

Polymer Impregnated Adsorbents for Direct Air Capture

Master's Degree

Abdulkadir Bozarslan

Master's thesis

2023/2024



Tomas Bata University in Zlín
Faculty of Technology

Tomas Bata University in Zlín
Faculty of Technology
Department of Polymer Engineering

Academic year: 2023/2024

ASSIGNMENT OF DIPLOMA THESIS

(project, art work, art performance)

Name and surname:	Abdulkadir Bozarslan
Personal number:	T22460
Study programme:	N0722A130002 Polymer Engineering
Type of Study:	Full-time
Work topic:	Polymer Impregnated Adsorbents for Direct Air Capture

Theses guidelines

1. Literature review – CO₂ emissions, global warming, reduction of CO₂ emissions versus negative carbon technologies, concept of “direct air capture” (DAC), overview of material base and methods of capturing CO₂ directly from the air.
2. Adsorbents preparation, impregnation of selected substrates by polymers, especially branched polyethylenimines but also others, eventually grafting, characterization (SEM, BET, FTIR).
3. Testing of thermal stability of prepared adsorbents, measurement of CO₂ adsorption/desorption, adsorption capacity, cyclic stability (TG).
4. Results evaluation, discussion.
5. Summary and conclusions.

Form processing of diploma thesis: **printed/electronic**
Language of elaboration: **English**

Recommended resources:

1. Lackner, K. et al. Carbon Dioxide Extraction From Air: Is It An Option? 24th Annual Technical Conference on coal Utilization & Fuel Systems, March 8-11, 1999, Clearwater, Florida.
2. Shi, X. et al. Sorbents for the Direct Capture of CO₂ from Ambient Air. *Angew. Chem. Int. Ed.* 2020, 59, 6984 – 7006. <http://doi.org/10.1002/anie.201906756>
3. Goepfert, A. et al. Carbon Dioxide Capture from the Air Using a Polyamine Based Regenerable Solid Adsorbent. *J. Am. Chem. Soc.* 2011, 133, 50, 20164–20167. <http://doi.org/10.1021/ja2100005>
4. Sakwa-Novak, M. A., Tan, S., Jones, Ch. W. Role of Additives in Composite PEI/Oxide CO₂ Adsorbents: Enhancement in the Amine Efficiency of Supported PEI by PEG in CO₂ Capture from Simulated Ambient Air. *ACS Appl. Mater. Interfaces* 2015, 7, 24748–24759. <http://doi.org/10.1021/acsami.5b07545>
5. Debashish, P., Vaishnavi, K., Sanjay, K.S. Evaluation of amine-based solid adsorbents for direct air capture: a critical review. *React. Chem. Eng.*, 2023, 8, 10–40. <http://doi.org/10.1039/d2re00211f>

Supervisors of diploma thesis: **Ing. Michal Machovský, Ph.D.**
Centre of Polymer Systems

Date of assignment of diploma thesis: **January 2, 2024**
Submission deadline of diploma thesis: **May 10, 2024**

prof. Ing. Roman Čermák, Ph.D. m.p.
Dean

L.S.

Ing. Jana Navrátilová, Ph.D. m.p.
Head of Department

In Zlín March 4, 2024

MASTER'S THESIS AUTHOR'S DECLARATION

I take cognizance of the fact that:

- my Master's thesis will be stored in electronic form in the university information system and will be available for viewing;
- my Master's thesis fully adheres to the Act No. 121/2000 Coll. on Copyright and Related Rights and on Amendments to Certain Acts (Copyright Act), as amended, in particular to § 35 Paragraph 3;
- in accordance with § 60 Paragraph 1 of the Copyright Act, Tomas Bata University in Zlín is entitled to conclude a licence agreement on the utilisation of a school work within the scope of § 12 Paragraph 4 of the Copyright Act;
- in accordance with § 60 Paragraph 2 and 3 of the Copyright Act, I may use my work – Master's thesis – or grant the licence for the utilisation thereof to another party only with prior written consent by Tomas Bata University in Zlín, which is in such a case entitled to claim from me an appropriate contribution to the reimbursement of the costs incurred by Tomas Bata University in Zlín due to the creation of the work (up to the full amount of this cost);
- if a software was provided for the preparation of the Master's thesis by Tomas Bata University in Zlín or by other entities only for study and research purposes (i.e. for non-commercial use), the results of the Master's thesis cannot be used for commercial purposes;
- if the output of the Master's thesis is a software product, the source codes and/or the files of which the project is comprised are considered as an inseparable part of the thesis. Failure to submit this part may be a reason for failure to defend the thesis.

I declare

- that the Master's thesis has been solely the result of my own work and that I have cited all the sources I had used. In case of publication of the results, I will be listed as a co-author.
- **that the submitted version of the Master's thesis and the version uploaded in electronic form in the IS/STAG system are identical in terms of their content.**

In Zlín on:

Name and surname of student:

.....

Signature of student

"The only limit to our realization of tomorrow will be our doubts of today."

Franklin D. Roosevelt

ABSTRAKT

Předložená diplomová práce je zaměřena na přípravu a charakterizaci aminy funkcionalizované pevné adsorbenty pro zachyt CO_2 , včetně možnosti přímého zachytu z atmosféry. V teoretické části je diskutován vliv CO_2 na klimatickou změnu a uveden koncept přímého zachytu CO_2 ze vzduchu. Pozornost je věnována obecným principům designu adsorbentů CO_2 a jejich přehledu, s důrazem na aminy funkcionalizované pevné adsorbenty a jejich specifickou interakci s CO_2 . V navazující experimentální části je vybrán komerční substrát na bázi kalcium silikátu funkcionalizován vybranými aminy. Kromě impregnace substrátu rozvětvenými polyethyleniminy o různé molekulové hmotnosti metodou smykových sil generovaných při vysokorychlostním míchání byla připravena série vzorků graftováním vybraných aminosilanů klasickou mokrou cestou. Adsorpce/desorpce CO_2 připravených vzorků byla testována metodou termogravimetrie v podmínkách simulujících vysokou koncentraci CO_2 (10 %), tak i přímý zachyt ze vzduchu (400 ppm).

Klíčová slova: zachyt CO_2 ; přímý zachyt ze vzduchu; pevné adsorbenty; polyetyleniminy; impregnace; termogravimetrie

ABSTRACT

This master thesis deals with preparation, characterization, and evaluation of amine functionalized solid adsorbents for CO_2 removal, including direct air capture. The theoretical part discusses the role of CO_2 in climate change and introduce the concept of direct air capture. Great attention is paid to adsorbents design rules and principles. Overview of up-to date solid adsorbents is given with emphasis of amine based solid adsorbents, including amine – CO_2 interactions. The experimental part focused on functionalization of commercial calcium silicate support material using various amines and techniques. Set of samples was prepared by impregnation support material with branched polyethyleneimines of various molecular weight via high-speed shear mixing, while another set was obtained by aminosilanes grafting following classic wet route. Performance of prepared solid adsorbents for CO_2 removal was evaluated by using thermogravimetry in a simulated flue gas atmosphere (10 % CO_2) as well as direct air capture simulated conditions (400 ppm CO_2).

Keywords: CO_2 removal; direct air capture; solid adsorbents, polyethyleneimines; impregnation; thermogravimetry

ACKNOWLEDGMENTS

I extend my deepest gratitude to Prof. Ing. et Ing. Ivo Kuritka, Ph.D. et Ph.D., whose insightful guidance and encouragement initiated this journey. His invaluable advice laid the foundation for this research endeavor.

I am indebted to my supervisor, Ing. Michal Machovsky, Ph.D., whose unwavering support and expertise were instrumental in shaping the research questions and methodology. His mentorship has been invaluable throughout this process.

I would like to thank my colleagues from research direction Nanomaterials and Advanced Technologies at Centre of Polymer Systems for their technical assistance, patience, and mentorship. I would also like to express gratitude to Dr. Eva Domincova Bergerova for elemental analysis.

I would like to acknowledge the support of the Centre of Polymer System and Faculty of Technology, Tomas Bata University whose resources and facilities were instrumental in the completion of this research.

Lastly, I cannot adequately express my gratitude to my parents, Vezir and Saadet Bozarslan, as well as to Asyumi Noraina for their endless love, encouragement, and sacrifices.

I hereby declare that the print version of my Master's thesis and the electronic version of my thesis deposited in the IS/STAG system are identical.

CONTENTS

PREFACE	10
1. INCREASE OF CO₂ EMISSION AND CLIMATE CHANGE	12
1.1 CO ₂ EMISSION AND ITS CONTRIBUTION TO GLOBAL WARMING.....	12
1.2 THE IMPORTANCE OF REDUCING CO ₂ EMISSIONS	14
1.3 CONCEPT OF DIRECT AIR CAPTURE IN MITIGATING GLOBAL WARMING	17
2. DIRECT AIR CO₂ CAPTURE	21
2.1 SOLID – DIRECT AIR CAPTURE (S- DAC).....	21
2.2 LIQUID - DIRECT AIR CAPTURE (L- DAC)	22
2.3 ADVANTAGES AND CHALLENGES OF DIRECT AIR CAPTURE.....	23
3. ADSORBENTS FOR DIRECT AIR CO₂ CAPTURE.....	25
3.1 CO ₂ ADSORBENTS BENCHMARK	25
3.2 ADSORBENTS DESIGN PRINCIPLES.....	26
3.3 ADSORBENTS CLASSIFICATION.....	27
3.4 PHYSICAL ADSORBENTS.....	28
3.4.1 Zeolites	28
3.4.2 Activated Carbon.....	28
3.4.3 Metal – Organic Frameworks (MOFs)	28
3.4.4 Covalent – Organic Frameworks (COFs).....	28
3.5 CHEMICAL ADSORBENTS.....	29
3.5.1 Metal Oxides	29
3.5.2 Metal Salts.....	29
3.5.3 Hydrotalcites and Double Salts.....	29
3.5.4 Amine Based Solid Sorbents.....	30
3.5.4.1 Amine Impregnated Sorbents (Class I)	31
3.5.4.2 Amine Grafted Sorbents (Class II)	31
3.5.4.3 In Situ Polymerization (Class III).....	32
3.5.4.4 Double Functionalization (Class IV)	32
4. CO₂ INTERACTION WITH AMINE.....	33
5. GOALS OF EXPERIMENTAL PART.....	36
5.1 AMINE GRAFTING WITH ZEOFREE	36
5.2 IMPREGNATION OF PEI AND/OR PEG WITH ZEOFREE	36
6. MATERIALS AND SYNTHESIS	38
6.1 MATERIALS	38
6.2 GRAFTING METHOD	40
6.2.1 Dry Grafting.....	41
6.2.2 Wet Grafting.....	41
6.3 IMPREGNATION METHOD	42
6.3.1 Amine-Impregnated Adsorbents	42
6.3.2 Dry Impregnation.....	42
6.3.3 Wet Impregnation.....	43
6.4 CHARACTERIZATIONS OF ADSORBENTS.....	45
6.4.1 Scanning Electron Microscopy Measurements	45
6.4.2 Thermal Stability Measurements.....	45
6.4.3 Specific Surface Area Evaluation.....	46
6.4.4 Fourier Transform Infrared Spectroscopy (FTIR) Measurements	47
6.4.5 Elemental Analysis Measurement	47
6.4.6 Adsorption Desorption Measurements in 10% CO ₂ Environment.....	48
6.4.7 Adsorption Desorption Measurements in 400 ppm CO ₂ Environment	50

7. RESULTS AND DISCUSSION.....	51
7.1 SURFACE MORPHOLOGY ANALYSIS (SEM) OF ADSORBENTS.....	51
7.2 THERMAL STABILITY AND ORGANIC CONTENT DETERMINATION OF AMINE-GRAFTED ADSORBENTS.....	54
7.3 THERMAL STABILITY AND ORGANIC CONTENT DETERMINATION OF AMINE-IMPREGNATED ADSORBENTS.....	56
7.4 SURFACE AREA AND POROSITY DETERMINATION (BET) OF ADSORBENTS	58
7.5 CHEMICAL CHARACTERIZATION (FTIR) OF AMINE-GRAFTED ADSORBENTS	60
7.6 CHEMICAL CHARACTERIZATION (FTIR) OF AMINE-IMPREGNATED ADSORBENTS	61
7.7 ELEMENTAL ANALYSIS OF ADSORBENTS	62
7.8 CO ₂ ADSORPTION CAPACITY AND CYCLIC STABILITY OF AMINE-GRAFTED ADSORBENTS IN 10% CO ₂ ENVIRONMENT	64
7.9 CO ₂ ADSORPTION CAPACITY AND CYCLIC STABILITY OF AMINE-IMPREGNATED ADSORBENTS IN 10% CO ₂ ENVIRONMENT	70
7.10 CO ₂ ADSORPTION CAPACITY OF AMINE-GRAFTED ADSORBENTS IN 400 PPM CO ₂ ENVIRONMENT	76
7.11 CO ₂ ADSORPTION CAPACITY OF AMINE-IMPREGNATED ADSORBENTS IN 400 PPM CO ₂ ENVIRONMENT	77
CONCLUSIONS.....	81
REFERENCES	83
LIST OF ABBREVIATIONS.....	89
LIST OF FIGURES	92
LIST OF TABLES	94

PREFACE

Nowadays, the research on Carbon Dioxide Removal (CDR) has gained momentum reflecting the growing concern about global warming. In contrast to concept of Carbon Capture, Storage and Utilization (CCSU), which focused on reduction CO₂ entering atmosphere from point emissions sources, its permanent storage underground and/or conversion to valuable industrial products such as chemicals and fuels, concept of CDR aimed to remove CO₂ that is already in atmosphere. While emission reduction, including CCSU is key to meet obligations declared in Paris Agreement, CDR technologies can help to counterbalance emissions from diffused small source which cannot be simply abated by other means. Within the CDR family of technologies, so called “direct air capture” (DAC) is a leading innovative technology for stabilizing the CO₂ concentration in the atmosphere and provides an important tool for carbon management in net zero pathways.[1]

In the hearth of both concepts is the process of CO₂ capture, therefore, research and development of high-performance CO₂ adsorbent become a new research hotspot in the field of material science. While liquid based CO₂ adsorbents, such as aqueous alkaline or amine solutions offer many pros, high energy input required for regeneration is hard to overcome.

In 2001 Satyapal et al demonstrated excellent performance and long-term stability of solid amine beads, known as HSC+, for application in aerospace vehicles and triggered a research interest in amine based solid adsorbents. The material system developed by Hamilton Sundstrand Space Systems International (HSSSI) consists of a polyethyleneimine (PEI) bonded to a high-surface-area polymethyl methacrylate solid support followed by second liquid phase coating with poly(ethylene glycol) (PEG) to enhance CO₂ adsorption/desorption rates and stability.[2] A privileged status of amine functionalized solid adsorbents can be ascribed to the almost ideal amine – CO₂ binding energy, which offer best trade-off between high selectivity and regeneration cost among current state of the art solid based CO₂ adsorbents.

THEORETICAL PART

1. INCREASE OF CO₂ EMISSION AND CLIMATE CHANGE

1.1 CO₂ Emission and Its Contribution to Global Warming

Increasing CO₂ levels in our atmosphere are a significant concern as they are the primary driver of climate change, leading to global warming. The burning of fossil fuels, deforestation, and various industrial processes have rapidly increased the concentration of carbon dioxide, trapping more heat in the Earth's atmosphere. This enhanced greenhouse effect results in climate anomalies, melting ice caps, rising sea levels, and extreme weather events. Addressing this increase is critical for the stability of global climates and the preservation of ecosystems worldwide.[3]

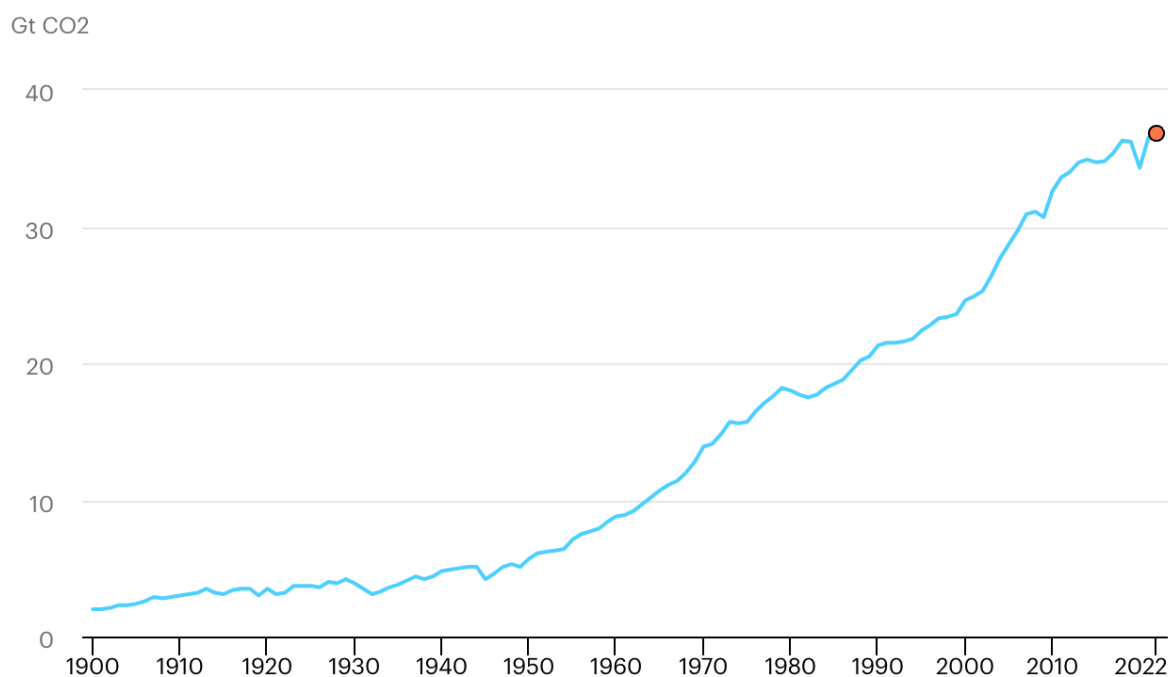


Figure 1 Worldwide emissions of carbon dioxide due to the burning of energy sources and industrial activities from the year 1900 to 2022. [4]

The graph illustrates a significant and continuous rise in global CO₂ emissions from energy combustion and industrial processes over the past century, particularly from the mid-20th century onwards. This trend reflects the expansion of industrial activity, the increased use of fossil fuels, and the impact of economic growth on the environment. Despite fluctuations, the overall trajectory indicates a pressing environmental concern, with emissions reaching an all-time high by 2022, underscoring the urgent need for effective climate change mitigation strategies.[3]

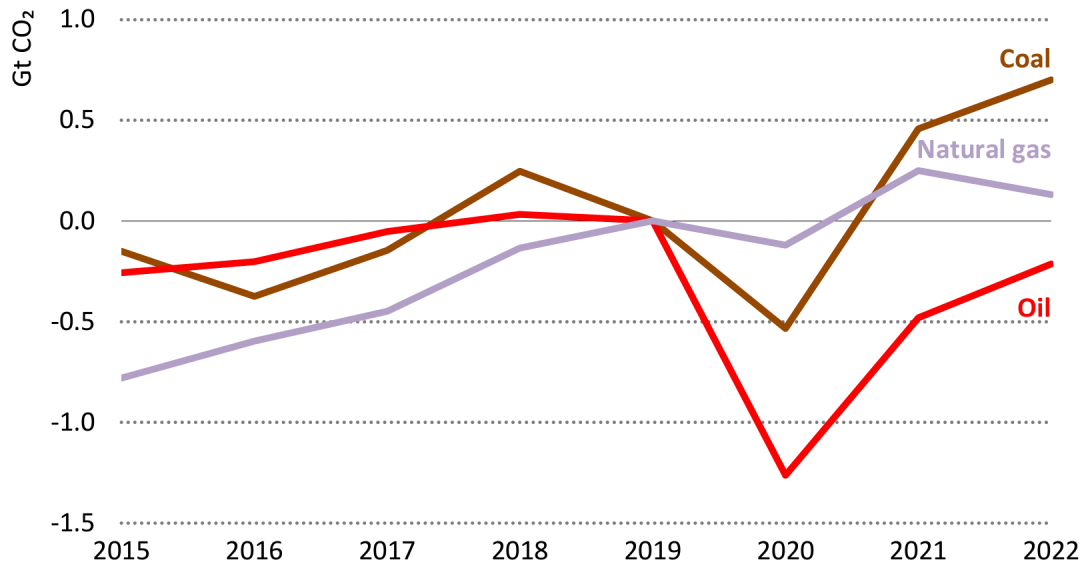


Figure 2 Variation in worldwide carbon dioxide emissions from different fuels, compared to the baseline of 2019, from the years 2015 to 2022. [3]

Fossil fuels are the primary energy source for most of the world's energy demands, with coal alone accounting for about 40% of the world's total energy consumption, a figure that is rising over time. The increased burning of these fuels has significantly raised CO₂ emissions, making anthropogenic CO₂ the main greenhouse gas contributing to global climate change. [3] [5]

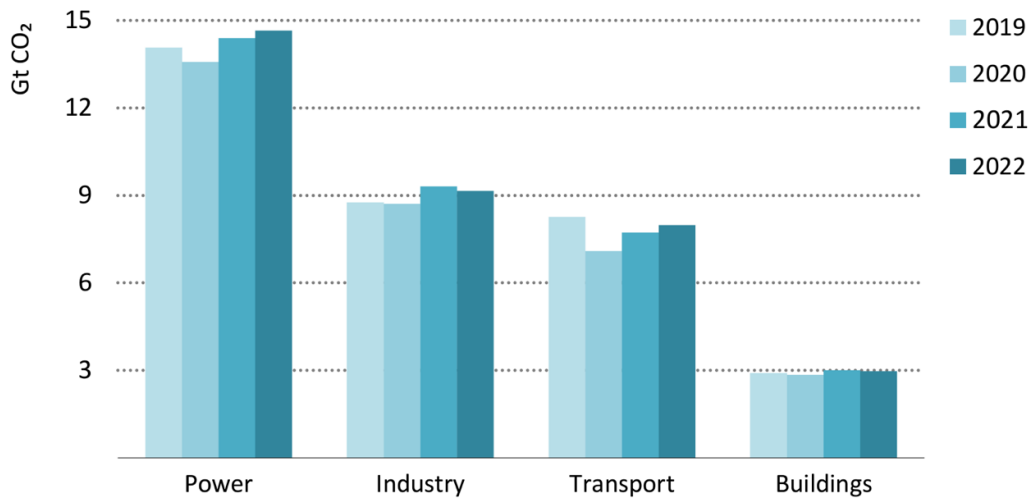


Figure 3 Worldwide carbon dioxide emissions categorized by industry, 2019 to 2022. [3]

Despite a rise in renewables, power sector emissions saw the most significant increase in 2022, mainly due to gas-to-coal switching, especially in Asian economies. Emissions from electricity and heat generation rose by 1.8% to a record 14.6 Gt. [3] By embracing renewable energy sources such as solar photovoltaic systems, wind turbines, and hydroelectric power for electricity generation, alongside the adoption of electric vehicles for transportation, we can significantly reduce carbon dioxide emissions.

1.2 The Importance of Reducing CO₂ Emissions

Reducing CO₂ emissions is crucial for addressing climate change and its impacts on the planet and humanity. Countries worldwide are making commitments to achieve "net zero" emissions, a critical step in combating climate change. Net zero means balancing any emissions made by absorbing/adsorbing an equivalent amount from the atmosphere.[6] This effort aims to limit global temperature increases to 1.5°C above pre-industrial levels, as per the Paris Agreement.

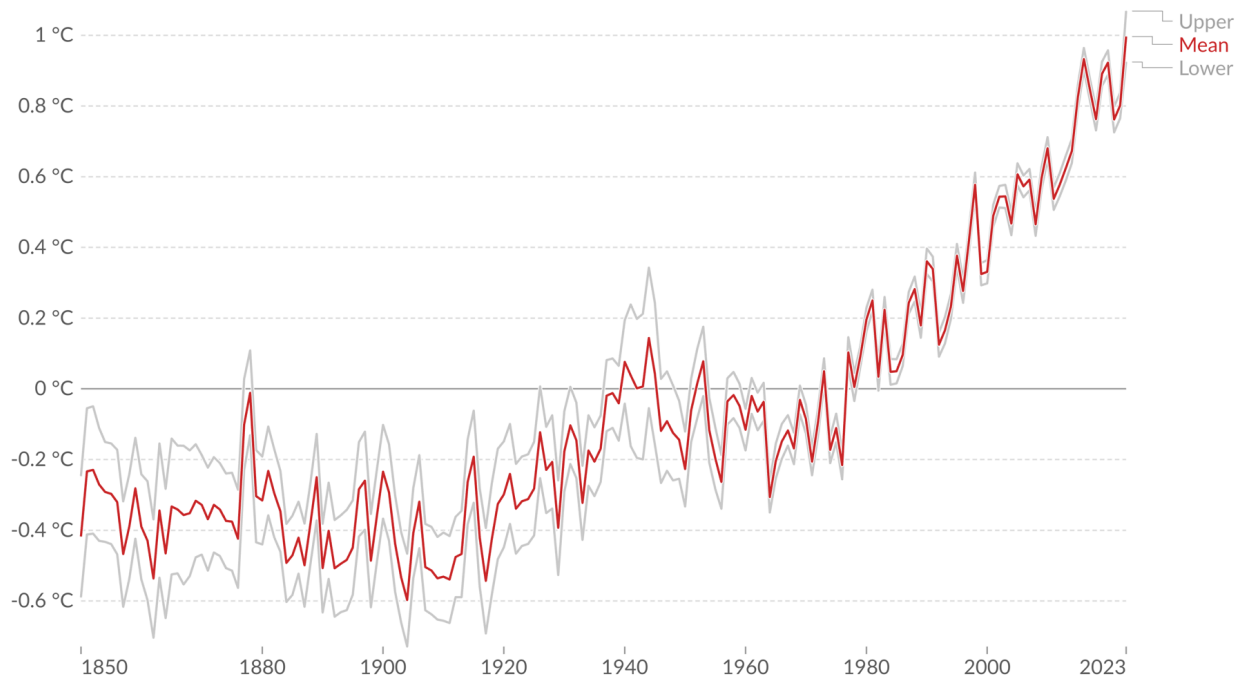


Figure 4 Global average temperature variation. [4]

The impact of climate change is being felt globally, with each continent facing unique challenges. Small islands are particularly vulnerable, experiencing a loss of biodiversity, food and water security risks, economic disruptions, and increased displacement due to habitat degradation. In North America, climate change is affecting mental health outcomes, ecosystem degradation, and water resources, leading to risks in food security and well-being. Europe faces flooding risks, temperature-related stress and mortality, ecosystem disruptions, water scarcity, and agricultural losses. [3], [6]

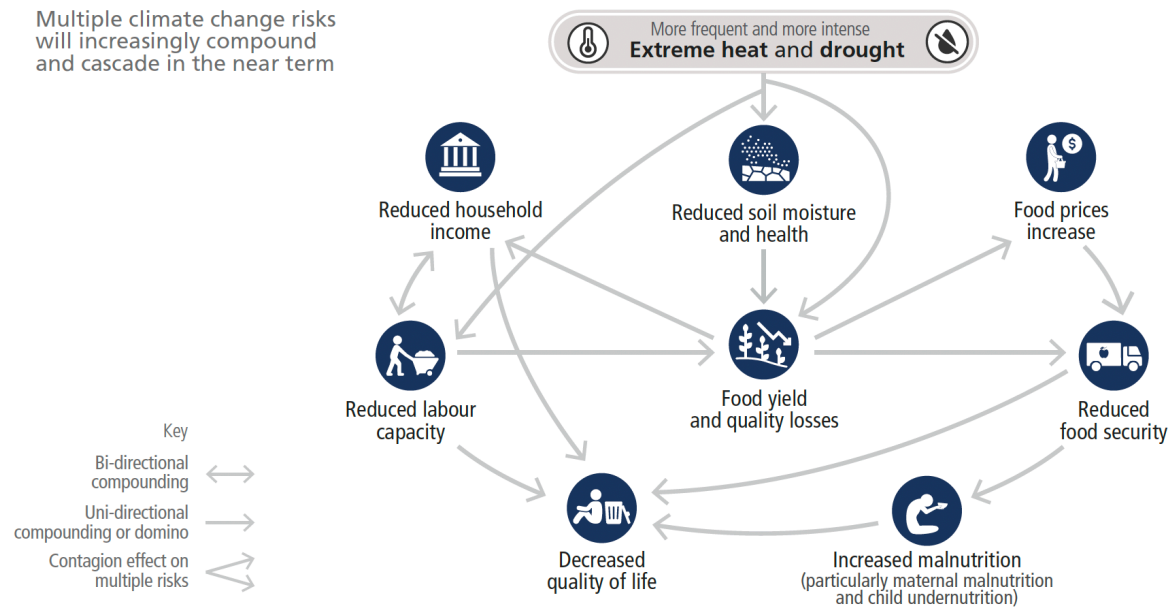


Figure 5 Extreme climate events harm smallholder farmers, reducing crop yields, food security, income, and well-being. [3]

Asia's challenges include urban infrastructure damage from flooding, biodiversity loss, coral bleaching, fishery resource decline, and threats to food and water security. Finally, Africa is grappling with potential species extinction, risks to food security and health, marine ecosystem degradation, economic challenges, and increased water and energy security risks due to drought and heat. These diverse impacts underscore the global nature of climate change and the need for concerted efforts to address these challenges.[3], [6]



Figure 6 Air pollution in New Delhi November 3, 2023 [7]

Air pollution is a significant global health risk, leading to around 7 million (according to WHO) or 6.7 million (according to IHME) deaths annually. This includes deaths from both outdoor and indoor pollution, stemming from man-made and natural sources. Especially PM_{2.5} (particulate matter 2.5 micrometers), is a key harmful component, penetrating deep into the lungs and bloodstream. Recent studies suggest the health impacts of pollution are more severe than previously thought.[8]



Figure 7 Every year, numerous forests endure drought conditions. [9]

Extremely dry circumstances, such as drought, heat waves, and strong winds, increase the risk of wildfires. A variety of dangerous air pollutants, including PM_{2.5}, NO₂, ozone, aromatic hydrocarbons, and lead, are combined to form wildfire smoke. Apart from discharging harmful substances into the environment, wildfires also have an impact on the climate by releasing copious amounts of greenhouse gases, such as carbon dioxide, into the atmosphere. [10]

The fire season is beginning earlier and ending later due to climate change, which is causing greater temperatures and drier conditions as well as increased urbanization of rural areas. The number of acres burned, their duration, and their intensity are all increasing during wildfire events, which can also interfere with communications, transportation, the provision of water, power, and gas.[10]

1.3 Concept of Direct Air Capture in Mitigating Global Warming

The idea of directly capturing CO₂ from the atmosphere is not a new concept. The necessity to capture CO₂ from the surrounding atmosphere emerged with the development of submarines, spaceships, and stations. Carbon dioxide is a by-product of human metabolic processes, and in enclosed spaces, if not actively removed, its concentration gradually rises. According to NASA research, cognitive abilities begin to deteriorate when CO₂ concentration exceeds 0.5%. [11]

Historically, on spacecraft until the 1990s, support systems that maintained a stable atmosphere relied on lithium hydroxide (LiOH). Despite the high adsorption capacity of alkaline hydroxides in general, these systems were unsuitable for long-term missions due to the impracticality of regenerating these adsorbents under the given conditions. Regeneration occurs at very high temperatures, making it highly energy intensive. For instance, regeneration of NaHCO₃, Na₂CO₃, and NaOH requires temperatures > 927°C, while CaO and Ca(OH)₂ require temperatures > 400°C. [12] Therefore, solid-state adsorbents based on amines deposited on a suitable substrate have emerged as viable alternatives in these high-tech space applications.

While these adsorbents may have lower adsorption capacities compared to alkaline hydroxides, they offer the advantage of easy regeneration, balancing the lower capacity. [2] The interaction of CO₂ with amines is highly specific and occurs at the interface of physisorption and chemisorption, with energy values typically falling within the range of 40-50 kJ/mol. [13] Aminated compounds exhibit significant selectivity at normal temperatures and pressures, addressing a common issue with physisorbents.

Additionally, they enable CO₂ desorption, allowing for the regeneration of the adsorbent at reasonable energy costs, unlike chemisorption. CO₂ desorption is typically achieved through a temperature cycle (temperature swing). However, to further reduce energy requirements, alternative desorption methods are also being investigated, such as vacuum swing [14], moisture swing [15], or electrochemical swing. [16]

These solid-state adsorbents, based on amines deposited on substrates, which have proven themselves in successful space applications, have regained the interest of the wider scientific community. This renewed interest is due to factors such as climate change, the necessity to decarbonize the economy, and the emergence of negative emission technologies. The technical feasibility and socio-economic aspects of innovative Direct Air Capture (DAC) technology as a solution to combat global warming were first presented by Klaus Lackner at the 24th Annual Technical Conference on Coal Utilization and Fuel Systems held in Clearwater, Florida in 1999. [17]

He demonstrated that capturing CO₂ directly from the surrounding atmosphere is technically feasible and represents an innovative solution for offsetting CO₂ emissions from numerous small, scattered sources such as cars, households, and small operations. This approach is particularly useful where it is not economically viable to install filters and other CO₂ capture systems, as is typically done with single point sources such as power plants, cement plants, and chemical plants. In the case of single point sources, the concentration of CO₂ is high (10-15%), as well as the temperature at which CO₂ capture takes place and when physisorbents (activated carbon, zeolites) are used.[18]



Technology Provider	Plant Type	Solid DAC 	Liquid DAC 	Location	Approx capture capacity (tCO ₂ per year)	Market Application
Climeworks	16 Pilots	✓		Across Europe	2,000	Utilisation
	Commercial (Orca)	✓		Iceland	4,000	Utilisation & Storage
	Under construction (Mammoth)	✓		Iceland	36,000	TBD
Carbon Engineering	Pilot		✓	Canada	350	Utilisation
	Under Construction		✓	USA	Up to 1,000,000	EOR & Storage
Global Thermostat	2 pilots - not operating	✓		USA	14,000	N/a
	Under construction	✓		USA	4,000	Utilisation

Figure 8 Leading Direct Air Capture companies around the world.

Direct Air Capture (DAC) technology is rapidly emerging as a critical solution in the fight against climate change. Currently, there are 18 DAC plants worldwide, capturing a total of 8,000 tonnes of CO₂ annually. Notably, a 1 million-tonnes/year DAC plant in Texas is set to become operational by late 2024, while a 36,000 tCO₂/year facility is under construction in Iceland, representing a significant increase in capacity. Interest and investment in DAC have surged, driven by the Bipartisan Infrastructure Law and Inflation Reduction Act in the United States, which provide substantial funding and tax credits for DAC development. The private sector has also committed substantial resources, with investments from the Frontier Fund, Bill Gates' Breakthrough Catalyst Fund, and Lowercarbon Capital.[19]

DAC's importance in achieving net-zero targets is increasingly recognized, with significant policy support and investments. Since 2020, nearly \$4 billion in funding has been allocated for DAC research and development and plans for nine new DAC facilities are in the pipeline. If realized, DAC deployment could reach approximately 3 MtCO₂ by 2030, a substantial increase from current levels but still a fraction of what is needed in the Net Zero Scenario.[6]

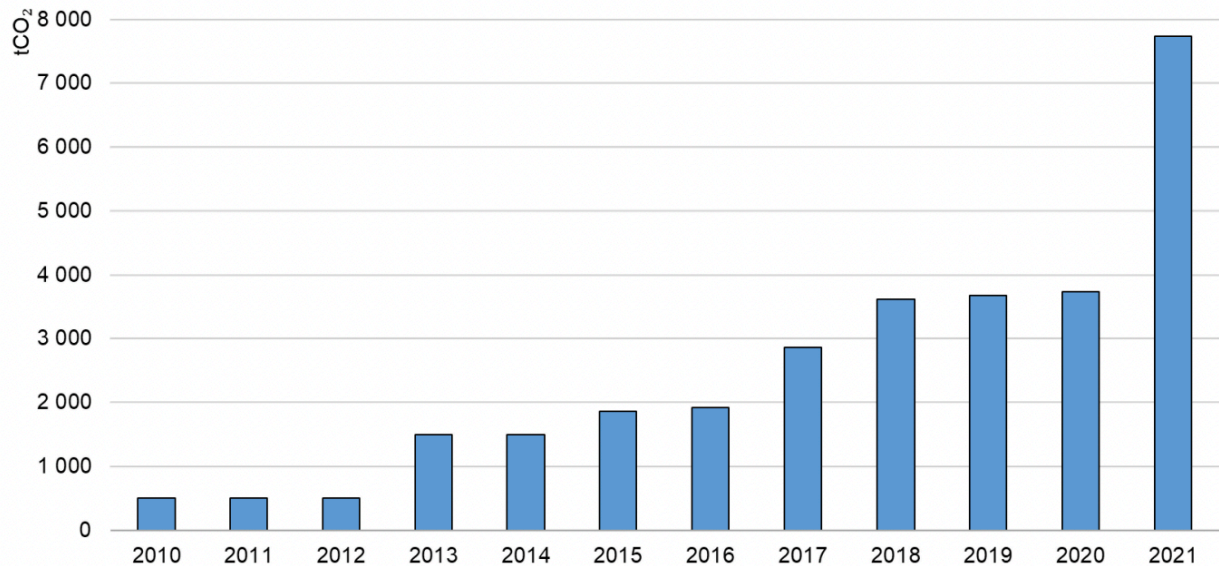


Figure 9 Direct Air Capture global operating capacity, 2010–2021 [6]

DAC is crucial for removing CO₂ from the atmosphere and can provide a climate-neutral feedstock for various products. In the Net Zero Scenario, DAC deployment accelerates, aiming for 980 MtCO₂ capture by 2050, contributing to a net-zero emissions energy system. Scaling up DAC deployment implies the addition of over 30 DAC plants capturing 1 Mt/year annually from 2020 to 2050, contingent on cost competitiveness, access to low-carbon energy, and essential consumables.[6], [19]

According to International Energy Agency (IEA), in the Delayed Action Scenario, reducing the global average temperature increase to below 1.5 °C would necessitate a significant ramp-up of CO₂ removal from the atmosphere. This would be achieved through the deployment of bioenergy with carbon capture and utilization or storage (BECCS) and direct air capture and storage (DACS), totaling over 5 billion metric tons of CO₂ removal annually in the latter half of this century. In the Delayed Action Scenario, it is assumed that this requirement is divided between BECCS, contributing 2 billion metric tons per year by 2100, and DACS, contributing 3.3 billion metric tons per year by 2100.[6]

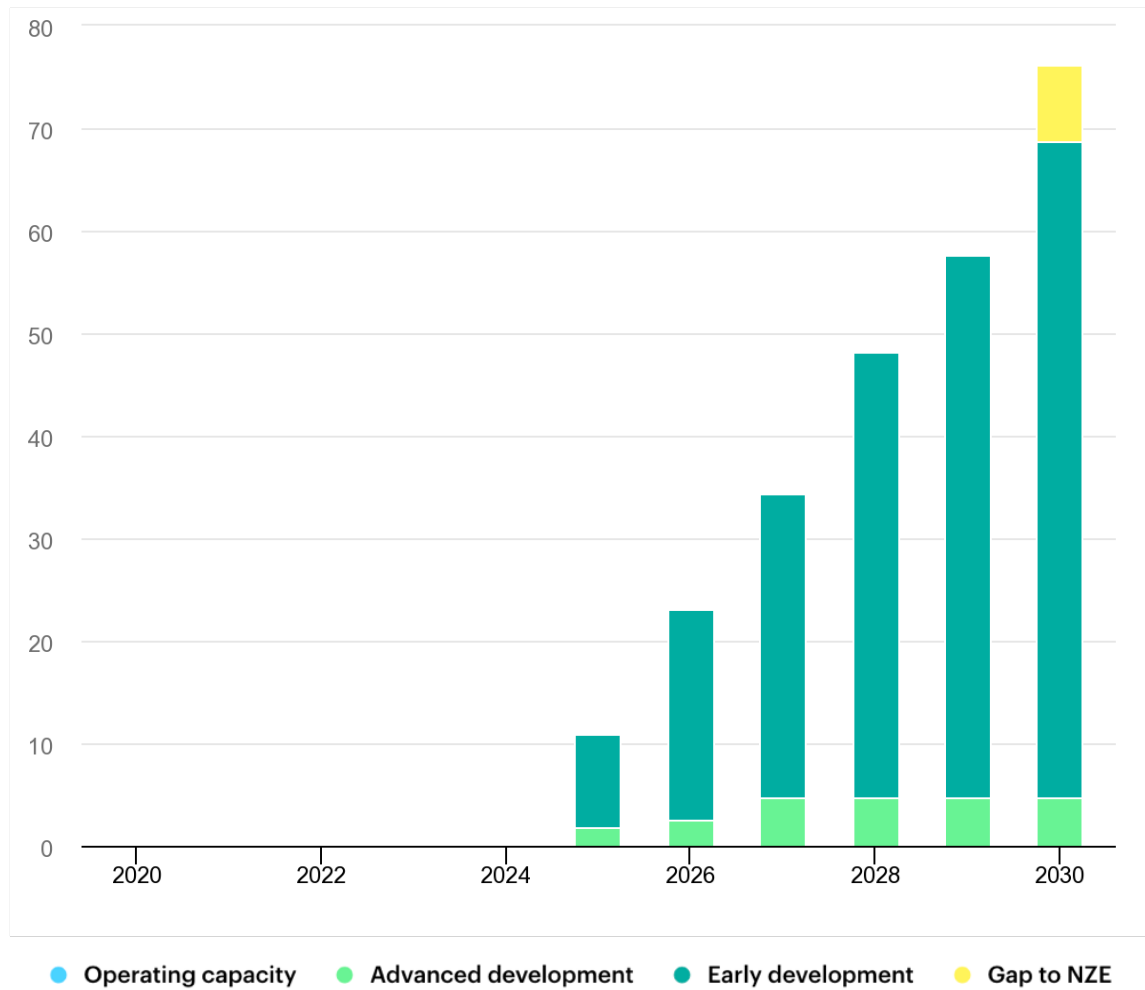


Figure 10 CO₂ capture by Direct Air Capture, planned projects and in the Net Zero Emissions by 2050 Scenario, 2020-2030 [6]

In conclusion, Direct Air Capture technology is gaining momentum and holds significant promise in addressing climate change. By removing CO₂ directly from the atmosphere, Direct Air Capture offers a powerful solution to reduce greenhouse gas emissions. With increased support from governments and the private sector, Direct Air Capture is poised to make a substantial contribution to achieving net-zero emissions targets. As we continue to advance this technology and scale up its deployment, we move closer to a sustainable and carbon-neutral future.

2. DIRECT AIR CO₂ CAPTURE

Despite low concentration, DAC has significant potential to remove substantial amounts of CO₂ annually. This is achieved by bringing vast quantities of air into contact with sorbents, specifically engineered to capture CO₂. Two technology approaches are currently being used to capture CO₂ from the air: solid and liquid DAC.[19]

An alternative to the strong base type of DAC commonly employs solid chemical compounds known as amines. Figure 11 showcases the process of amine-based adsorbents capturing CO₂ directly from the air under regular conditions. After reaching CO₂ saturation, these adsorbents undergo desorption by being subjected to pressures between 20–400 mbar and temperatures of 80–130 °C. The cost of CO₂ capture can be significantly reduced if these adsorbents are regenerated using waste heat or renewable energy sources.[20], [21], [22]

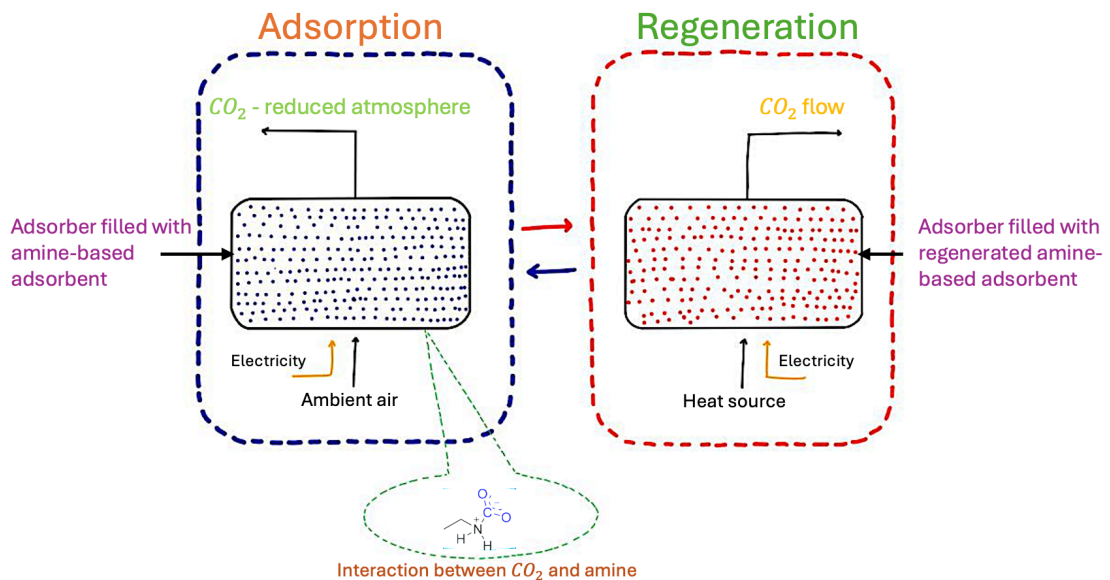


Figure 11 Adsorption and regeneration process of adsorbents. (Redrawn from [20])

2.1 Solid – Direct Air Capture (S- DAC)

- Air is drawn in through a fan located inside the collector. Once sucked in, it passes through an amine-based adsorbent filter located inside the collector which traps the carbon dioxide particles.
- When the filter is completely full of CO₂, the collector closes, and the temperature rises to about 80°C - 130°C.
- This causes the filter to release the CO₂ so we can finally collect it. The CO₂ can then be safely and permanently stored underground.[23]

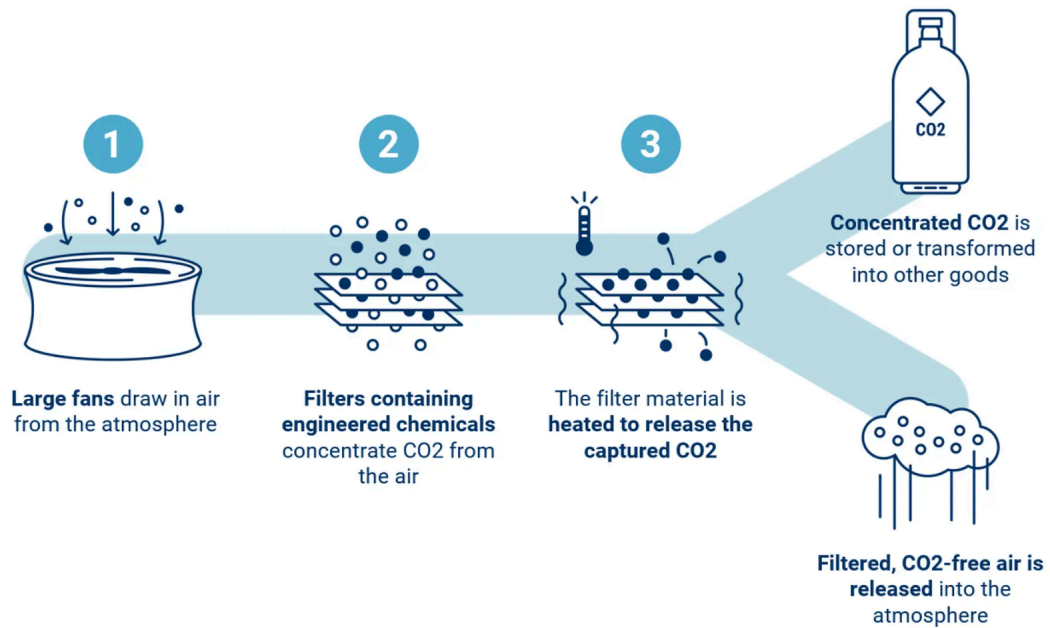


Figure 12 Solid Direct Air Capture process. (Climeworks [24])

2.2 Liquid - Direct Air Capture (L- DAC)

The process initiates with an air contactor, a sizable construction resembling industrial cooling towers. A massive fan draws air into this structure, guiding it over thin plastic surfaces coated with a potassium hydroxide solution. This harmless solution chemically binds with the CO₂ molecules, extracting them from the air and imprisoning them within the liquid as carbonate salt.[25]

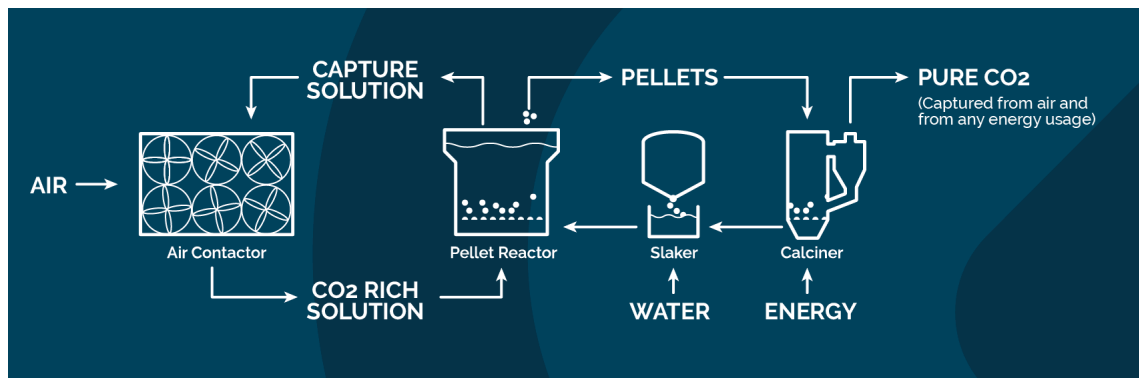


Figure 13 Liquid Direct Air Capture process. (Carbon Engineering [25])

Next, the CO₂ within the carbonate solution undergoes a series of chemical procedures to heighten its concentration, refine it, and compress it into a gas state, making it suitable for immediate use or storage. This entails segregating the salt from the solution and transforming it into small pellets within a structure known as a pellet reactor, which was adapted from water treatment technology. [25]

During this chemical reaction, not only are calcium carbonate pellets precipitated, but also the initial capture chemical for the air contactor is rejuvenated. Subsequently, these pellets are subjected to heat in third step, a calciner, to liberate the CO₂ in its pure gaseous form. This stage also leaves behind calcium oxide, which is mixed with water in the slaker to rehydrate it. It is then reintroduced into the pellet reactor, thus commencing the cycle anew.[25]

2.3 Advantages and Challenges of Direct Air Capture

DAC, in comparison to capturing it from concentrated sources like power plants or cement factories it requires more energy and costly because it's more challenging to extract CO₂ from the ambient air. This is mainly because the CO₂ in the air is much more diluted, requiring more energy and resources to extract. [19]

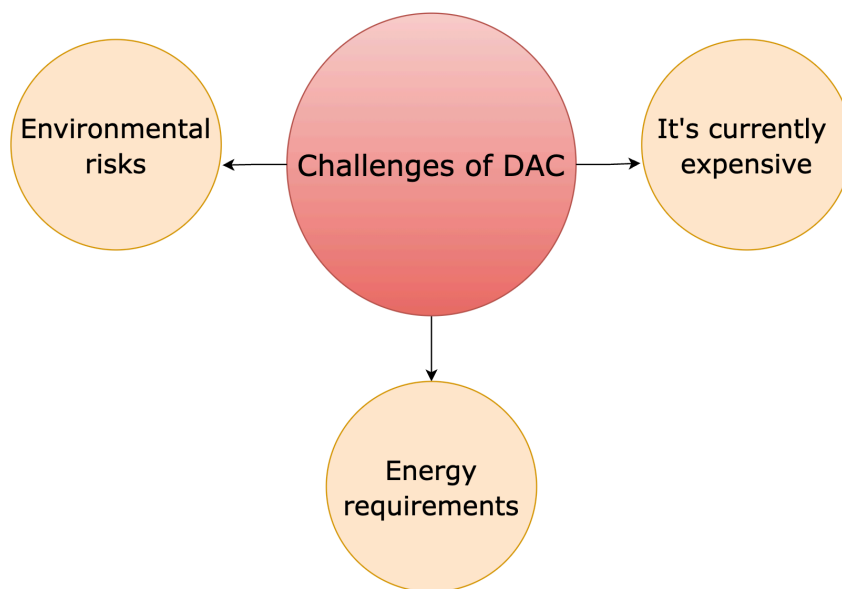


Figure 14 Challenges of Direct Air Capture Technology.

The ambient air has a CO₂ concentration that is 100 to 300 times less than the concentrated CO₂ found in the flue gases of coal and gas power stations. As a result, DAC facilities need a significantly larger area of CO₂-capturing chemicals exposed to the air than the areas or volumes used in CCS for contact with flue gases. This leads to DAC being roughly three times more energy-intensive per ton of CO₂ removed from the atmosphere than CCS.[19]

The cost of DAC for large-scale applications (1 million tons of CO₂ per year) typically falls between \$125 to \$335 per ton of CO₂, depending on various factors. Lower energy costs can bring these estimates closer to the industry target of \$100 per ton of CO₂. If there's a carbon pricing scheme in place, the cost of DAC capture could become even more competitive. [19]

The US Department of Energy aims to bring DAC costs below \$100 per ton of CO₂ in the coming decade, making it an attractive option, especially when combined with tax credits and carbon credits. [19]

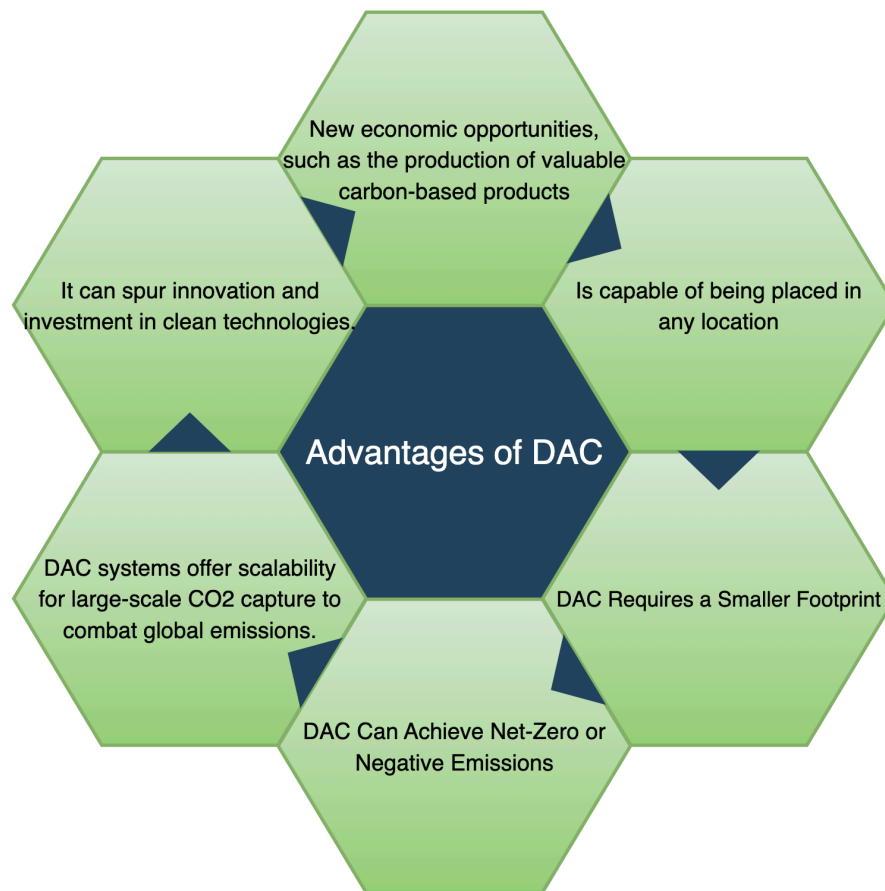


Figure 15 Advantages of Direct Air Capture Technology.

Capture costs below USD 200-250/tCO₂ could already be commercially attractive in the United States where facilities are able to access the California LCFS credits (around USD 200/tCO₂) together with tax credits such as the 45Q (USD 50/tCO₂). As DAC technology continues to evolve and sees widespread deployment, costs are expected to decrease further in the next five to ten years.[19]

Nevertheless, DAC offers unique benefits over conventional CCS that could be key for its large-scale implementation. DAC plants can be located virtually anywhere, as long as they have access to low-carbon energy and suitable CO₂ storage or transportation options. Unlike conventional CCS, which typically needs to be near fossil fuel power plants or industrial sites, DAC facilities can be independent of these locations and can even be situated offshore. This flexibility allows DAC to potentially capture CO₂ emissions from widespread sources like transportation, buildings, and land use in forestry and agriculture. These sources account for about 35% of global anthropogenic CO₂ emissions and are not addressed by conventional CCS. [26]

3. ADSORBENTS FOR DIRECT AIR CO₂ CAPTURE

3.1 CO₂ Adsorbents Benchmark

In practical application, CO₂ adsorbents must satisfy some key checkpoints to ensure efficiency. First and foremost, the adsorbent should have a high adsorption capacity, ideally capturing at least 2 mmol of CO₂ per gram of adsorbent. This high adsorption capacity is paramount for effective CO₂ capture. Secondly, the adsorbent must be cyclable, capable of enduring at least 1000 cycles of adsorption and desorption processes without significant degradation. Thirdly, selectivity is crucial. The adsorbent must exhibit high CO₂ selectivity, ensuring efficient capture without capturing other gases. [20]

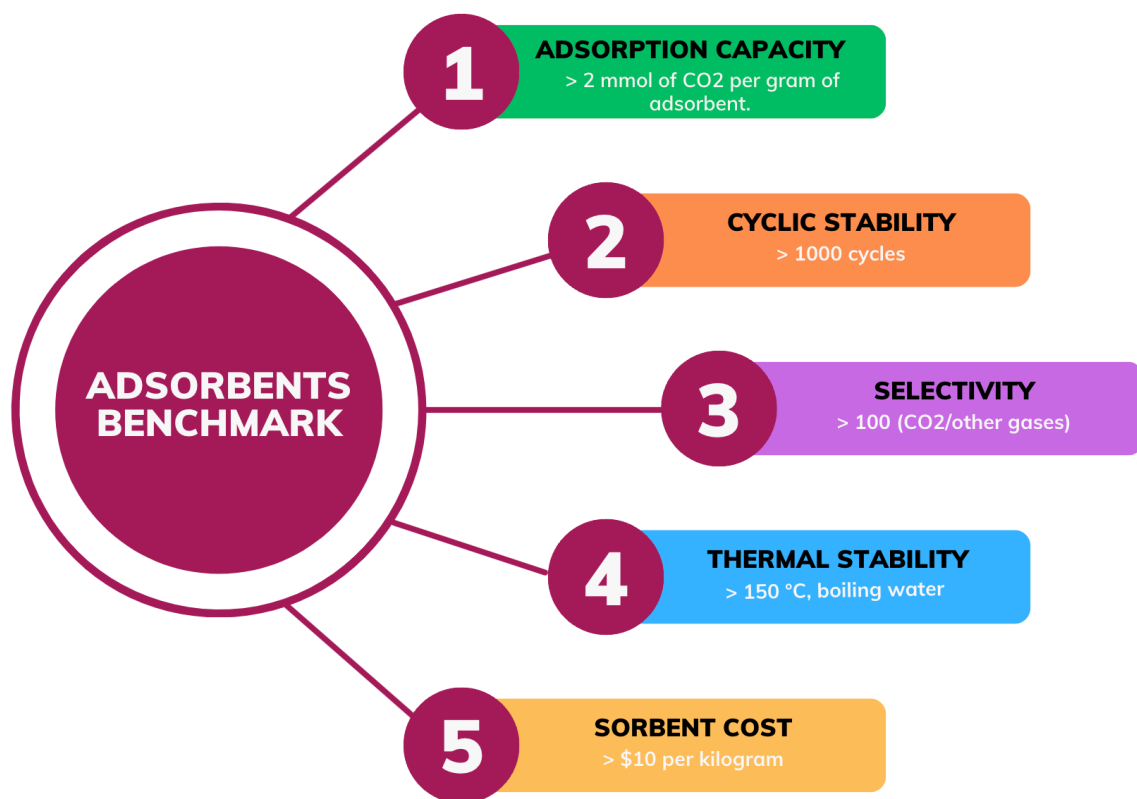


Figure 16 Some of significant checkpoints for an effective CO₂ adsorbent.

Furthermore, the adsorbent should possess good stability properties to maintain its performance over multiple cycles. Cost-effectiveness is another crucial factor. The cost of the sorbent should be economical, ideally under \$10 per kilogram. Lastly, a good kinetic performance is essential. The adsorbent should have a kinetic performance of over 1 mmol (g x min)⁻¹. Additionally, low pressure drops, and practical sorbent regeneration should be considered to ensure efficient Direct Air Capture.[12], [20]

3.2 Adsorbents Design Principles

In addition to surface chemistry, the specific surface area and porosity of an adsorbent play crucial roles in CO₂ adsorption. It is intuitive to expect that a microporous adsorbent with a high specific surface area would perform the best. However, the small pore size of such adsorbent's limits CO₂ diffusion. Therefore, the textural properties of the adsorbent must be carefully tailored to balance these opposing requirements. Similarly, the chemistry of the adsorbent is crucial in designing high performing adsorbents. By optimizing both the textural properties and chemistry of the adsorbent, it is possible to achieve enhanced CO₂ adsorption performance. [27]

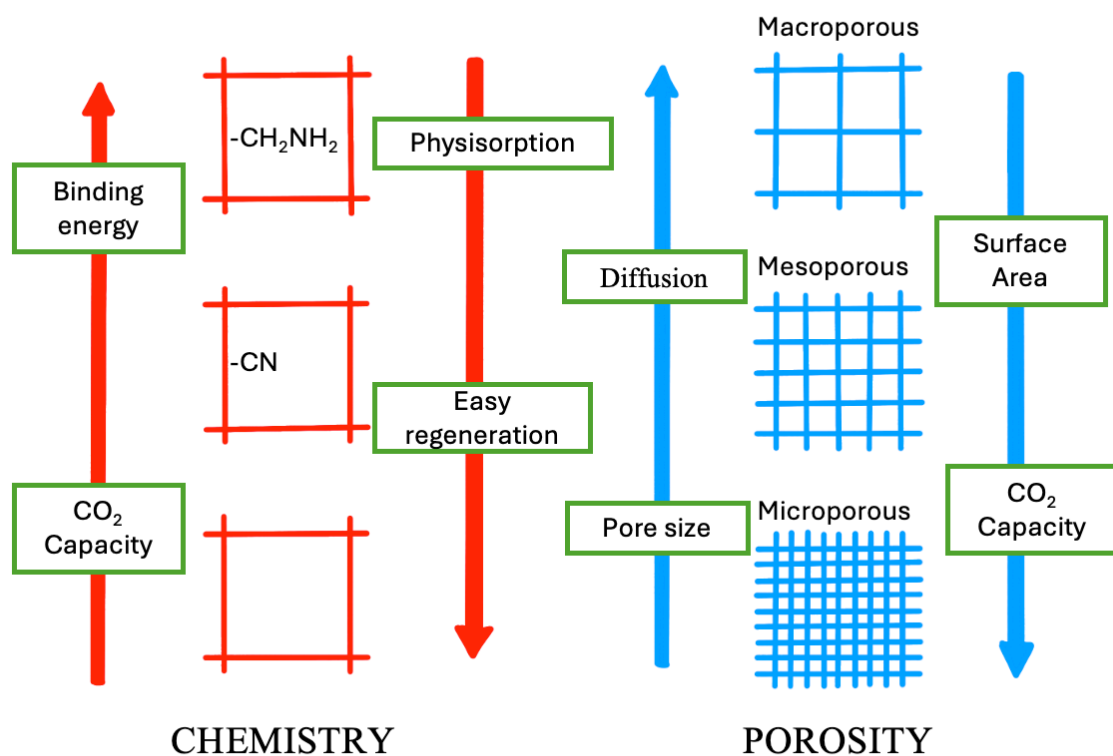


Figure 17 Porosity and chemistry have to be considered together in optimizing a sorbent choice.
(Redrawn from [27])

This delicate balance between surface area, porosity, and chemical composition is key to the development of efficient CO₂ adsorbents for various applications, including carbon capture and storage.

3.3 Adsorbents Classification

Carbon dioxide separation and capture technologies are broadly categorized into five main types: membrane, absorption, adsorption, cryogenic distillation, and chemical looping. Among these, carbon dioxide absorption is a widely used method where CO_2 is dissolved in a medium through physical or chemical interactions. Adsorption, on the other hand, involves capturing CO_2 using a physical or chemical adsorbent. Cryogenic separation operates under high pressure and extremely low temperatures, leveraging the different boiling points of gases for separation.[28]

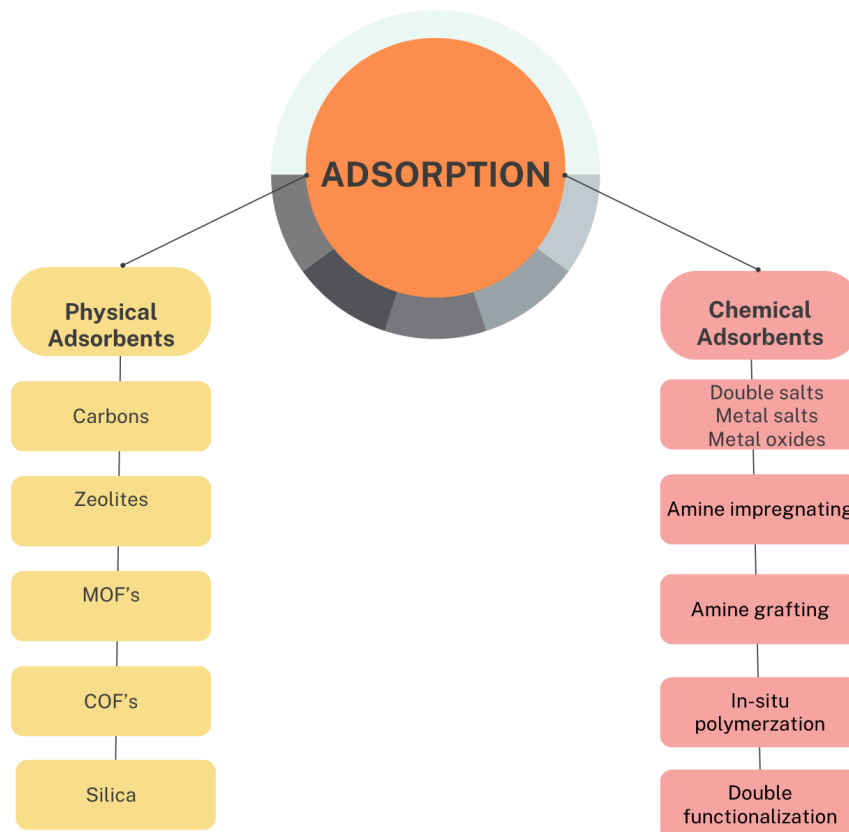


Figure 18 Classification of adsorbents materials.

For physical adsorbents, attributes like the size of the adsorbent, surface area, and the architecture of the pores are crucial for determining how effectively they can adsorb gases. The most efficient physical adsorbents typically have a large surface area and pore diameters smaller than 0.7 nanometers.[29] Moreover, the ideal enthalpy of sorption should align with the requirements for both adsorption and desorption to optimize carbon dioxide capture.

Chemical adsorbents, in contrast, are often metallic elements available in forms such as salts or oxides, for example, magnesium oxide and calcium oxide, or as alkali-metal and hydrotalcite compounds like lithium silicate and lithium zirconate. These materials react with acidic gases like carbon dioxide to form strong chemical bonds, resulting in metal carbonates. [28], [29], [30]

3.4 Physical Adsorbents

Common materials used as physical adsorbents like zeolites, activated carbon, metal-organic frameworks (MOFs), and covalent organic frameworks (COFs) are pivotal. These materials are chosen due to their high surface area, which is desirable for adsorption processes. The mechanism of action in physical adsorbents relies on physical interactions between the sorbent material and the substance being adsorbed. These interactions are often governed by van der Waals or ion quadrupole forces, which bind the molecules to the surface of the sorbent. [29], [30]

3.4.1 Zeolites

Zeolites are silicate-based materials with a crystalline structure, high surface area, and adjustable pore design. The alumina content and pore diameter greatly affect their adsorption capabilities. Zeolites with larger pore diameters, such as zeolite 13X, demonstrate enhanced adsorption abilities compared to other types. Despite their effectiveness in carbon dioxide adsorption, challenges include reduced efficiency at higher temperatures, low selectivity, and decreased performance in humid conditions.[30]

3.4.2 Activated Carbon

Activated carbon is characterized by its carbon-rich composition and well-organized porosity, making it suitable for diverse applications ranging from wastewater treatment to air pollution control. It stands out for its hydrophobic nature, large surface area, and stability, making it a favored choice for carbon dioxide capture. However, challenges include its low selectivity for specific gas separations, prompting research into its modification for improved performance.[30]

3.4.3 Metal – Organic Frameworks (MOFs)

MOF consist of metal ions/clusters and organic ligands, known for their remarkably high surface area and pore size. They exhibit unique adsorption kinetics and can be regenerated at low temperatures. While they show great potential in carbon dioxide capture, challenges include high production costs and instability under humid conditions also, complicated synthesis process. [20]

3.4.4 Covalent – Organic Frameworks (COFs)

COFs made of crystalline, highly porous polymers linked by covalent bonds, are noted for their stability and tunable pore sizes. They have gained attention in carbon dioxide adsorption due to their high surface area and adaptability. Challenges in COFs include the cost and complexity of synthesis methods, which are areas of ongoing research.

All these adsorbents, as they generally demand less energy for regeneration due to non-chemical bond formation with the adsorbate. Their operation at lower temperatures and the high reversibility of the

adsorption and desorption cycles accentuates their energy-saving benefits. However, the necessity for strong vacuum conditions or gentle heating during regeneration brings an inevitable energy penalty. Weak interactions may need more frequent regeneration than chemical adsorbents, which bond stronger with molecules.[28], [29], [30], [31], [32], [33]

3.5 Chemical Adsorbents

Chemical adsorption, a subset of adsorption processes, involves a chemical reaction occurring on a surface to capture substances like CO₂. Various metals and compounds have been explored for this purpose.

3.5.1 Metal Oxides

Examples include calcium oxide (CaO) and magnesium oxide (MgO). They are involved in a reversible reaction with CO₂, where one mole of metal compound reacts with one mole of CO₂. In practical applications, metal oxides like CaO are transformed into metal carbonates (e.g., CaCO₃) through a cyclic process involving temperature variations, which helps in regenerating the sorbent and producing a concentrated CO₂ stream suitable for storage. [20]

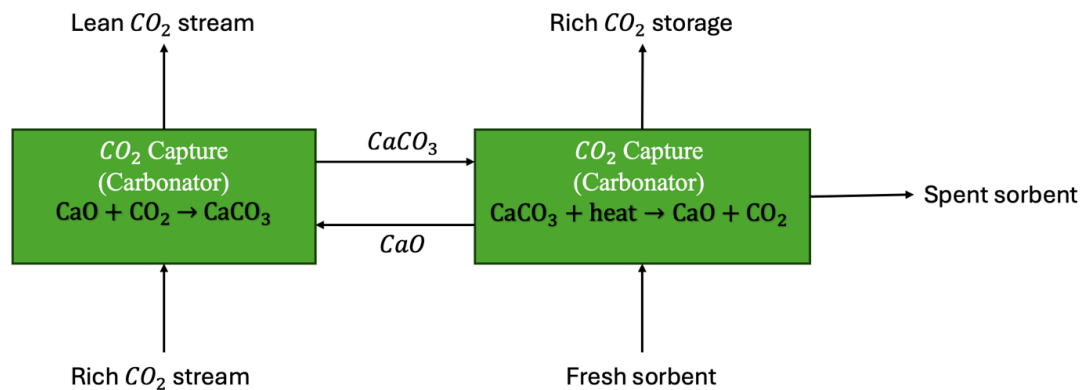


Figure 19 Capturing CO₂ via calcination and carbonation with a calcium oxide (CaO) sorbent.

3.5.2 Metal Salts

These range from alkali metal compounds like lithium silicate and lithium zirconate to alkaline earth metal compounds. Although lithium-based salts show promising CO₂ adsorption performance, their high production cost limits their widespread use.

3.5.3 Hydrotalcites and Double Salts

These materials have layered structures and are noted for their easy regeneration due to low energy requirements. However, their stability is yet to be thoroughly examined.

Also, lithium zirconate (Li_2ZrO_3) has been identified as an effective high-temperature CO_2 absorbent. Its reaction with CO_2 is reversible within a specific temperature range, and this reversibility can be controlled simply by adjusting the temperature. The addition of eutectic carbonates (like a mix of Li_2CO_3 and K_2CO_3) can further enhance the CO_2 absorption efficiency.

Another material is lithium silicate (Li_4SiO_4), which has been found to have a greater CO_2 adsorption capacity than lithium zirconate. Lithium silicate undergoes a reaction with CO_2 below 720°C and releases CO_2 above this temperature. Its large capacity, quick absorption rate, stability, and effectiveness across various temperatures and CO_2 concentrations make it a strong candidate for commercial CO_2 adsorbent development. However, its energy-intensive due to high temperatures.[33]

3.5.4 Amine Based Solid Sorbents.

Amine-based adsorbents have recently attracted attention for their proficiency in Direct Air Capture (DAC) due to their high CO_2 adsorption capacities, especially at ultra-dilute concentrations and in humid conditions. However, the effectiveness of these adsorbents is significantly influenced by their synthesis method and the governing process parameters. There are four primary methods for synthesizing these adsorbents. [34] Physical Impregnation (class I), Chemical grafting (class II), In situ polymerization (class III), Double functionalization (class IV).

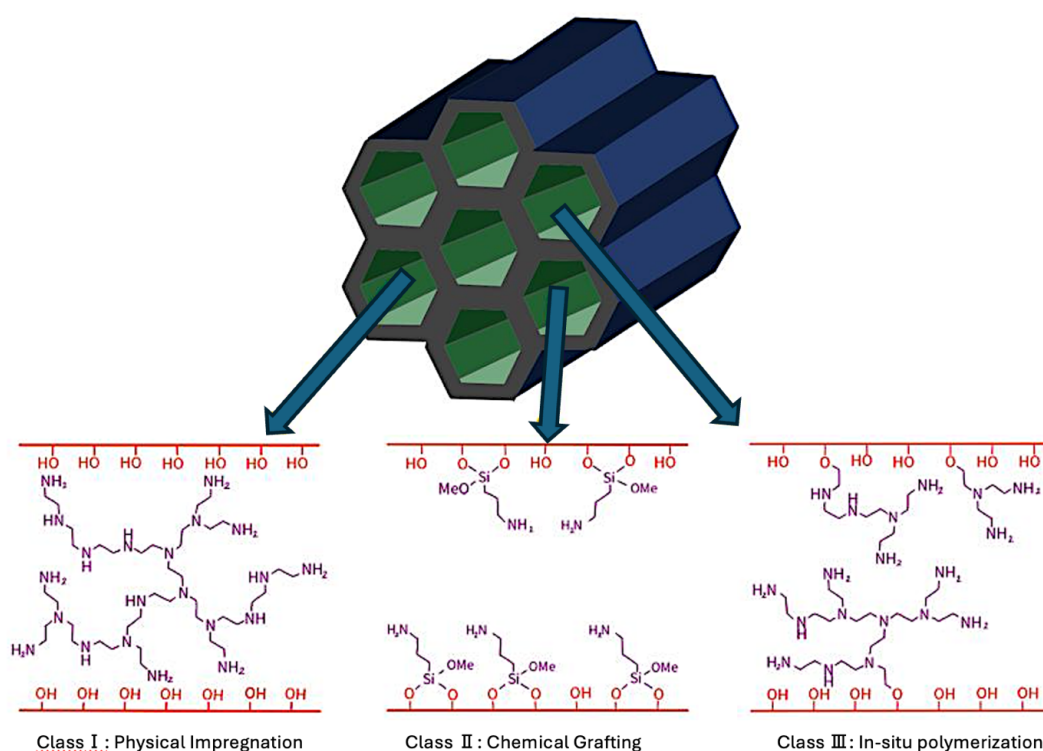


Figure 20 Schematic representation of classification of amine based solid adsorbents. Redrawn from [20]

3.5.4.1 Amine Impregnated Sorbents (Class I)

Physical Impregnation (Class I Adsorbents) method involves dispersing amines like TEPA or PEI (polyethyleneimine) in a solvent,[35], [36] followed by mixing with a porous support. This method is favored for its simplicity and its ability to house substantial amounts of amine. However, challenges such as amine degradation and evaporation. Despite these challenges, there have been successful attempts in using low-volatile, high-molecular-weight amines to address these issues. One effective approach involves the impregnation of PEI molecules of varying molecular weights into sorbents.

For instance, impregnating PEI molecules with an average molecular weight (Mw) between 400 and 25 000 Da into sorbents maximizes the effective content of amine in the adsorbent. Notably, the literature reported that adsorbents with branched PEI (Mw of 800 Da) achieved the highest CO₂ adsorption capacity.[20], [37], [38], [39], [40]

Notably, temperature and pressure influence CO₂ adsorption capacities. For instance, when assessing the performance of certain adsorbents under varying temperatures and pressures, specific trends have emerged that shed light on the mechanisms behind CO₂ adsorption in amine-based adsorbents. As the temperature rises, for instance, there's a change in the dynamics of CO₂ penetration, when the temperature rises, the films produced by the crosslink between CO₂ and PEI (formation of ammonium carbamate ion pairs) become less dominating over CO₂ penetration, resulting in increased capacity.[20], [41]

3.5.4.2 Amine Grafted Sorbents (Class II)

Amine grafted adsorbents are lauded for their high stability and easy regeneration during CO₂ adsorption–desorption cycles, even in humid conditions, compared to those obtained by the physical impregnation method. Class II materials are made up of amino silanes covalently bound to the surface of the porous support. The covalent binding of the amino silane to the support lends these materials significant thermal stability, although they tend to have a relatively low concentration of amine. Furthermore, Class II materials have been predominantly utilized in basic research to explore how different types of amines (primary, secondary, tertiary) affect CO₂ capture efficiency and resistance to oxidation. Also, one must acknowledge their limitation in CO₂ uptake capacity. This arises due to surface saturation with amino silane species. [20], [30] This reaction predominantly occurs between amino silane species and the hydroxyl group found on the support surface. It generally commences with the mixing of the chosen porous solid support in a solvent, with anhydrous toluene being a common choice. This is then combined with amino silane, followed by a phase of stirring and refluxing. After the reaction is complete, the solution is filtered and washed to remove any remaining unreacted amine molecules from the sorbent.[20]

3.5.4.3 In Situ Polymerization (Class III)

Class III materials are synthesized through a specialized process of in situ polymerization, where amino polymers are covalently bonded inside the porous support, utilizing amine-rich monomers such as aziridine. This method grants these materials superior thermal stability due to the robust covalent linkages between the support and the polymer. However, the rapid polymerization of aziridine, while beneficial for securing the amino polymers firmly onto the support, poses challenges in controlling the polymer's final structure, making these materials more complex to produce on a laboratory scale. Moreover, the polymer can obstruct the pores of the support, leading to diffusion issues that slow down the adsorption and desorption processes. The hazardous properties of aziridine further diminish the attractiveness of this method for lab-based research, due to the difficulties in managing the swift and potentially unsafe polymerization process. [20], [42]

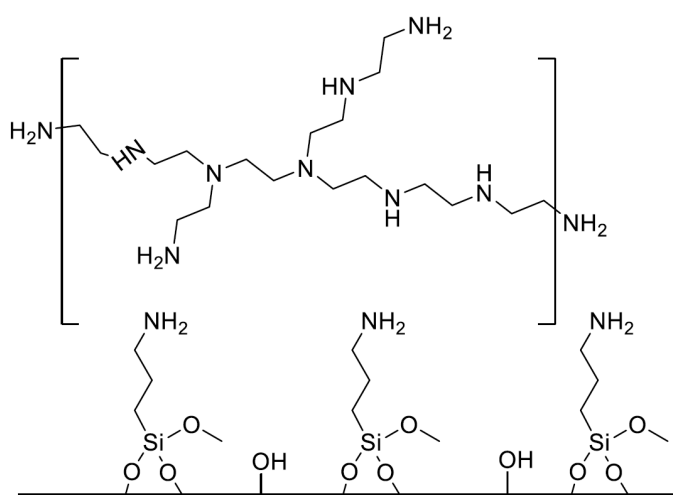


Figure 21 Representation of double functionalization. (Redrawn from [43])

3.5.4.4 Double Functionalization (Class IV)

Class IV adsorbents embody a hybrid methodology, blending the advantages of both grafting and impregnation techniques through a "double-functionalized method." This innovative process involves the synthesis of amine-based sorbents that, after initial grafting, are further enriched by impregnation with amino silanes, potentially increasing their adsorption capacity by introducing additional amine species. These materials merge the traits of Class 1 and Class 2 materials, featuring both chemically grafted molecular amino silanes and physically embedded amino polymers. This combination has been shown to enhance stability over Class 1 materials, thanks to the hydrogen bonding between the amines on the amino polymer and those covalently bonded to the surface. Despite these improvements, Class IV adsorbents may still face diffusion issues due to pore blockage.[18], [20], [43], [44], [45], [46], [47], [48]

4. CO₂ INTERACTION WITH AMINE

Since the 1930s, solutions of primary and secondary amines in water have been utilized for capturing CO₂ from natural gas and hydrogen under high partial pressures. These solutions, however, are limited by their significant heat capacities and losses due to evaporation, making the regeneration process costly and energy demanding. To mitigate these energy costs, employing amines and polyamines on solid supports has been introduced.

Solid adsorbents based on amines, which are a combination of amines with a porous solid support, show enhanced performance in capturing CO₂. This improvement is attributed to the synergistic effect of CO₂ chemisorption by the amines and physisorption by the solid support.

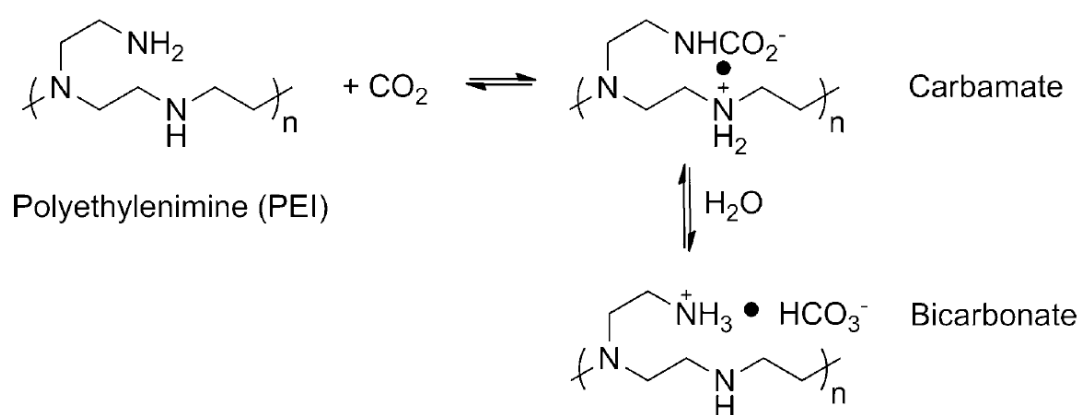


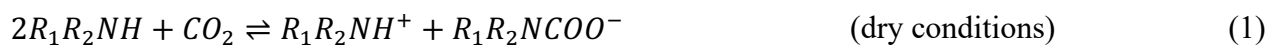
Figure 22 Interaction of PEI with CO₂. (Redrawn from [40])

The reaction of CO₂ with PEI is depicted in Figure 22. The polymer's repeating unit in Figure 22 offers a simplified model representation, illustrating the three different types of amines present in PEI. The primary and secondary amino groups in PEI react with CO₂ to form carbamates. These carbamates can further react to form bicarbonates in the presence of water. Under dry conditions, two amino groups are required for every CO₂ molecule to be captured.

Conversely, under humid conditions, theoretically, only one amino group is needed to capture a molecule of CO₂. Consequently, the CO₂ adsorption capacity of PEI is expected to be higher under humid conditions. Additionally, the presence of water significantly stabilizes the adsorbents based on PEI and grafted amines by inhibiting the formation of urea species.[40]

In situ IR spectroscopy has shown that under dry conditions, CO₂ adsorbs on primary amine sites as strongly bound ammonium carbamate and on secondary amine sites as weakly bound carbamic acid.

Additionally, a secondary amine may also weakly adsorb ammonium carbamate. Under moist conditions, amines react with CO₂ to produce bicarbonate, as demonstrated by equations (1) and (2) for the reaction of secondary amines with CO₂ under both conditions.[49]



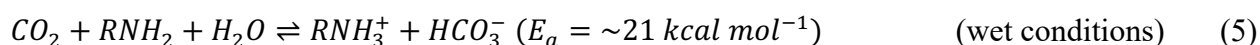
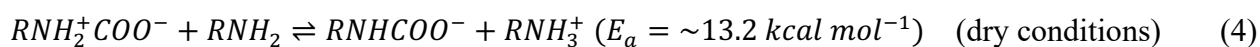
For primary amines (R₂ = hydrogen atom), the carbamate reaction [Eq. (1)] and the carbonation reaction [Eq. (2)] may compete. However, in some amines, the carbamate reaction is suppressed due to steric hindrance. Tertiary amines (R₁R₂R₃N) cannot undergo carbamation since the COO⁻ group needs to replace a hydrogen atom.[50]

Pinto et al. studied CO₂ sorption by amine-modified materials under dry conditions using solid-state NMR spectroscopy. The study noted that when a large amount of CO₂ is incorporated and only a small amount of R-NH₂ is available, a fraction of carbamic acid could remain unreacted, leading to its presence during CO₂ sorption.

The reaction mechanisms for CO₂ adsorption on amine-based adsorbents are categorized as follows (outlined in eqn (3)–(8)):

The Zwitterion mechanism (type I):

CO₂ reacts with amine to form a zwitterion (eqn (3)), which is then deprotonated by a free base (such as amine, OH⁻, or H₂O) to yield carbamate (dry conditions) or bicarbonate (wet conditions). [20]



The single-step mechanism (type II):

Amine reacts with CO₂ and a base simultaneously, bypassing the formation of a stable zwitterion. Here, water molecules serve as proton acceptors instead of amines.[20]



The carbamic acid mechanism (type III):

A two-step reaction where the amine first combines with CO₂ to create carbamic acid, which then undergoes a proton transfer with another amine to form carbamate:



Among these, the zwitterion mechanism is frequently observed in studies addressing CO₂ capture by amines, whether in solutions or on solid adsorbents, in both dry and humid conditions. Species such as carbamic acid, alkylammonium carbamate, and/or bicarbonate are identified during CO₂ adsorption over amine-based adsorbents, depending on the amine concentration and adsorption conditions.[20]

Kortunov et al. reported the nucleophilic attack of amine (Lewis base) on CO₂ carbon leading to the formation of zwitterion $\text{RH}_2\text{N}^+-\text{COO}^-$ (referred to as 1,3-zwitterion, with 1 and 3 denoting the positive and negative centers, respectively). Depending on the conditions, 1,3-zwitterion may convert to ammonium carbamate through intermolecular proton transfer with amine (Brønsted base) or to carbamic acid through intramolecular hydrogen transfer. Notably, in anhydrous conditions, two primary amines react with CO₂ to form ammonium carbamate. In the presence of water, water acts as a nucleophile, reacting with CO₂ to create carbonic acid, which then forms carbonate/bicarbonate upon reacting with an amine. Additionally, water can convert carbamate anion into carbonate or bicarbonate, releasing the amine for further CO₂ reaction, leading to a maximum theoretical amine efficiency (molar CO₂/N ratio) of 0.5 in anhydrous conditions and 1.0 in hydrous conditions.

Primary and secondary amines can react with CO₂ under both dry and humid conditions, while tertiary amines only do so in the presence of moisture. The formation of carbamic acid or carbamate depends on the amine loading, with alkylammonium carbamate being predominant at high amine loadings, whereas carbamic acid or hydronium carbamate is more likely at lower amine loadings. In humid conditions, water can also assist the nucleophilic attack of CO₂ with the amine to generate hydronium carbamate, or it can act as a nucleophile that amines assist in producing ammonium bicarbonate at expense of carbamate. For highly hindered amine or tertiary amines, water acts as a more competitive Lewis base, leading to the formation of ammonium bicarbonate in comparison to carbamate.[20]

5. GOALS OF EXPERIMENTAL PART

The experimental goals of this thesis focused on the modification of ZEOFREE support material through chemical grafting and impregnation processes, aimed at enhancing their adsorption properties for capturing CO₂ under flue (%10 CO₂) and dilute (400 ppm CO₂) conditions.

5.1 Amine Grafting with ZEOFREE

- Explored two different aminosilanes, APTMS (amino propyl trimethoxy silane) and AEAPTMS 3-[2-(2-aminoethylamino) ethyl amino] propyl-trimethoxy silane, for grafting onto ZEOFREE to enhance its CO₂ adsorption capabilities as well as thermal and cyclic stability.
- Assessed the influence of water by grafting under dry and wet conditions. Additionally, undried ZEOFREE support was used to observe the effects of inherent water without additional water.

5.2 Impregnation of PEI and/or PEG with ZEOFREE

- Investigated the impregnation of PEI (polyethyleneimine) onto ZEOFREE to enhance its CO₂ capture potential.
- Examined the effect of the addition of PEG (polyethyleneglycol) on the impregnation process and resulting adsorption properties and cyclic stability.
- Implemented both dry and wet impregnation methods (where 'wet' means without additional water; PEI2000 and PEI750000 already contain 50% inherent water) using PEIs of different molecular weights (800, 25000, 2000, 750000).

These experimental objectives aimed to advance the understanding of surface modification techniques for adsorbent materials and to develop adsorbents with enhanced CO₂ adsorption capabilities, as well as their cyclic stability, thermal stability, and textural properties suitable for flue and dilute conditions.

EXPERIMENTAL PART

6. MATERIALS AND SYNTHESISSES

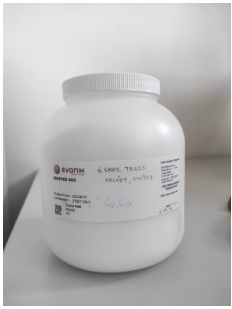
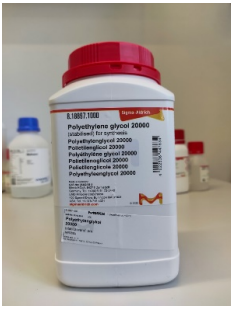
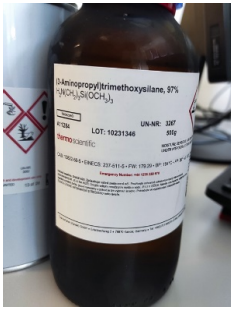
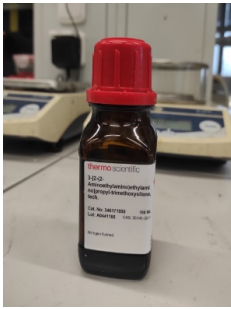
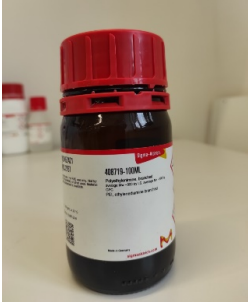

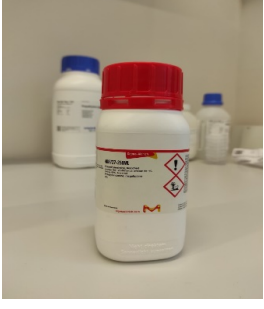

6.1 Materials

ZEOFREE were obtained from Evonik, anhydrous toluene were obtained from PENTA, For amine-grafting APTMS (amino propyl trimethoxy silane) (%97) and AEAPTMS 3-[2-(2-aminoethylamino) ethyl amino] propyl-trimethoxy silane were obtained from Thermo Scientific. While for amine-impregnation PEI branched (polyethyleneimine) (molecular weight 800 and 25000), PEI branched (molecular weight 2000 and 750000) and PEG (polyethylene glycol) (molecular weight 20000) were obtained from Sigma Aldrich.

Table 1 List of materials and chemicals used for the syntheses.

Materials / Chemicals	Used for	Obtained from
ZEOFREE	Support material.	EVONIK
APTMS (amino propyl trimethoxy silane) (%97)	Amino silane, used for grafting method.	THERMO SCIENTIFIC
AEAPTMS 3-[2-(2-aminoethylamino) ethyl amino] propyl-trimethoxy silane	Amino silane, used for grafting method.	THERMO SCIENTIFIC
Anhydrous toluene	Solvent	PENTA
PEI branched (Mw 800)	Used for impregnation	SIGMA ALDRICH
PEI branched (Mw 25000)	Used for impregnation	SIGMA ALDRICH
PEI branched (Mw 2000) 50% water solution	Used for impregnation	SIGMA ALDRICH
PEI branched (Mw 750000) 50% water solution	Used for impregnation	SIGMA ALDRICH
PEG (Mw 20000)	Used for impregnation	SIGMA ALDRICH

Table 2 Materials and chemicals used for the syntheses.

 <p>ZEOFREE (Precipitated Calcium Silicate)</p>	 <p>PEG Mw 20000 poly(ethylene glycol)</p>
 <p>APTMS (amino propyl trimethoxy silane) (%97)</p>	 <p>AEAPTMS 3-[2-(2-aminoethylamino) ethyl amino] propyl-trimethoxy silane</p>
 <p>PEI branched (polyethyleneimine) Mw 800</p>	 <p>PEI branched (polyethyleneimine) Mw 2000</p>
 <p>PEI branched (polyethyleneimine) Mw 25000</p>	 <p>PEI branched (polyethyleneimine) Mw 750000</p>

6.2 Grafting Method

ZEOFREE, a specialized synthetic calcium silicate, boasts an extraordinarily high absorption capacity due to its precipitated nature. This product features highly porous particles. For this reason, we selected ZEOFREE sorbent as the support material for the adsorption process, capturing CO₂ directly from air at concentrations of 10% and 0.04%. In our first experiment, we systematically worked to remove water from the ZEOFREE. The support material, weighing 20g, were subjected to a controlled environment inside the MEMMERT VO400 oven. The drying conditions were set at a temperature of 100°C and a pressure of 10 millibar. After a 24-hour duration, the material was extracted and weighed, and it was observed that ZEOFREE was 18.9 g. We also kept some support sorbent that had not gone through the drying process for sample ZEO-3, and ZEO-6. Therefore, for ZEO-3 and ZEO-6 there was no additional water injected.

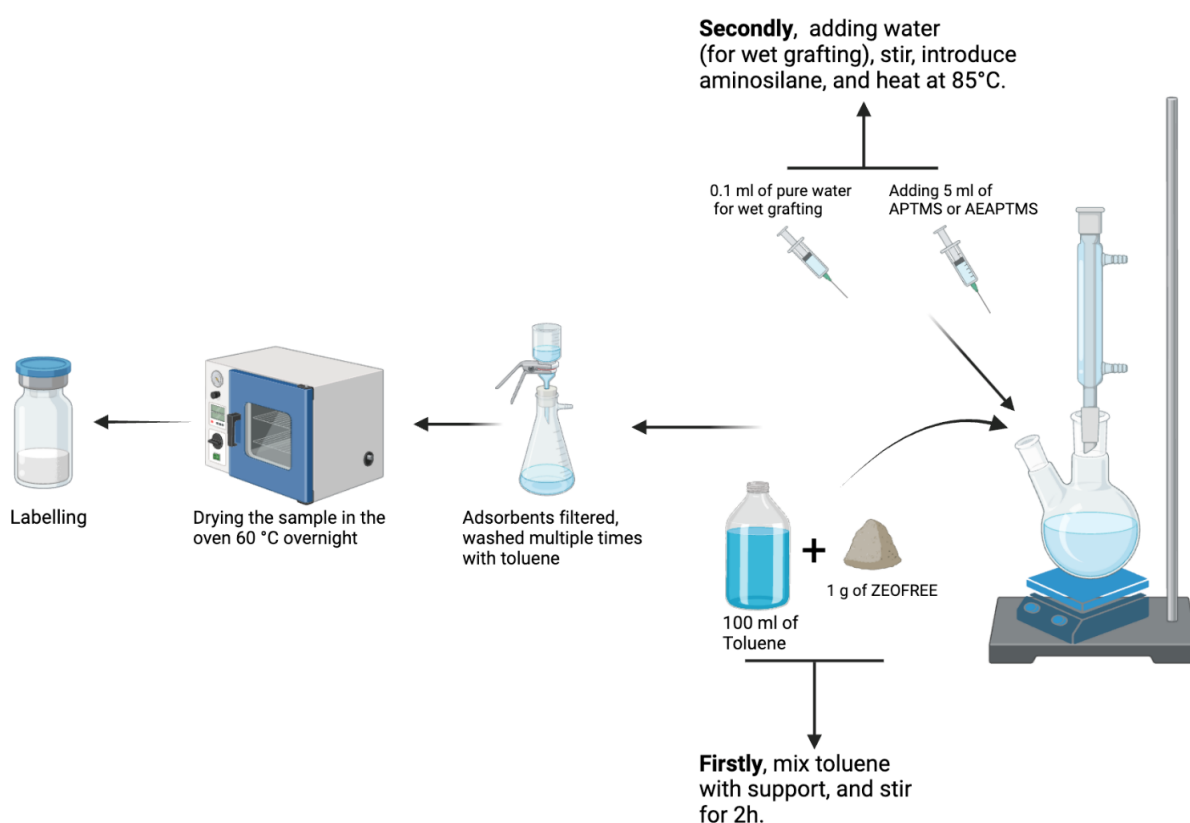


Figure 23 Synthesis of amine-grafting with ZEOFREE. (Created with BioRender.com)

Before each grafting experiment, the flask, filtration apparatus used for the experiments was thoroughly cleaned for each sample. This entailed washing the flask and other necessary equipment with a combination of HNO₃, water, and acetone.

6.2.1 Dry Grafting

The initial step for this method involves combining 100 mL of anhydrous toluene with 1 g of ZEOFREE in a flask. This mixture is stirred at room temperature for 2 hours. Depending on the specific experiment, either 5 mL of APTMS (amino propyl trimethoxy silane) (%97) or 5 mL of AEAPTMS 3-[2-(2-aminoethylamino) ethyl amino] propyl-trimethoxy silane is introduced. The mixture is then subjected to a temperature of 85°C for a duration of 6 hours. Post-reaction, grafted adsorbents material was filtered and washed multiple times with toluene, followed by drying in a vacuum oven at 60°C overnight.

Table 3 Comparative table of grafting experiments performed using ZEOFREE support.

Grafting type	Support Material and Amount	Amount of Toluene	Initial Mixing Time	Initial Mixing Temp.	Amount of water	Amino silane Type and Amount	Amino silane Mixing Time	Amino silane Mixing Temp.
Dry ZEO-1	1 g of ZEOFREE	100 mL	2 hours	Room temp.	-	5 mL APTES	6 hours	85°C
Wet ZEO-2	1 g of ZEOFREE	100 mL	2 hours	Room temp.	0.1 mL	5 mL APTES	6 hours	85°C
Undried support ZEO-3	1 g of ZEOFREE	100 mL	2 hours	Room temp.	-	5 mL APTES	6 hours	85°C
Dry ZEO-4	1 g of ZEOFREE	100 mL	2 hours	Room temp.	-	5 mL AEAPTMS	6 hours	85°C
Wet ZEO-5	1 g of ZEOFREE	100 mL	2 hours	Room temp.	0.1 mL	5 mL AEAPTMS	6 hours	85°C
Undried support ZEO-6	1 g of ZEOFREE	100 mL	2 hours	Room temp.	-	5 mL AEAPTMS	6 hours	85°C

6.2.2 Wet Grafting

For wet grafting, the procedure starts similarly by combining 100 mL of anhydrous toluene with 1 g of ZEOFREE support in a flask and stirring at room temperature for 2 hours. After the initial stirring, 0.1 mL of ultrapure water is added, and the mixture is stirred for an additional 3 hours. Depending on the specific experiment, either 5 mL of APTMS or 5 mL of AEAPTMS is introduced. Post-reaction, the grafted adsorbent material was filtered and washed multiple times with toluene, followed by drying in a vacuum oven at 60°C overnight.

6.3 Impregnation Method

6.3.1 Amine-Impregnated Adsorbents

Amine-functionalized adsorbents have been synthesized through a novel approach utilizing a high-speed shear mixing impregnation technique. In this process, a precisely measured amount of PEI, ZEOFREE, and/or Polyethylene glycol (PEG) are combined in a small cup. This mixture is then placed into a speed mixer device. The device is set to operate at a specific speed (up to 3000 rpm) and is allowed to spin for one minute. This method ensures a thorough and uniform distribution of the components, leading to the effective synthesis of the amine-functionalized adsorbents. Following high-speed shear mixing, the adsorbents were left to dry at 60°C throughout the night.

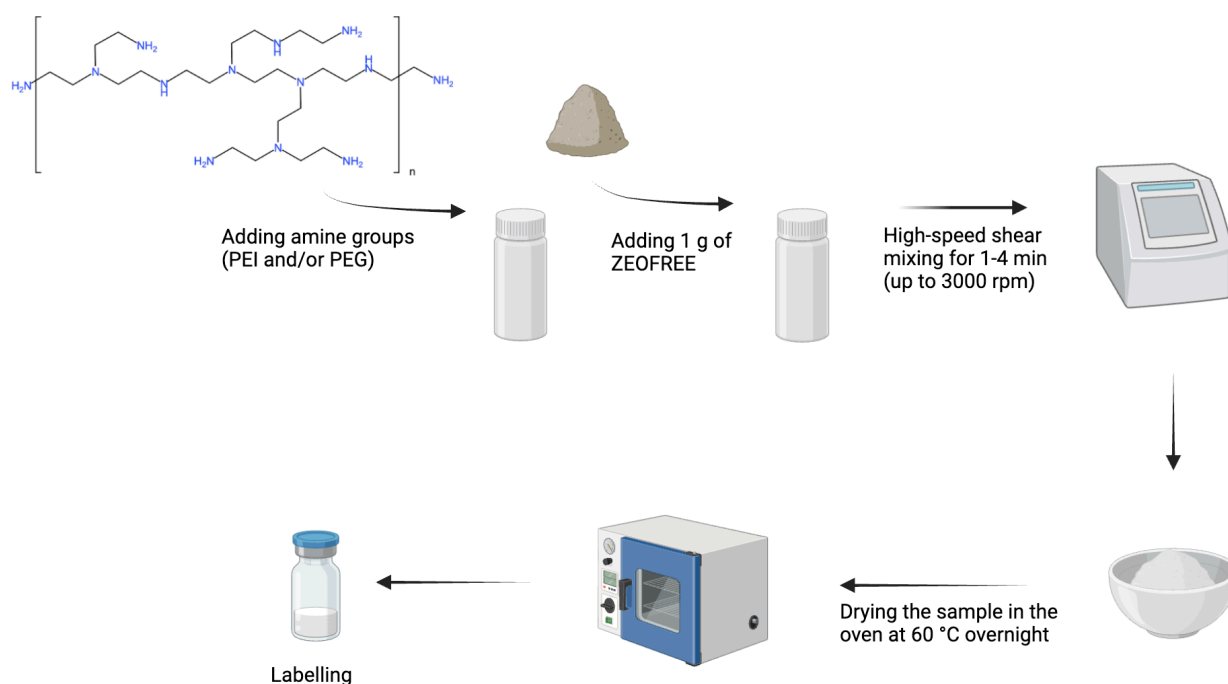


Figure 24 Synthesis of amine impregnating with ZEOFREE. (Created with BioRender.com)

6.3.2 Dry Impregnation

In the dry synthesis for amine-functionalized adsorbents, we developed several samples with distinct compositions. The first sample combined 1 gram of PEI (800 molecular weight) with 1 gram of ZEOFREE, undergoing two spins at 1000 and 3000 rpm, respectively, for effective homogenization. The second sample, slightly modified, included 0.95 gram of PEI (800 molecular weight), 1 gram of ZEOFREE, and 0.05 gram of PEG (20000 molecular weight), subjected to three spins at 1000, 2000, and 3000 rpm. This process included a manual mixing step after the second spin to ensure even distribution of components.

The third sample shifted focus to a higher molecular weight, PEI (25000), mixed with 1 gram of ZEOFREE, and followed a two-spin process at 1000 and 2000 rpm for homogenization. Lastly, the fourth sample mirrored the second but used PEI (25000 molecular weight), incorporating three spinning cycles at 1000, 2000, and 3000 rpm to achieve a uniformly functionalized material. This approach demonstrates the adsorbents' properties by adjusting the molecular weight of PEI and the inclusion of PEG.

Table 4 Comparative table of dry impregnation synthesis.

Dry Impregnation	ZEOFREE	PEI	PEG
PEI800_ZEO	1 gram	1 gram (800 molecular weight)	-
PEI800_ZEO_PEG	1 gram	0.95 gram (800 molecular weight)	0.05 gram (20000 molecular weight)
PEI25000_ZEO	1 gram	1 gram (25000 molecular weight)	-
PEI25000_ZEO_PEG	1 gram	0.95 gram (25000 molecular weight)	0.05 gram (20000 molecular weight)

6.3.3 Wet Impregnation

In the wet synthesis approach for amine-functionalized adsorbents, the unique aspect was the inherent moisture content of PEI, given its 50% water composition. Therefore, there was no need to add water additionally.

The first sample utilized 2 grams of PEI (2000 molecular weight) and 1 gram of ZEOFREE support, subjected to three spinning cycles at 1000, 1500, and 2000 rpm, ensuring thorough mixing and homogenization. For the second sample, the composition was slightly adjusted to include 1.95 grams of PEI (2000 molecular weight), 1 gram of ZEOFREE, and an addition of 0.05 gram of PEG (20000 molecular weight). This sample underwent a more intensive mixing process with four spins at speeds of 1000, 2000, 1500, and finally, 3000 rpm.

The third sample utilized 2 grams of PEI (750000 molecular weight), combined with 1 gram of ZEOFREE. It was spun twice, both times at 2000 rpm, to achieve effective functionalization. The final sample mirrored the second in terms of process but utilized PEI with a molecular weight of 750000 (1.95 grams), 1 gram of ZEOFREE, and the standard 0.05 gram of PEG (20000 molecular weight). This sample was spun four times at 1000, 1500, 2000, and 3000 rpm to ensure uniformity and effective adsorbent preparation.

Table 5 Comparative table of wet impregnation synthesis.

Wet Impregnation	ZEOFREE	PEI	PEG
PEI2000_ZEO	1 gram	2 grams (2000 molecular weight)	-
PEI2000_ZEO_PEG	1 gram	1.95 gram (2000 molecular weight)	0.05 gram (20000 molecular weight)
PEI750000_ZEO	1 gram	2 grams (750000 molecular weight)	-
PEI750000_ZEO_PEG	1 gram	1.95 gram (750000 molecular weight)	0.05 gram (20000 molecular weight)

This wet synthesis method capitalized on the water content within PEI to facilitate the adsorbent's functionalization, demonstrating the adsorbents' properties by adjusting the molecular weight of PEI and the inclusion of PEG.

6.4 Characterizations of Adsorbents

6.4.1 Scanning Electron Microscopy Measurements

Scanning Electron Microscopy (SEM) is crucial for analyzing the surface patterns of adsorbents at various levels. By providing a close-up view of the adsorbent's structure, SEM enables researchers to understand its morphology, topography, and composition, essential for optimizing its performance in CO₂ capture.

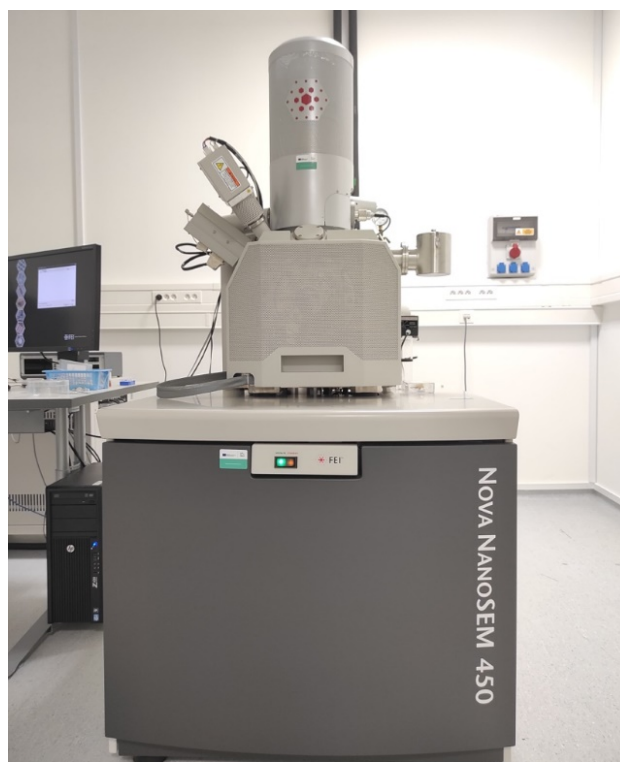


Figure 25 Scanning Electron Microscope (FEI, Nova NanoSEM 450)

The surface topographies of the adsorbents were recorded by scanning electron microscopy (SEM) using FEI Nova NanoSEM 450 at an accelerating voltage of 10 kV. Figure 31 and 32 illustrates SEM images for ZEO and PEI series. ZEO series including ZEOFREE pristine support material at 20 μm and 2 μm scales with magnifications of 5000x and 50000x, respectively, therewithal, for PEI series at 20 μm and 3 μm scales with magnifications of 5000x and 30000x, respectively.

6.4.2 Thermal Stability Measurements

TGA is a crucial technique for understanding the thermal stability, decomposition behavior, water evaporation, amine evaporation of adsorbents. By subjecting the adsorbent to a controlled temperature ramp in an inert atmosphere, TGA allows us to observe weight changes as a function of temperature. TGA enables adsorption-desorption experiments, providing insights into the adsorbent's behavior under different temperature conditions.

The thermal stabilities and organic content of the adsorbents were evaluated using thermogravimetric analysis (TGA) with a TGA Q500 Thermogravimetric Analyzer. The analysis was conducted from 30°C to 800°C at a rate of 10°C/min under a 50 mL/min N₂ flow in a platinum crucible. TA Instruments Universal Analysis 2000 software recorded weight loss versus temperature data and derivative weight. The results were analyzed in the software, peaks and weight losses were calculated based on the graphs conducted from the software.

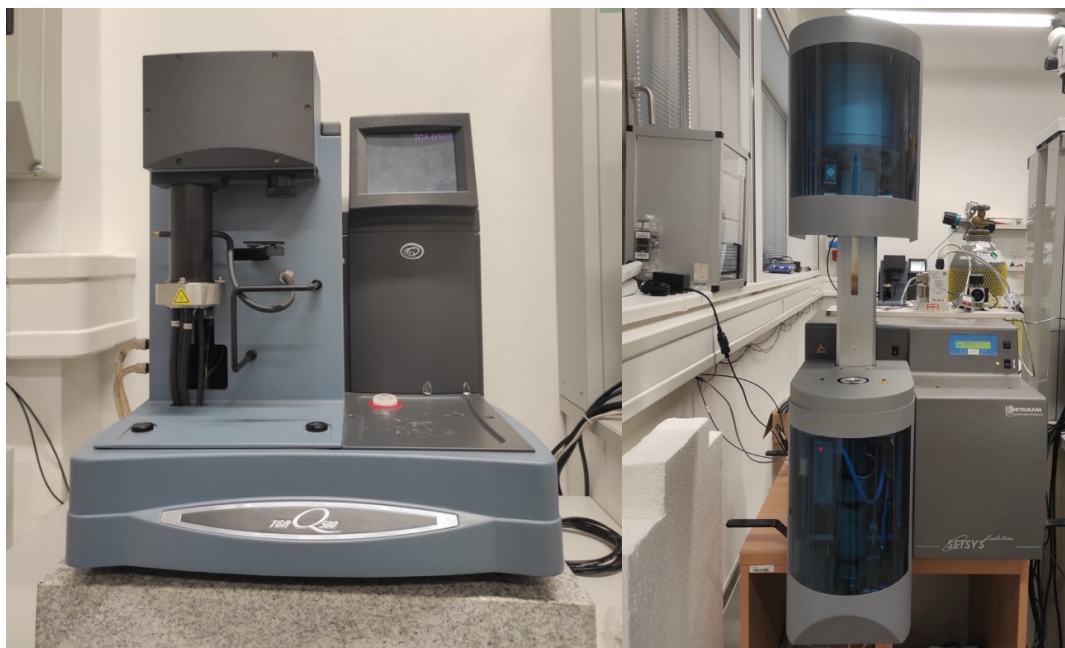


Figure 26 Thermo-gravimetric analyzer (TGA Q500 Thermogravimetric Analyzer) (left) and SETARAM Scientific & Industrial Equipment (SETSYS Evolution) TGA (right)

6.4.3 Specific Surface Area Evaluation

Brunauer-Emmett-Teller (BET) analysis is essential for determining the specific surface area of adsorbents, which is crucial for understanding their CO₂ capture efficiency. BET analysis utilizes nitrogen gas adsorption to measure the surface area of the adsorbent material. By providing precise information about the surface area, BET analysis helps optimize the adsorbent's performance and efficiency in CO₂ capture applications.

The surface area of the support material ZEOFREE, and synthesized adsorbents were determined through nitrogen-adsorption/desorption isothermal measurements at 77 K with Brunauer-Emmett-Teller (BET) using BELSORP-mini II Analyzer. All samples including support material ZEOFREE were degassed under vacuum for 4 hours at 80 °C. N₂ adsorption-desorption isotherms were collected at – 196 °C, surface area and pore volume were calculated from the isotherm data using the Brunauer-Emmett-Teller.

6.4.4 Fourier Transform Infrared Spectroscopy (FTIR) Measurements

Fourier Transform Infrared Spectroscopy (FTIR) is a powerful technique for analyzing the chemical composition and surface functional groups of adsorbents. By examining the adsorbent's infrared absorption spectrum, FTIR provides valuable insights into the types of chemical bonds present on the surface. With FTIR, we can determine whether CO₂ is bonded to the adsorbents, identify grafting agents on the surface, and analyze various functional groups, providing crucial information for optimizing the adsorbent's performance in CO₂ capture applications.

The chemical groups of the adsorbents were determined by Fourier transform infrared spectroscopy (FTIR) using an infrared spectrometer NICOLET 6700 FT-IR, Thermo Scientific in the range of wavenumber from 4000 to 400 cm^{-1} during 64 scans, with 4 cm^{-1} resolution. The materials were mounted directly in the sample holder and data was collected after scanning the background.



Figure 27 Brunauer-Emmett-Teller (BET) BELSORP-mini II Analyzer (left) and Fourier Transform Infrared Spectroscopy (FTIR) NICOLET 6700 FT-IR, Thermo Scientific (right)

6.4.5 Elemental Analysis Measurement

Elemental analyzers are essential tools, designed to accurately determine the composition of various materials by measuring elements like carbon, hydrogen, nitrogen, and sulfur. The contents of carbon (C), hydrogen (H), nitrogen (N), and Sulphur (S) in the adsorbents also including amino silanes, PEI, PEG, and pristine support ZEOFREE were measured by Elemental Analyzer using Flash 2000 CHNS/O+MAS200R, Thermo Scientific.

The samples, weighing approx. 2-3 mg, were placed into an aluminum cup and weighed three times on an analytical balance. After weighing, the crucible was packed to remove all air, weighed again, and the value was recorded in the FLASH CHNS program. The sample was transferred to the dispenser of the device, where a blank sample (blank – empty cup) was first inserted, two bypasses

(selected standard 1-3 mg) - for internal calibration of the device and calibration standards (three different amounts of a suitable standard), where they are represented in precisely defined quantities of all analyzed elements. The samples were then inserted into the autosampler in the correct order, in which they were also marked in the instrument software. FLASH and analysis and subsequent evaluation of individual amounts (mass percentages) of each analyzed element in the sample took place. Due to the large number of samples each sample was analyzed 3 times, the analysis was performed in two parts, each time together with the selected methionine standard (Table 9).



Figure 28 Flash Analyzer CHNS / O + MAS200R, Thermo Scientific

For set of ZEO series, amine loading was quantified as the millimoles of nitrogen (N) per gram of the adsorbent, determined through elemental analysis. Similarly, amine efficiency was evaluated as the millimoles of CO₂ adsorbed per millimole of nitrogen.

6.4.6 Adsorption Desorption Measurements in 10% CO₂ Environment

The CO₂ adsorption and desorption cycles for all adsorbents, including pristine ZEOFREE support, were conducted using a TGA Q500 Thermogravimetric Analyzer. The procedure began with a nitrogen equilibration step to ensure system stability. Samples were initially equilibrated under a nitrogen atmosphere at 30°C for 10 minutes. The temperature was then raised to 90°C at a rate of 10°C/min, followed by a 30-minute isothermal hold to stabilize the sample environment. Subsequently, the temperature was decreased to 30°C at the same rate, with an additional 30-minute isothermal period to prepare for the first adsorption cycle. Upon completion of the nitrogen step, the system's atmosphere was switched to 10 % of CO₂ with a flow rate of 14 mL/min. The samples were maintained isothermally at 30°C for 20 minutes to enable the first adsorption of CO₂. This step marks the transition from nitrogen to CO₂ atmosphere, capturing the initial adsorption behavior of the samples.

Following the first adsorption phase, the gas flow was reverted to nitrogen at a rate of 10 mL/min, and the temperature was once again raised to 90°C at a rate of 10°C/min. Another isothermal hold at 90°C for 30 minutes ensured the thorough desorption of CO₂ from the samples. The temperature was then decreased back to 30°C at the same rate, with a subsequent 30-minute isothermal period to prepare for the next adsorption cycle.

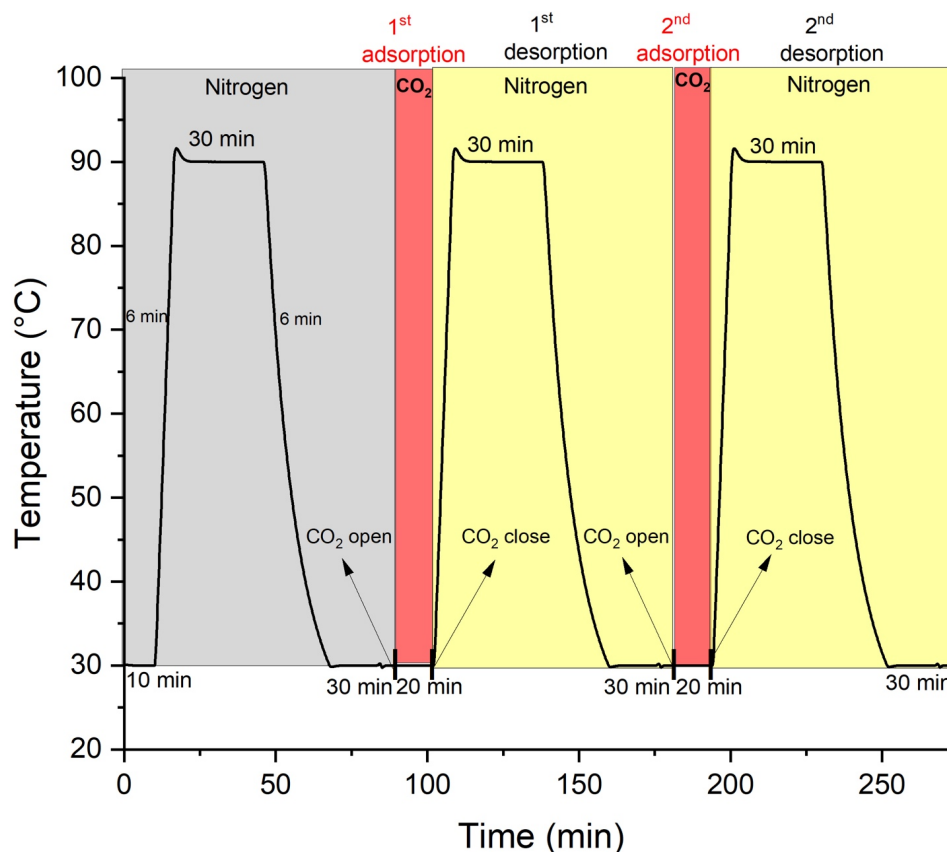


Figure 29 Representation of adsorption-desorption cycles by temperature profile in 10% CO₂ environment.

This sequence—comprising temperature ramping, isothermal holds under nitrogen, and CO₂ exposure for adsorption, followed by nitrogen purging for desorption—was repeated for a total of 20 cycles. This rigorous procedure aimed to assess the adsorption-desorption repeatability and stability of the adsorbents under 10% of CO₂ conditions.

Each adsorption and desorption step were carefully timed and temperature-controlled to ensure accurate data collection and reproducibility. Figure 29 illustrates the temperature profile and gas switching timeline, providing a visual representation of the experimental conditions and the cyclic nature of the adsorption-desorption process.

6.4.7 Adsorption Desorption Measurements in 400 ppm CO₂ Environment

The CO₂ adsorption desorption cycles in a 400 ppm CO₂ environment were conducted for all adsorbents and pristine ZEOFREE, using a SETARAM Scientific & Industrial Equipment (SETSYS Evolution) TGA.

The procedure began with a preliminary nitrogen step to ensure system equilibrium. Initially, the samples were equilibrated under a nitrogen atmosphere at 30°C for 90 minutes. The temperature was then gradually raised to 90°C at a rate of 10°C/min, followed by a 60-minute isothermal hold to stabilize the sample environment. Subsequently, the temperature was lowered back to 30°C at the same rate, with an additional 60-minute isothermal period to prepare for the single adsorption cycle.

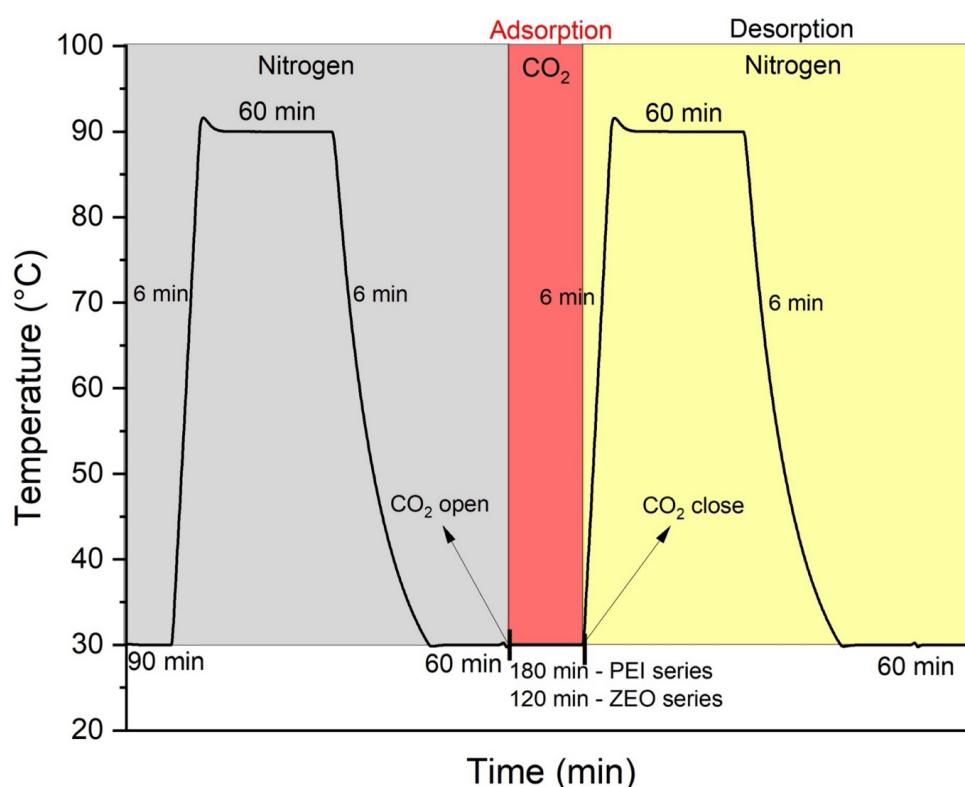


Figure 30 Representation of adsorption desorption cycle by temperature profile in 400 ppm CO₂ environment.

Upon completion of the nitrogen step, the system's atmosphere was switched to 400 ppm CO₂. The samples were maintained isothermally at 30°C for 180 minutes for the PEI series and 120 minutes for the ZEO series to facilitate CO₂ adsorption. After the single adsorption phase, the gas flow was switched back to nitrogen, and the temperature was once again raised to 90°C at a rate of 10°C/min. A 60-minute isothermal hold at 90°C ensured thorough desorption of CO₂ from the samples. The temperature was then lowered back to 30°C at the same rate, followed by another 60-minute isothermal period to complete the cycle.

7. RESULTS AND DISCUSSION

7.1 Surface Morphology Analysis (SEM) of Adsorbents

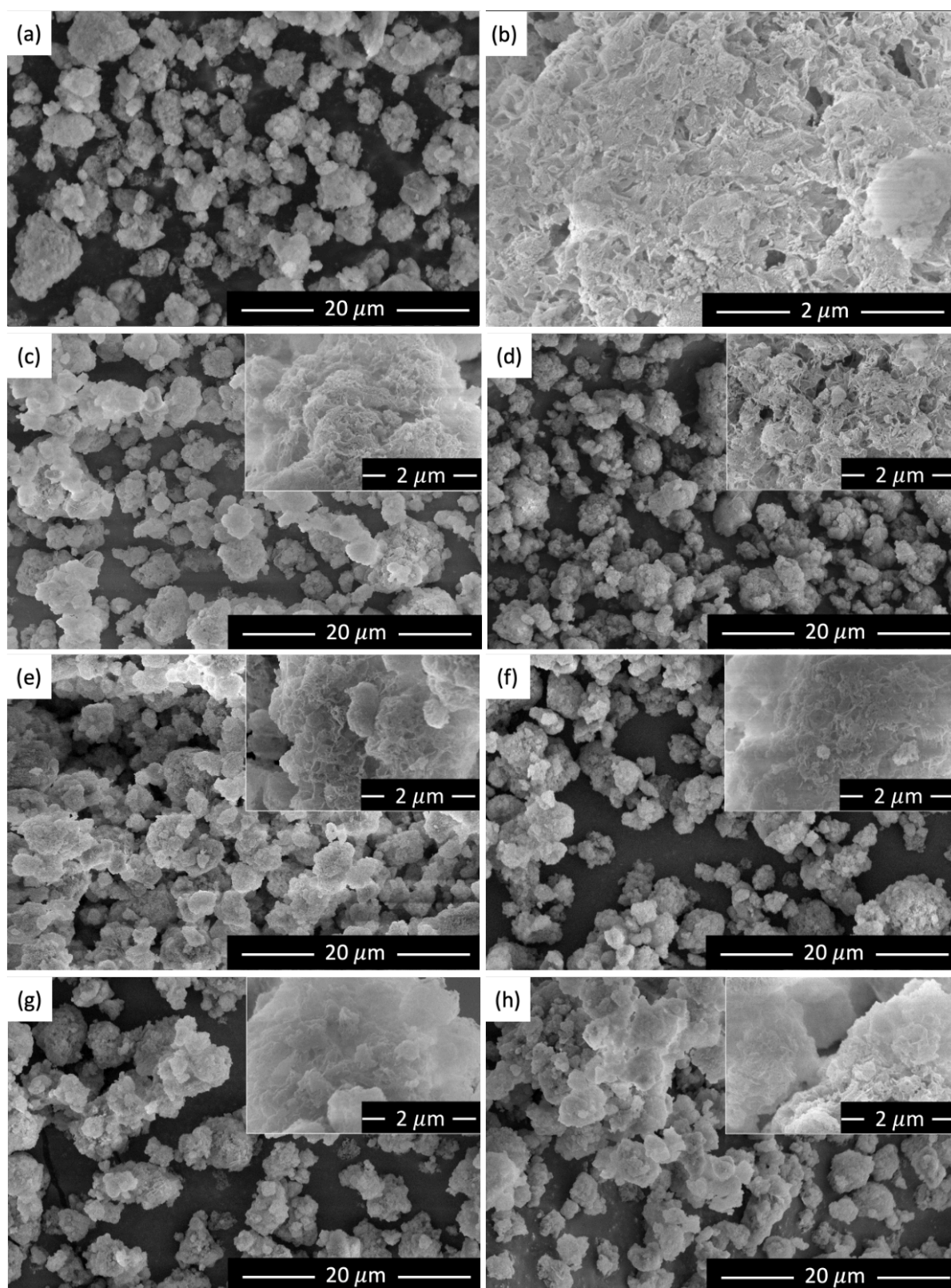


Figure 31 SEM images of ZEOFREE and ZEO series. a) and b) ZEOFREE c) ZEO-1 d) ZEO-2 e) ZEO-3 f) ZEO-4 g) ZEO-5 and h) ZEO-6.

Figure 31 SEM images offer a comparative study of ZEO support before and after silane grafting. The ungrafted ZEOFREE (Image a and b) displays a collection of particles with relatively smooth surfaces and homogenous morphology, providing a baseline for evaluating the effects of grafting.

Upon grafting with APTMS (Images c, d, e) and AEAPTMS (Images f, g, h), the ZEO particles retain their distinct shapes but show subtle textural changes. The magnified insets reveal a fine, granular coating on the particles, suggesting the presence of the grafting agent. This fine layer likely represents the initial stage of surface modification, where the APTMS or AEAPTMS molecules adhere to and slightly alter the original smoothness of the ZEO surface.

Based on the SEM images presented in Figure 32, it is evident that the morphology of the PEI-based adsorbents varies depending on the molecular weight of the PEI used in their synthesis. Samples PEI800_ZEO, PEI800_PEG_ZEO, PEI2000_ZEO, and PEI2000_PEG_ZEO exhibit bulkier particles with a more aggregated appearance. Conversely, PEI25000_ZEO, PEI25000_PEG_ZEO, PEI750000_ZEO, and PEI750000_PEG_ZEO display smaller particles without noticeable agglomeration, resulting in a powderier appearance.

This trend suggests that adsorbents synthesized with lower molecular weight PEI tend to have bulkier, more rounded, and more aggregated particles, whereas those synthesized with higher molecular weight PEIs display smaller, more dispersed particles without noticeable lump formations. Therefore, it can be concluded that the molecular weight of PEI influences the morphology of the resulting adsorbents.

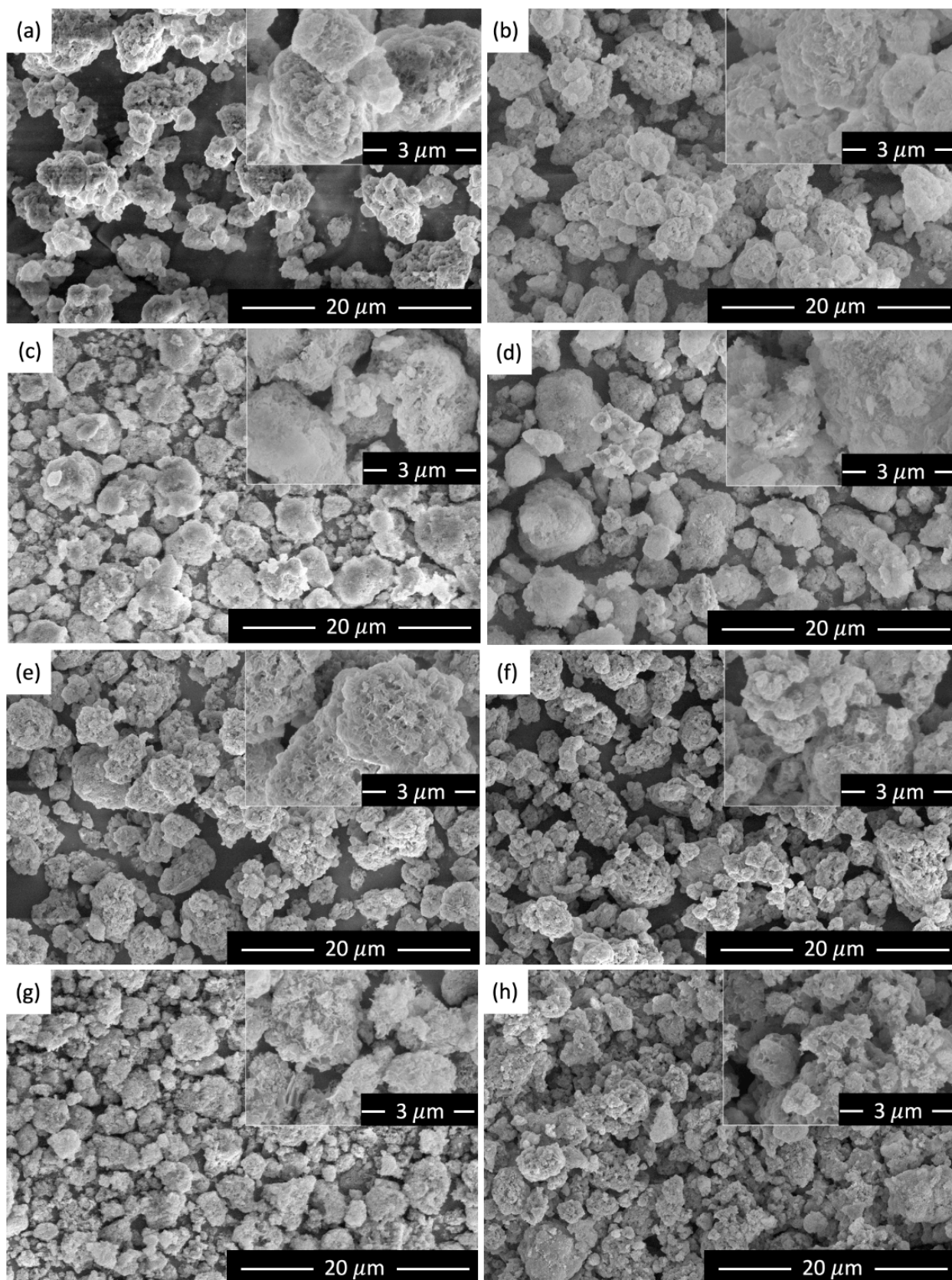


Figure 32 SEM images of PEI series. a) PEI800_ZEO b) PEI800_PEG_ZEO c) PEI25000_ZEO d) PEI25000_PEG_ZEO e) PEI2000_ZEO f) PEI2000_PEG_ZEO g) PEI750000_ZEO and h) PEI750000_PEG_ZEO

7.2 Thermal Stability and Organic Content Determination of Amine-Grafted Adsorbents

Figure 33 presents an in-depth analysis of the thermal stability for both pristine ZEOFREE and ZEOFREE support grafted with amino silanes. The associated Table 6 complements this analysis by quantifying the water loss and detailing the overall weight loss alongside the estimated loss in organic content. This loss in organic content is discerned by deducting the total weight loss of pristine ZEOFREE—water loss excluded—from that of the total weight loss of the grafted adsorbents.

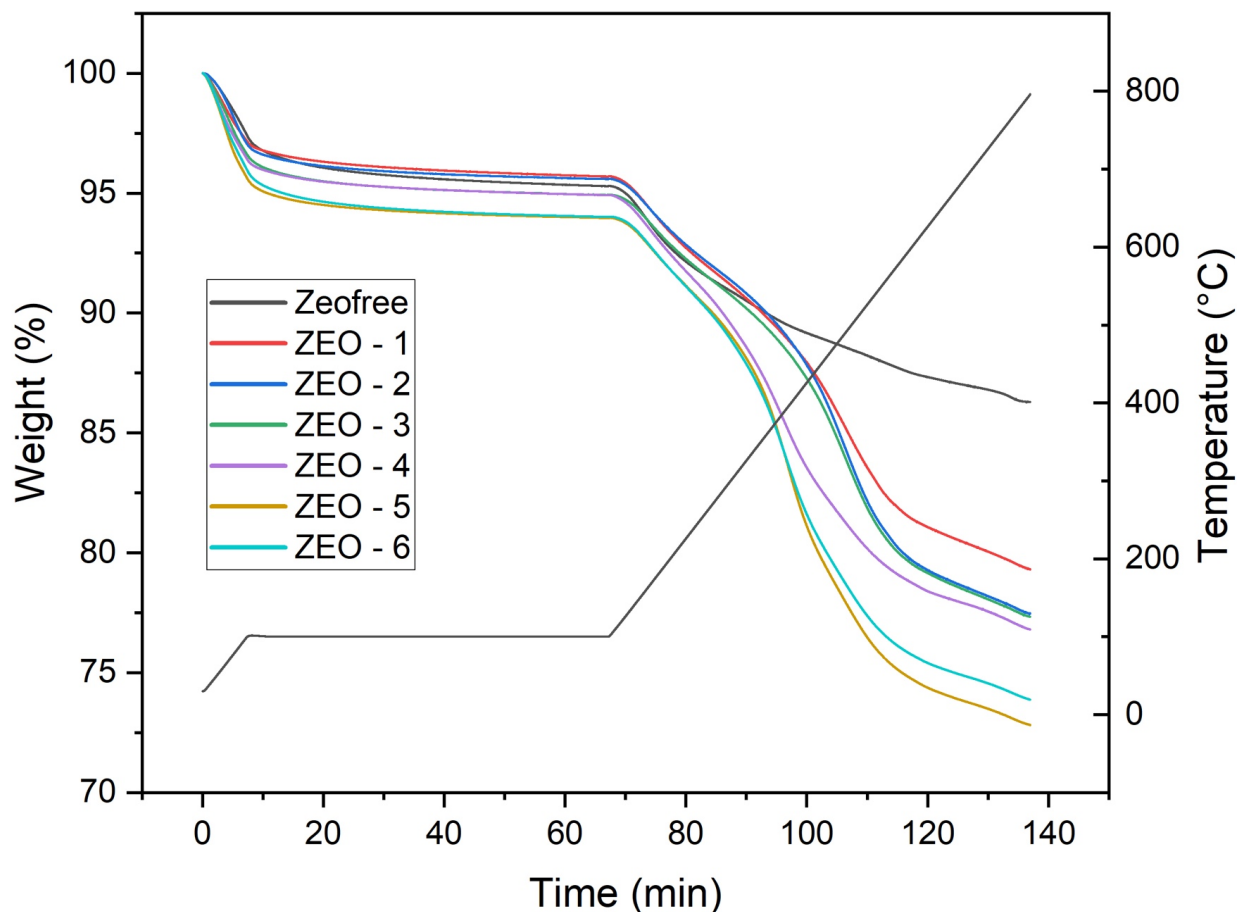


Figure 33 Thermal stability curves of ZEO series including ZEOFREE support.

The thermal stability graph indicating notable weight loss primarily during water evaporation, amine evaporation and at the decomposition stage. This was anticipated since ZEO-1 and ZEO-4 were synthesized under dry conditions, thus registering the lowest water content. In contrast, adsorbents synthesized in wet conditions (ZEO-2, ZEO-5) and adsorbents synthesized with undried support (ZEO-3, ZEO-6) manifested the expected higher water content levels.

ZEOFREE, serving as the support material, exhibits stable thermal properties up to temperatures between 157-200°C, where it undergoes an 8.98% weight loss due to water evaporation.

Subsequently, the material maintains relative stability, albeit with a slight ongoing weight loss, until reaching 766.41°C. At this point, it experiences an additional 4.93% weight loss, indicating the material decomposition.

Table 6 Corresponding table detailing water loss and overall weight loss as well as estimated organic content.

Sample name	Water content (%)	Organic content (%)	Total Weight loss (%)
ZEOFREE	8.98	N/A	13.64
ZEO – 1	8.93	11.53	20.46
ZEO – 2	9.33	13.12	22.45
ZEO – 3	9.02	13.40	22.42
ZEO – 4	7.85	15.03	22.88
ZEO – 5	9.11	17.72	26.83
ZEO – 6	9.06	16.72	25.78

ZEO-1, ZEO-2, ZEO-3 samples demonstrate significant weight loss between 485-495°C, which can be attributed to the amine evaporation of the APTMS grafting agent. ZEO-4, ZEO-5, ZEO-6, exhibit significant weight loss at slightly lower temperatures 385-395°C, indicating an earlier amine evaporation stage for the AEAPTMS grafting agent compared to APTMS. ZEO-5 and ZEO-6 show the highest organic content, suggesting a more effective grafting process of AEAPTMS, which has a larger molecular structure due to the additional aminoethyl group. Additionally, after water and amine evaporation, decomposition of ZEOFREE support in the adsorbents are observed at temperatures around 775-778 °C.

7.3 Thermal Stability and Organic Content Determination of Amine-Impregnated Adsorbents

Figures 34 and 35 illustrate thermal behavior of the adsorbents, ZEOFREE, and the difference between adsorbents modified with PEI and those modified with PEI including the addition of PEG.

The thermal gravimetric (TG) curve of the ZEOFREE support material showed a total weight loss of 13.64% from 30°C to 800°C, significantly lower than that of the PEI based amine-modified adsorbents. These results further confirm the successful loading of amine.

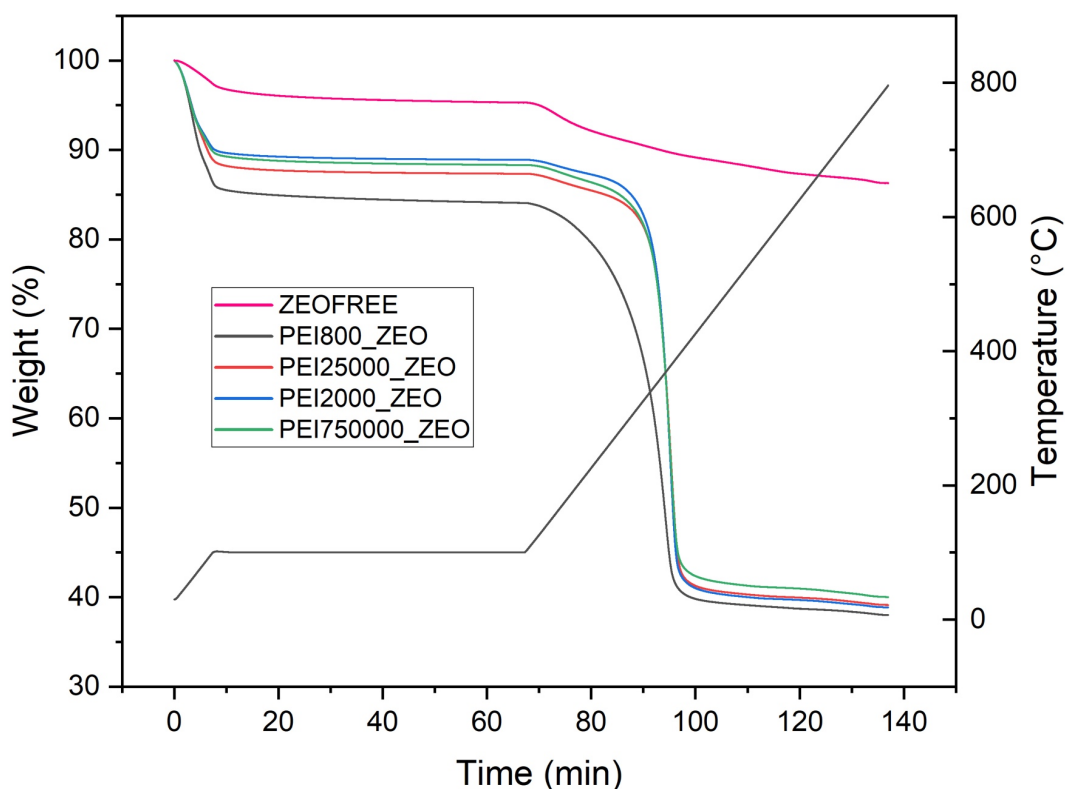


Figure 34 Thermal stability of PEI-based adsorbents without addition of PEG including ZEOFREE.

In Figures 34 and 35, the weight loss is observed in two stages, spanning from 30°C to 800°C. The first stage involves the desorption of adsorbate, including absorbed water, CO₂, and other compounds, occurring between 30°C and 150°C. This slow adsorbent activity in ambient air leads to a reversible loss of adsorption capacity, which can be mitigated by proper storage and degassing before use.

The second stage involves PEI evaporation and decomposition, occurring at temperatures between 200°C and 500°C. At this stage, the weight loss corresponds closely to the PEI loading.

For instance, theoretically PEI loading was 50% wt. for PEI800_ZEO, PEI25000_ZEO, PEI2000_ZEO, PEI750000_ZEO while it was 47.5% wt. for PEI800_PEG_ZEO, PEI25000_PEG_ZEO, PEI2000_PEG_ZEO and PEI750000_PEG_ZEO. This 47.5% amine loading was because of additional 2.5% wt. of PEG loading.

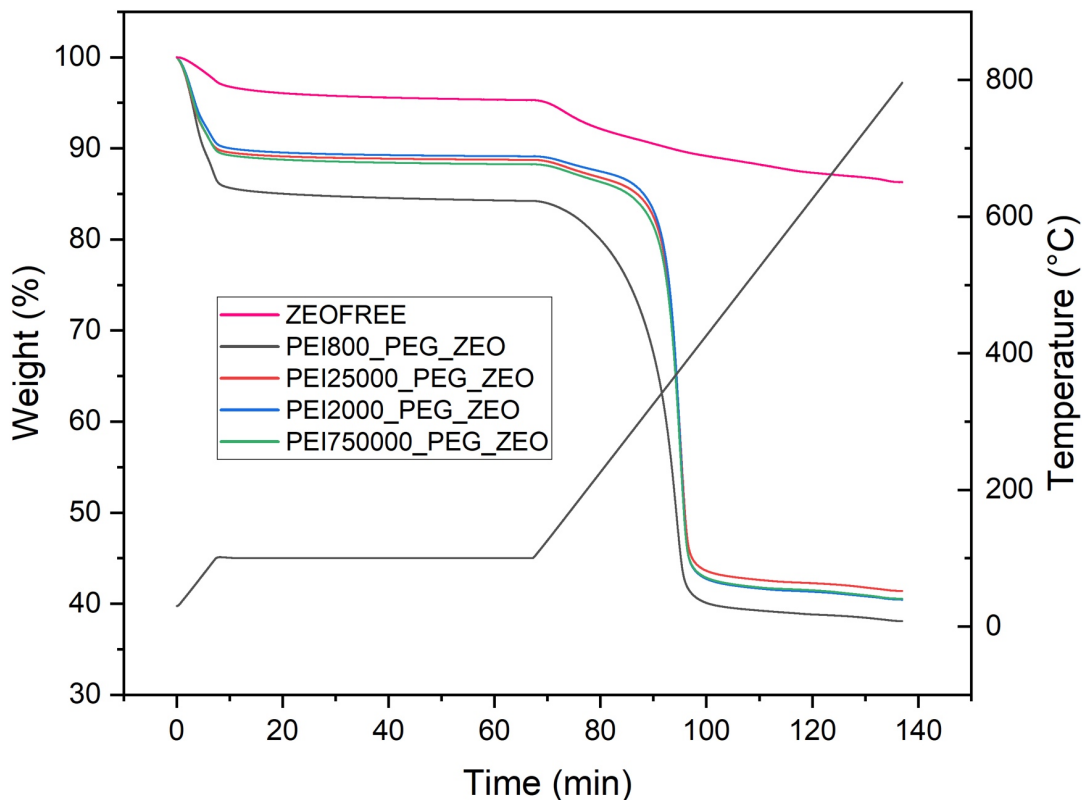


Figure 35 Thermal stability of PEI-based adsorbents with addition of PEG including ZEOFREE.

Adsorbents synthesized with lower molecular weight of PEI showed higher amine loading. The little rest of the loading might have been lost during synthesis, particularly in cases where PEI mixing with the support was required for better/manual homogenization. The adsorbents with the lowest actual amine loading appeared to be PEI750000_ZEO with 45.7% wt. while the highest actual amine loading appeared to be PEI800_PEG_ZEO with 47.07% wt.

Addition of PEG resulted in approximately 2% less total weight loss in TGA curves and calculations as well as adsorbents synthesized with addition of PEG showed higher amine loading across all samples.

Furthermore, the PEI loaded onto shallow and deep pores evaporates and decomposes at different temperatures. This leads to irreversible loss of adsorption capacity, necessitating that the temperature during CO₂ capture applications be limited to below 200°C.

Table 7 Actual amine loading and total weight loss of PEI series.

Adsorbents	Organic content (actual amine loading) (%)	Total weight loss (%)
PEI800_ZEO	47.34	60.98
PEI800_PEG_ZEO	47.07	60.71
PEI25000_ZEO	46.11	59.75
PEI25000_PEG_ZEO	43.77	57.41
PEI2000_ZEO	46.38	60.02
PEI2000_PEG_ZEO	44.95	58.59
PEI750000_ZEO	45.76	59.40
PEI750000_PEG_ZEO	45.32	58.96

7.4 Surface Area and Porosity Determination (BET) of Adsorbents

The surface area, total pore volume, and pore diameter of ZEOFREE were found to be 168 m²/g, 1.34 cm³/g, and 31.85 nm, respectively. After grafting with APTMS, a reduction in surface area and total pore volume was observed, accompanied by an increase in pore diameter.

Wet grafting synthesis of the adsorbents further decreased the surface area and total pore volume while increasing the pore diameter. Upon inoculation with AEAPTMS, a more significant decrease in surface area and total pore volume was observed compared to APTMS grafting. Similarly, the pore diameter increased more prominently after inoculation with AEAPTMS.

Textural properties of PEI-based adsorbents dramatically decreased upon inclusion different molecular weight of PEI. Adsorbents prepared using high molecular weight PEI exhibited a higher surface area compared to those prepared with low molecular weight PEI.

For instance, the addition of PEG increased the surface area of PEI800_ZEO from 12.84 m²/g to 19.93 m²/g, with a corresponding increase in pore diameter from 52.90 nm to 59.51 nm. Conversely, the addition of PEG reduced the surface area of PEI750000_ZEO from 21.94 m²/g to 17.85 m²/g PEI750000_PEG_ZEO. Also, adsorbents synthesized with low molecular weight PEIs generally exhibited higher pore diameters compared to those synthesized with high molecular weight PEIs which leads to increase in CO₂ adsorption capacity.

Table 8 Surface area, pore diameter and total pore volume of all samples including ZEOFREE support.

Adsorbents	Surface area (BET), m^2/g	Pore diameter, nm	Total pore volume ($p/p_0 = 0,990$) cm^3/g
ZEOFREE	168.80	31.853	1.3442
ZEO-1	108.38	40.655	1.1015
ZEO-2	93.823	40.637	0.9532
ZEO-3	94.011	40.838	0.9598
ZEO-4	101.95	43.073	1.0979
ZEO-5	83.829	50.085	1.0496
ZEO-6	90.041	50.886	1.1455
PEI800_ZEO	12.843	52.906	0.1699
PEI800_PEG_ZEO	19.935	59.515	0.2966
PEI25000_ZEO	32.975	52.777	0.4351
PEI25000_PEG_ZEO	33.648	50.907	0.4282
PEI2000_ZEO	14.360	57.290	0.2057
PEI2000_PEG_ZEO	14.455	60.841	0.2199
PEI750000_ZEO	21.942	53.281	0.2923
PEI750000_PEG_ZEO	17.858	53.779	0.2401

7.5 Chemical Characterization (FTIR) of Amine-Grafted Adsorbents

The ungrafted ZEOFREE spectrum serves as a baseline, highlighting the inherent functional groups or bonding within the material itself. The peaks at 1076 cm^{-1} , and 970 cm^{-1} , across all grafted samples, indicative of Si-O-Si asymmetric stretching and Si-OH bending, respectively. The peak around 1477 cm^{-1} , potentially associated with N-H bending vibrations, signifies the presence of aminopropyl and aminoethylamino groups.

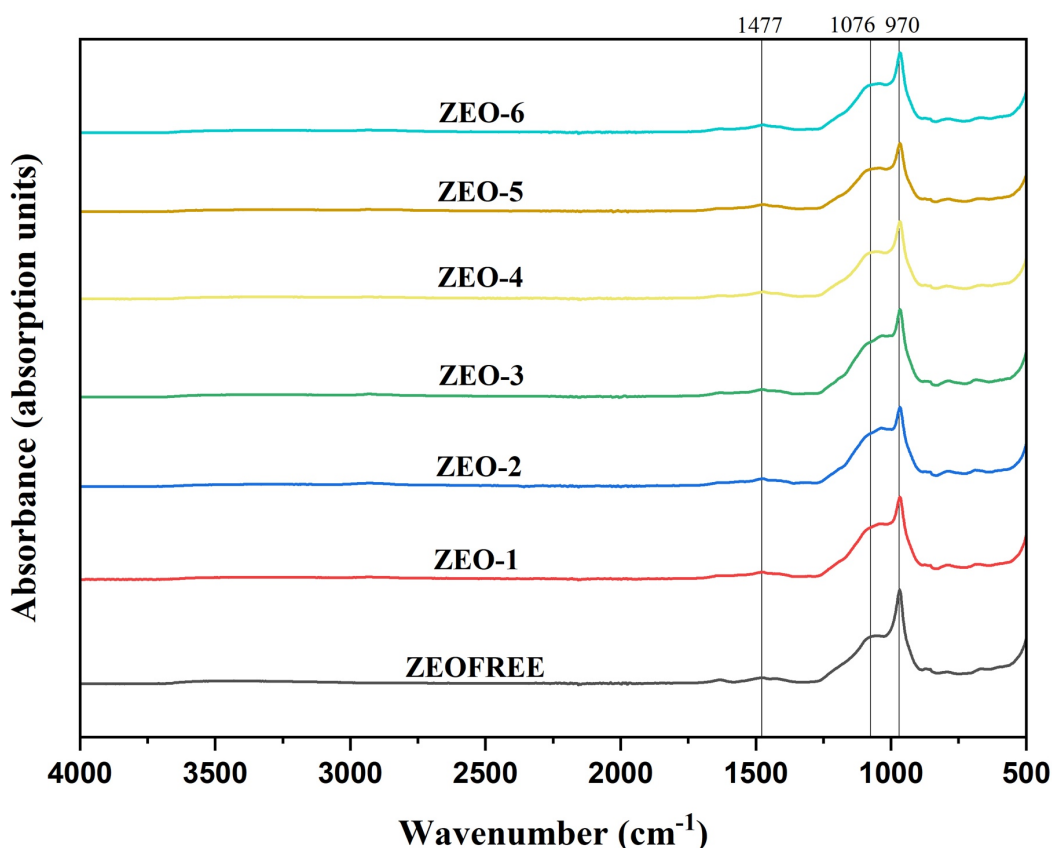


Figure 36 FTIR spectra of ZEO series including ZEOFREE support.

A comparative analysis of the peak intensities from ZEO-1 to ZEO-6 against the ungrafted ZEOFREE spectrum reveals a progressive increase, indicating an incremental amount of grafting. Notably, the intensity of these peaks is higher in ZEO-4 to ZEO-6 than in ZEO-1 to ZEO-3, implying a higher degree of grafting or more effective attachment of the silane molecules, possibly due to the different chemical structure of the aminosilane which is AEAPTMS used in ZEO-4 to ZEO-6, which may lead to stronger interactions or more efficient bonding with the ZEOFREE support.

7.6 Chemical Characterization (FTIR) of Amine-Impregnated Adsorbents

The peaks observed at 3364 and 3288 cm^{-1} in PEI800 and PEI25000 are attributed to N-H and N-H₂ stretching vibrations, respectively. Similar peaks are also observed in PEI2000 and PEI750000, but they appear as broad absorption bands, indicating O-H stretching vibrations due to inherent water. The peak at 1453 cm^{-1} is attributed to C-H deformations, while the peaks at 2950 and 2823 cm^{-1} are attributed to C-H₂ stretching vibrations. Additionally, the peak at 1477 cm^{-1} is attributed to N-H vibrations.

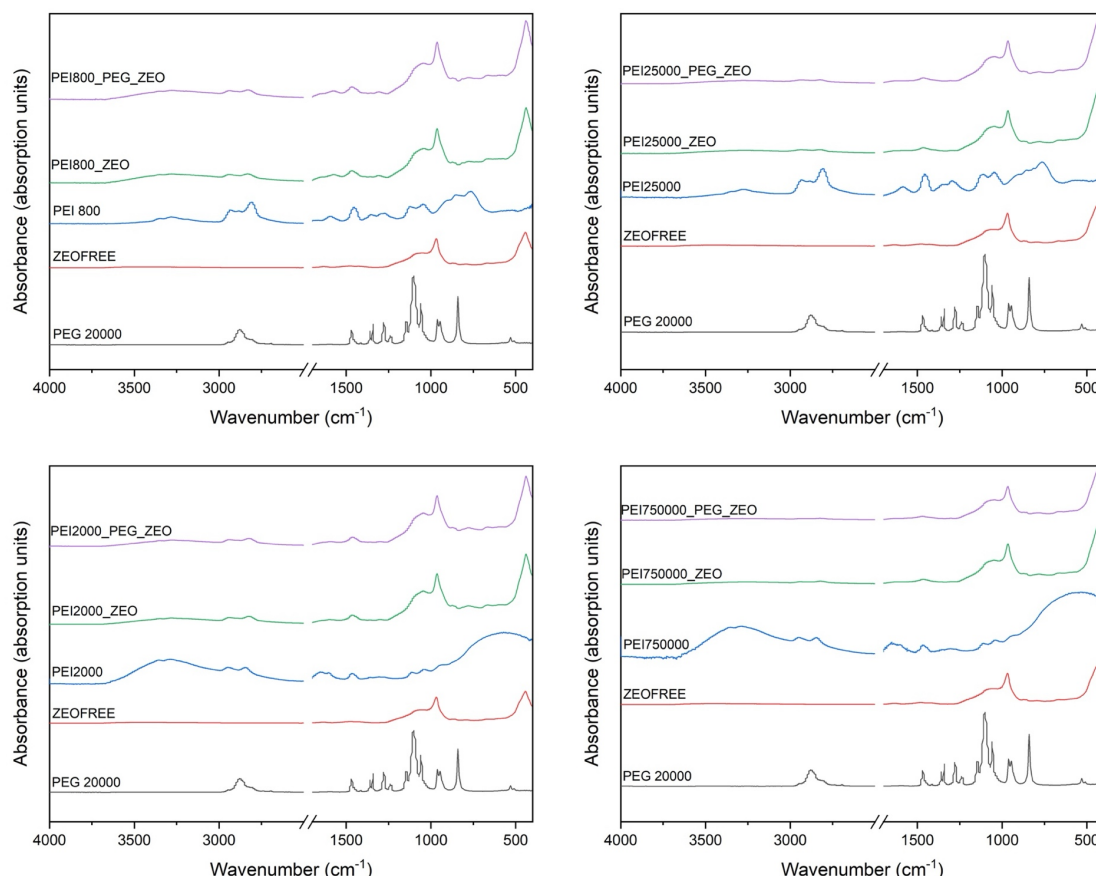


Figure 37 FTIR spectra of PEI series and pristine PEIs as well as PEG and ZEOFREE support.

After the surface modification of ZEOFREE with different molecular weights of PEI, as well as PEI containing inherent water, a series of new bands appeared. This indicates that the ZEOFREE sorbent has been impregnated with PEI. The peaks observed in the pristine PEIs also appear in the adsorbents. It is evident that PEI2000_ZEO, PEI2000_PEG_ZEO, PEI750000_ZEO, and PEI750000_PEG_ZEO adsorbents contain OH, N-H, and CH₂ groups, which can contribute to better cyclic stability. Since the peaks in PEI800_ZEO, PEI800_PEG_ZEO, PEI2000_ZEO, and PEI2000_PEG_ZEO are more pronounced, it is expected that their adsorption capacity will be higher based on the amine-CO₂ interaction.

7.7 Elemental Analysis of Adsorbents

Table 9 shows the analyzed values of nitrogen, carbon, hydrogen, and sulfur in mass % (m/m). Each sample was analyzed 3 times. For this, values show average results of samples. The LOD (limit of detection) is below 0.5% for FLASH analysis; amounts below 0.05% are evaluated by the method as undetectable.

All samples show no sulfur, indicating that the sulfur element in these samples is either absent or below the detection limit. For other elements, there's a variation across samples, APTMS, with its functional amine group, demonstrated a notable nitrogen presence, aligning with its expected chemical composition. In contrast, AEAPTMS displayed a higher nitrogen content due to its additional aminoethyl group. Also, ZEO-4 shows the highest nitrogen content and ZEO-5 shows the highest carbon and hydrogen content among the ZEOFREE based sorbents.

Among the different molecular weights of pristine PEIs tested, PEI with 25000 molecular weight exhibited the highest nitrogen (N) and carbon (C) content, with percentages of 30.07% and 62.24% respectively. On the other hand, PEI 800 displayed the highest hydrogen (H) content at 9.92%.

We also examined the effect of adding polyethylene glycol (PEG) to the PEI-based adsorbents. While the addition of PEG showed little variability in the N, H, and C values of other adsorbents, a significant increase in nitrogen content was observed when comparing PEI800_ZEO and PEI800_PEG_ZEO. Specifically, the addition of PEG increased the nitrogen content from 15.10% to 23.79%.

Additionally, PEI800_PEG_ZEO adsorbent exhibited the highest nitrogen and hydrogen content at 23.79% and 6.82% respectively. On the other hand, PEI25000_PEG_ZEO displayed the highest carbon content at 29.20%.

Table 9 Determination of C, H, N, (S) content in Diatoms (DE) and ZEOFREE based sorbents and samples using the FLASH method. Values given in weight percent % (m/m), methionine (C 5 H 11 NO 2 S) standard used.

Samples and Chemicals	N (%)	C (%)	H (%)	S (%)
Methionine	9,39	40,25	7,42	21,5
APTMS	9,25	22,03	4,65	-
AEAPTMS	36,44	4,52	7,46	-
ZEOFREE	3,39	0,87	0,84	-
ZEO-1	5,09	7,87	1,68	-
ZEO-2	5,26	9,59	1,53	-
ZEO-3	7,36	9,44	1,7	-
ZEO-4	18,92	7,86	1,34	-
ZEO-5	5,03	10,4	2,36	-
ZEO-6	11,91	8,94	1,16	-
PEG 20000	7,06	52,02	11,96	-
PEI 800	28,55	52,28	9,92	-
PEI 25000	30,07	62,14	7,56	-
PEI 2000	18,27	28,75	6,48	-
PEI 750000	20,81	31,87	7,34	-
PEI800_ZEO	15,10	24,10	5,78	-
PEI800_PEG_ZEO	23,79	25,52	6,82	-
PEI25000_ZEO	14,63	28,04	3,94	-
PEI25000_PEG_ZEO	15,49	29,20	3,40	-
PEI2000_ZEO	15,28	26,40	3,16	-
PEI2000_PEG_ZEO	14,13	25,80	3,22	-
PEI750000_ZEO	14,28	27,70	4,54	-
PEI750000_PEG_ZEO	14,28	25,98	3,53	-

7.8 CO₂ Adsorption Capacity and Cyclic Stability of Amine-Grafted Adsorbents in 10% CO₂ Environment

The adsorption time under 10% CO₂ conditions was consistently set to be 20 minutes across various samples, as illustrated in Figure 29. However, it was observed that upon closing the CO₂ valve to initiate the completion of the adsorption cycle, a residual amount of CO₂ remained present within the piping and on the balance. This residual CO₂ was found to be adsorbed by the adsorbent within approximately 4 minutes for all samples. Consequently, while the targeted adsorption time was achieved within the specified 20-minute duration, the overall adsorption process for all samples extended to 24 minutes. Consequently, capacity calculated based on adsorption peaks of the adsorbents, as depicted in Figure 38, it was imperative to consider this residual CO₂ effect.

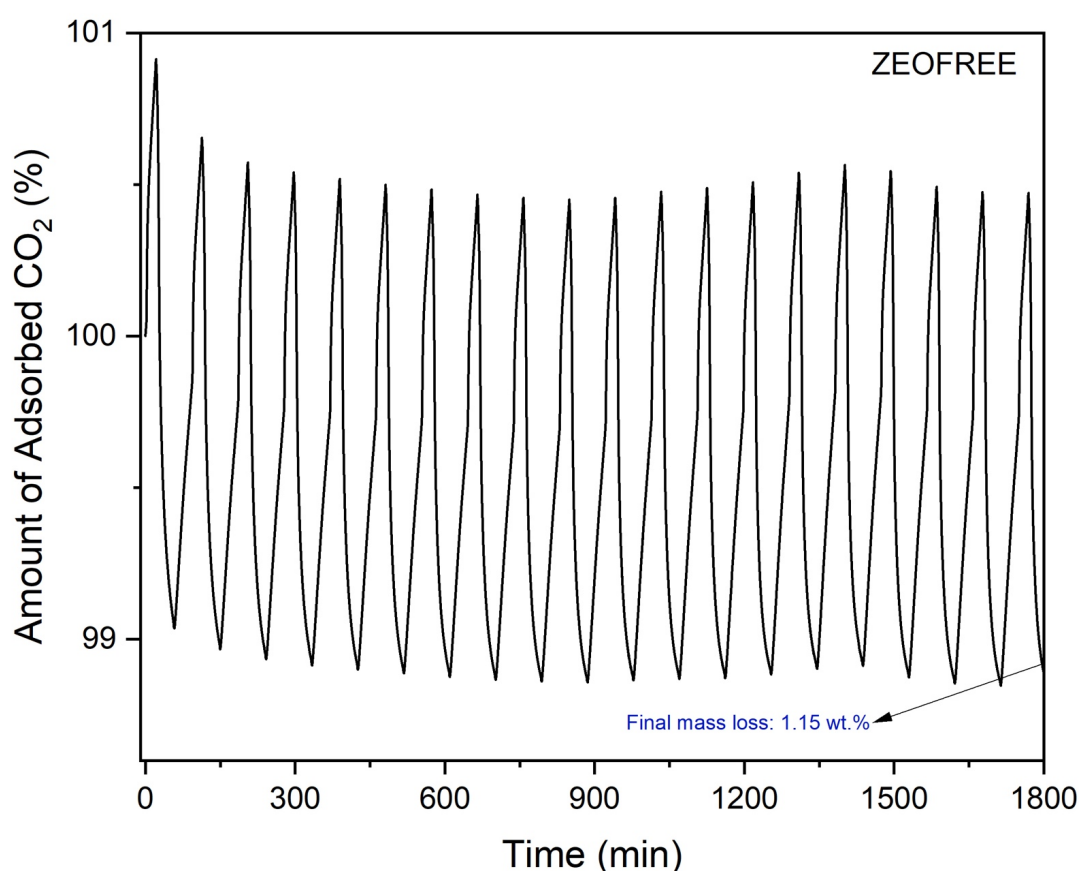


Figure 38 Adsorption-desorption measurements of pristine ZEOFREE support.

Moving on to the investigation of ZEOFREE substrate without any modifications, showcased in Figures 38 and 39, it's evident that even in its pristine state, ZEOFREE possessed a noteworthy adsorption capacity of 0.16 mmol/g. This inherent capacity can be attributed to ZEOFREE's exceptional porosity and high surface area, which can facilitate efficient adsorption.

Figure 38 presents the adsorption cycles along with the corresponding weight losses, with the final weight loss of ZEOFREE recorded at 1.15%. Notably, during the adsorption process, certain cycles, particularly between the 10th and 15th cycles, exhibited unexpected weight gains. These anomalies were likely induced by variations in temperature and gas switches within the system. Interestingly, such deviations were predominantly observed in the pristine ZEOFREE and ZEO-4 samples, while other samples did not exhibit any significant unexpected weight gain.

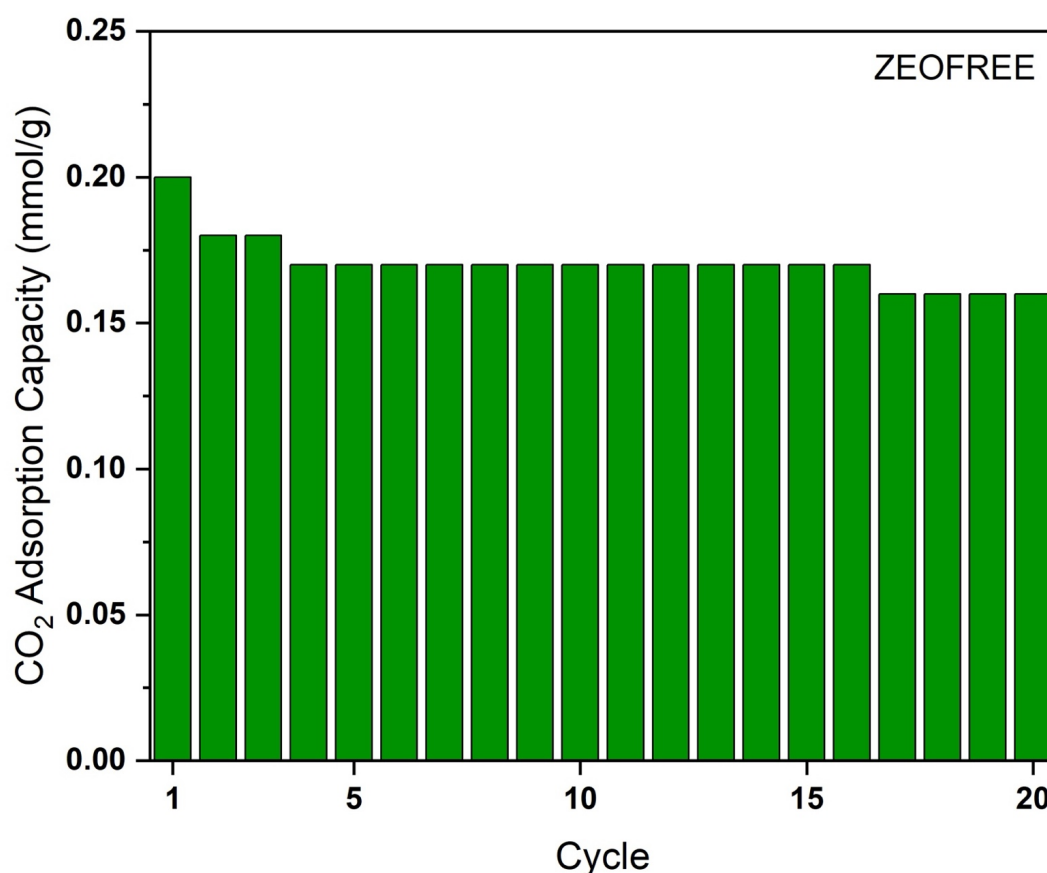


Figure 39 Cyclic stability and CO₂ adsorption capacity of ZEOFREE support over 20 cycles.

Long-term stability is paramount to ensure effective CO₂ capture over numerous successive adsorption-desorption cycles, without compromising performance. In pursuit of such stability, the performance of various materials, denoted as ZEO-1 to ZEO-6, was meticulously assessed, as depicted in Figure 41. These materials underwent rigorous testing involving 20 consecutive adsorption-desorption cycles. Upon the completion of these cycles, it was observed that ZEO-1, ZEO-2, and ZEO-3 exhibited final mass losses of 1.8 wt.%, 2.1 wt.%, and 2.32 wt.%, respectively. In contrast, ZEO-4, ZEO-5, and ZEO-6 displayed slightly lower final mass losses of 1.55 wt.%, 1.43 wt.%, and 1.77 wt.%, respectively.

Notably, ZEO-5 demonstrated the least amine loss, indicating its superior cyclic stability within the ZEO series. Moreover, ZEO-5 exhibited the highest CO₂ adsorption capacity of 0.60 mmol/g, as indicated in Table 10. It was observed that ZEO samples grafted with AEAPTMS displayed reduced amine loss during cyclic operations.

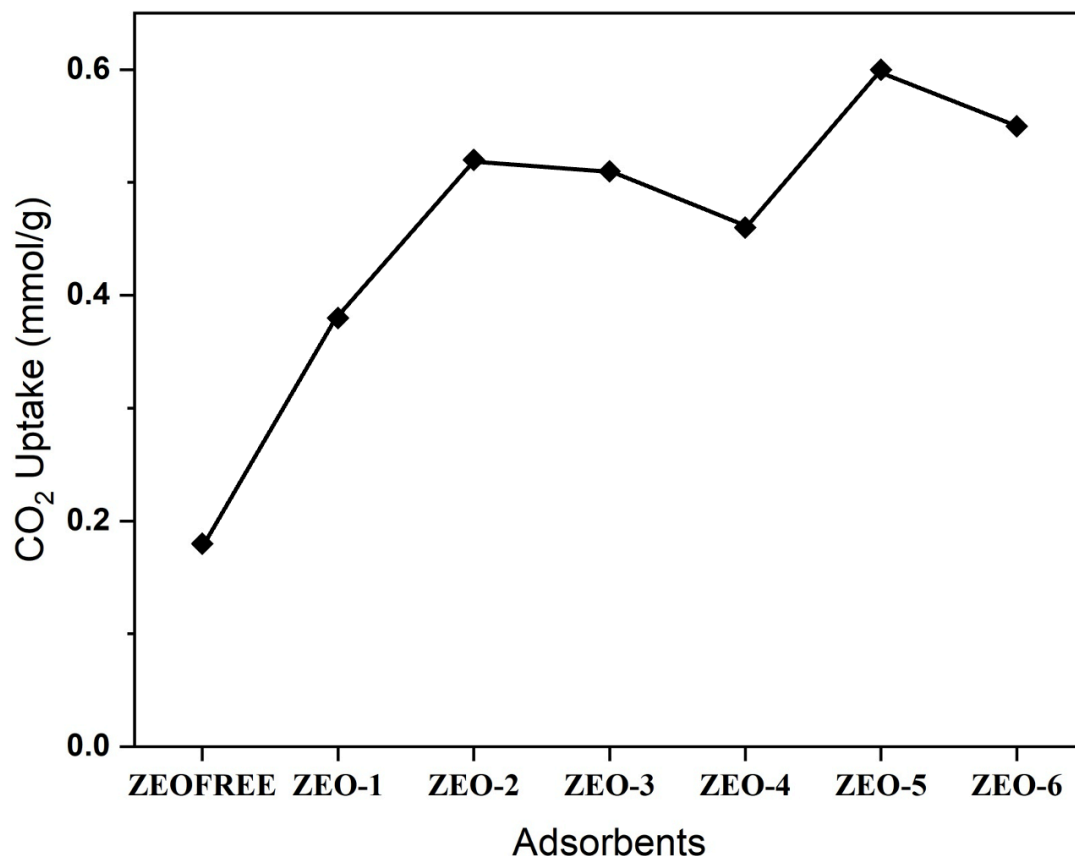


Figure 40 Comparative CO₂ uptake of the ZEO series under 10% CO₂ conditions.

Figure 42 provides insights into the adsorption capacity of each adsorbent across multiple cycles. It's evident that ZEO-4 to ZEO-6 consistently displayed higher CO₂ adsorption capacities compared to ZEO-1 to ZEO-3. This enhancement can be attributed to the presence of the grafting agent AEAPTMS, which introduces additional aminoethyl groups onto the adsorbent surface.

Across all examples, there was a notable decrease in capacity observed while passing from the first cycle to the second cycle, a trend observed in the PEI series as well, except for PEI2000_ZEO. To further investigate this rapid decrease, the materials underwent a one-time nitrogen cycle at 90 °C for 30 minutes before initiating the first adsorption cycle. Interestingly, when this period was extended to 1 hour for PEI2000_ZEO, the dramatic decrease in capacity observed in the initial step was not observed, suggesting a potential avenue for improving the stability of these materials.

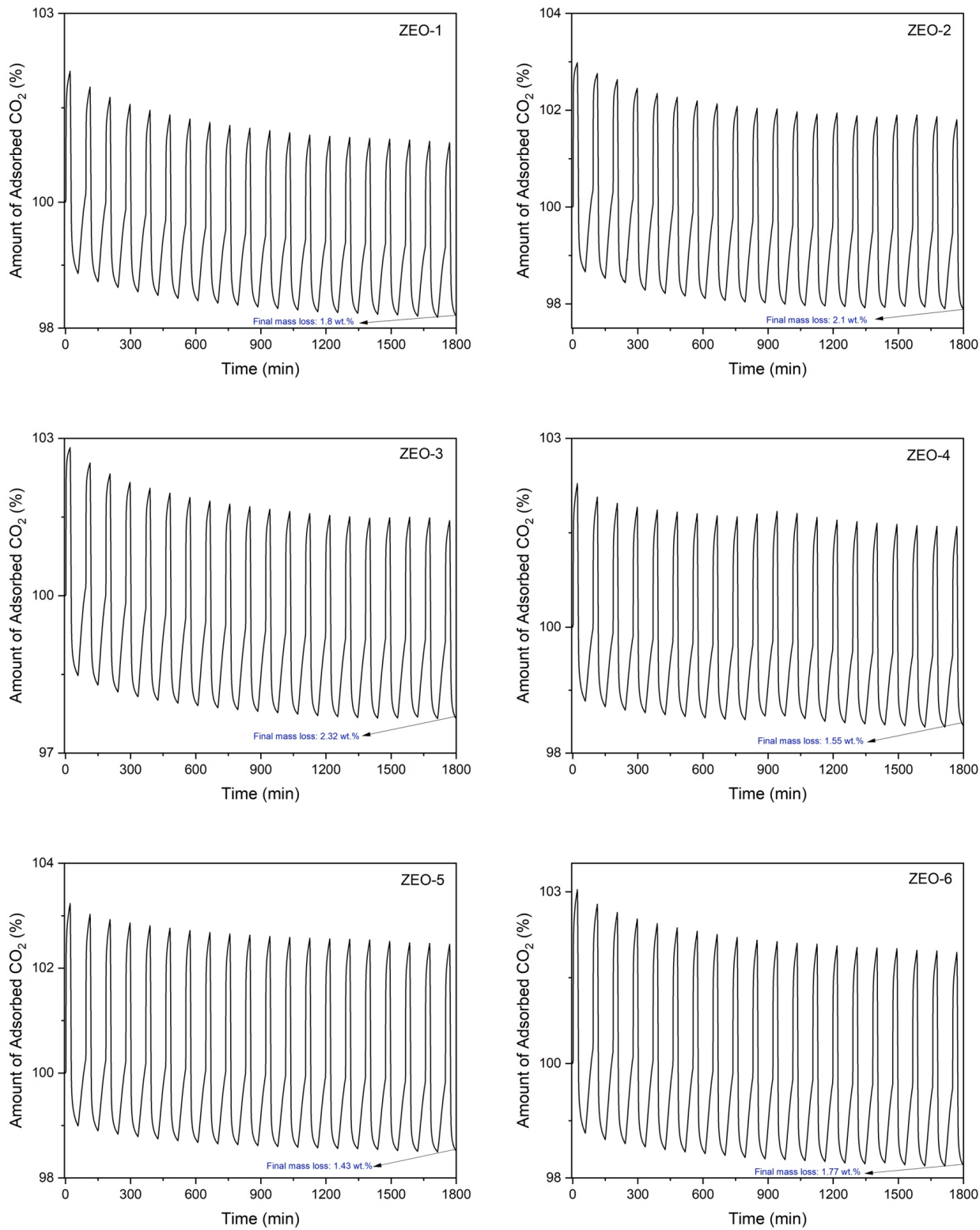


Figure 41 Adsorption-desorption measurements of ZEO series.

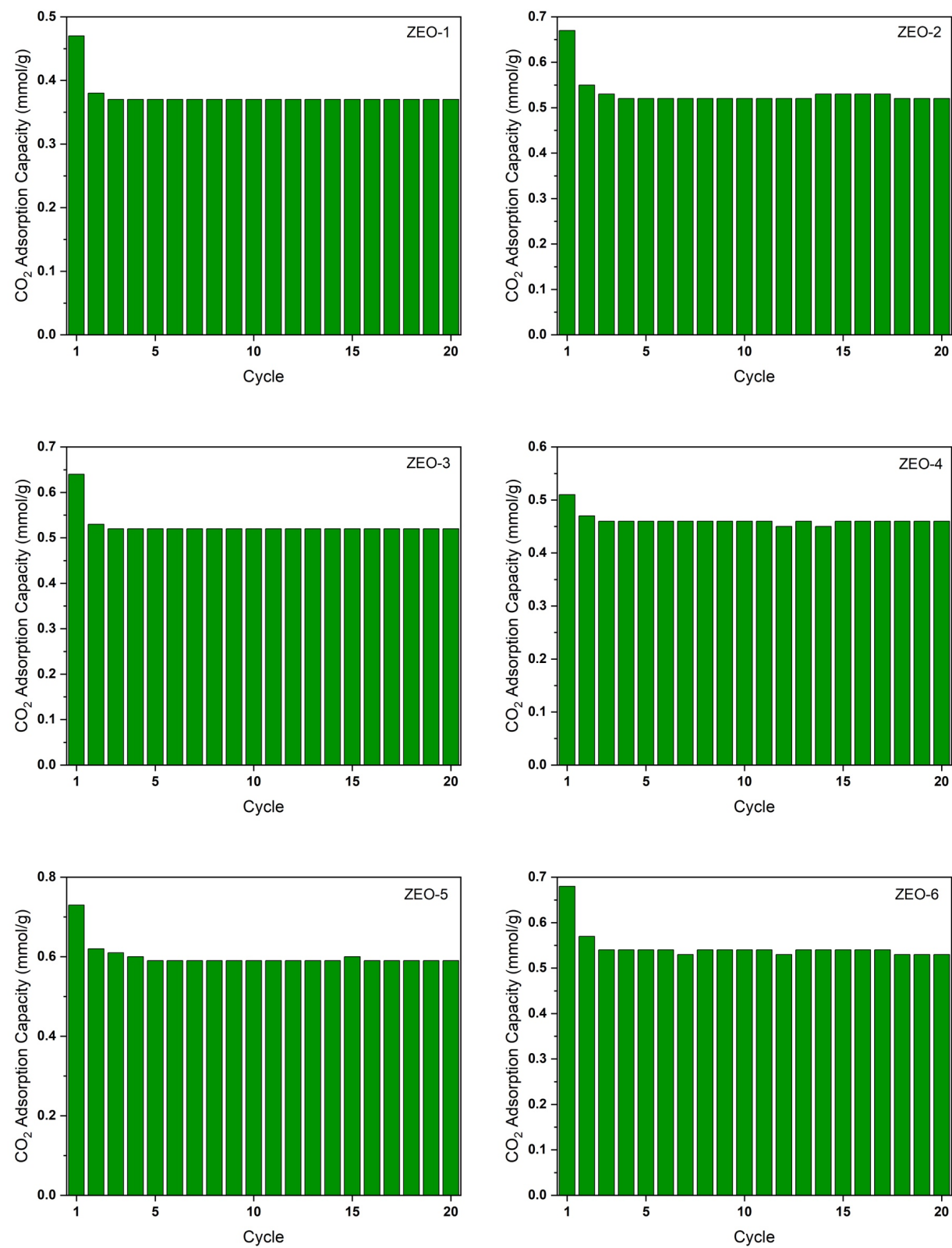


Figure 42 Cyclic stability and CO₂ adsorption capacity of ZEO series.

Table 10 CO₂ capture capacity of amine-functionalized ZEO series adsorbents synthesized by chemical grafting.

Adsorbent	Amine type	Temp (°C)	CO ₂ conc. (%)	Amine loading (mmol of N per g of the adsorbent)	CO ₂ adsorption capacity (mmol/g)	Amine efficiency (mmol of CO ₂ per mmol of N)
ZEOFREE	-	30	10	-	0.16	-
ZEO-1	APTMS	30	10	3.64	0.37	0.10
ZEO-2	APTMS	30	10	3.76	0.53	0.15
ZEO-3	APTMS	30	10	3.69	0.52	0.14
ZEO-4	AEAPTMS	30	10	23.29	0.46	0.020
ZEO-5	AEAPTMS	30	10	3.54	0.60	0.17
ZEO-6	AEAPTMS	30	10	12.08	0.54	0.044

The comparative study presented in Table 10 reveals insights into adsorbent performance concerning amine loading, amine efficiency, and CO₂ adsorption capacity. Notably, adsorbents synthesized under wet conditions demonstrate superior amine efficiency and CO₂ adsorption capacity compared to those synthesized under dry conditions or undried support conditions. This trend suggests that the wet synthesis method enhances the effectiveness of amine functionalization, leading to increased CO₂ adsorption capacity.

ZEO-4 and ZEO-6 show higher amine loading while lower amine efficiency compared to others. Elemental analysis reveals ZEO-4 has the highest nitrogen content at 18.92%, followed by ZEO-6 at 11.91%, while ZEO-5 exhibits 5.03% nitrogen and the highest carbon content at 10.4%, Table 9.

7.9 CO₂ Adsorption Capacity and Cyclic Stability of Amine-Impregnated Adsorbents in 10% CO₂ Environment

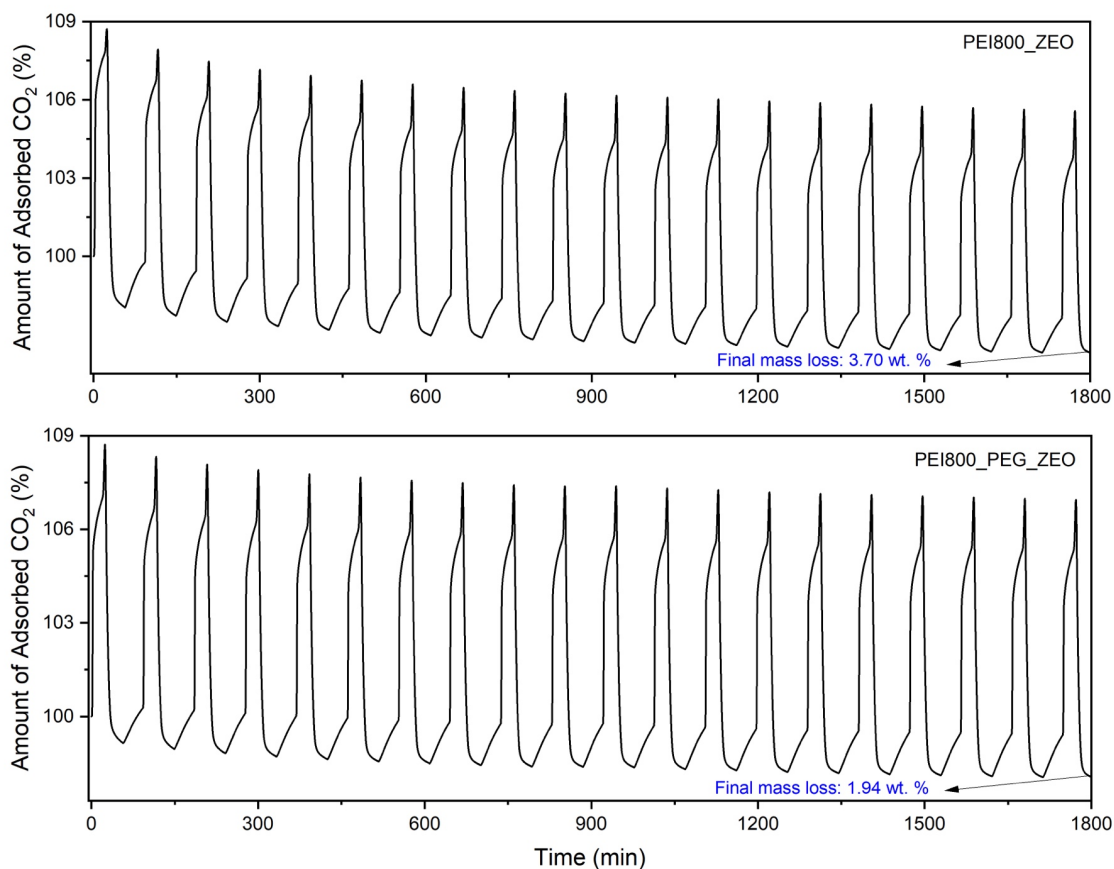


Figure 43 Adsorption-desorption measurements of PEI800_ZEO and PEI800_PEG_ZEO.

The investigation reveals a relationship between PEI molecular weight and cyclic stability, evidenced by a reduction in amine loss as molecular weight increases. Notably, PEI800_ZEO exhibited the highest final mass loss at 3.79%, followed by PEI2000_ZEO at 1.27%, PEI25000_ZEO at 0.99%, and PEI750000_ZEO at 0.83%.

The introduction of PEG with a molecular weight of 20000 yielded improvements in cyclic stability across several PEI adsorbents. Substantial decreases in final mass loss were observed, with PEI800_PEG_ZEO decreasing to 1.94%, PEI2000_PEG_ZEO decreasing to 0.72%, and PEI750000_PEG_ZEO decreasing to 0.78%. However, there was no discernible enhancement in cyclic stability for PEI25000_PEG_ZEO.

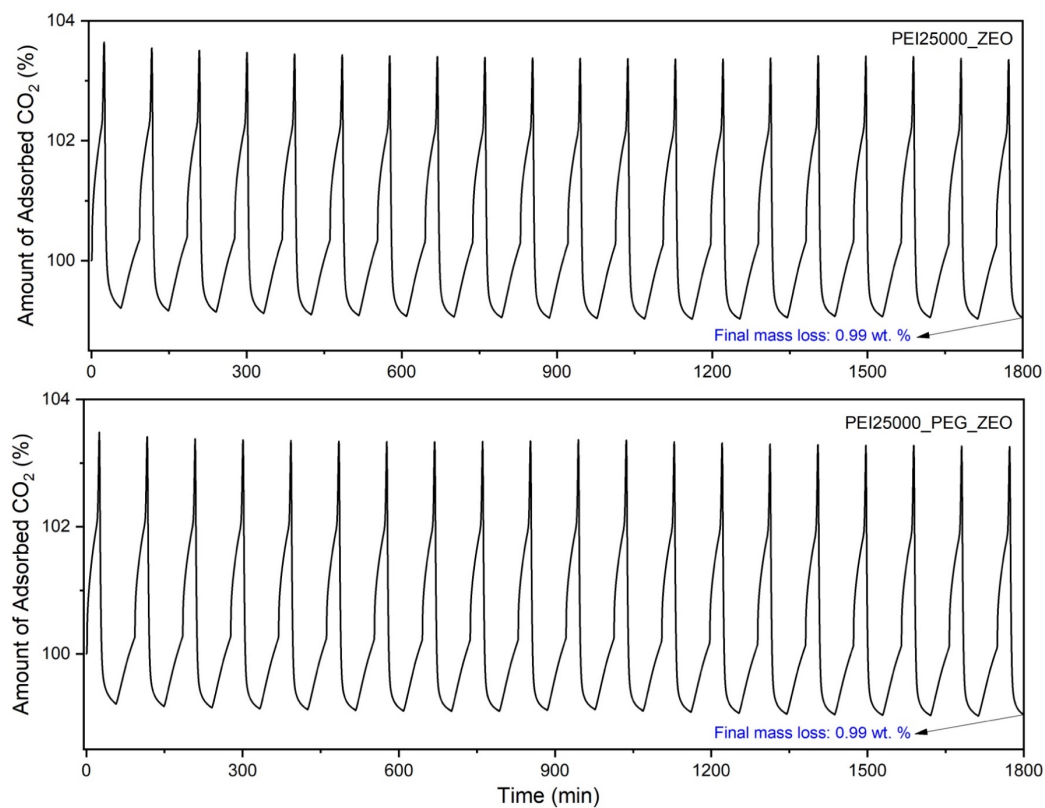


Figure 44 Adsorption-desorption measurements of PEI25000_ZEO and PEI25000_PEG_ZEO.

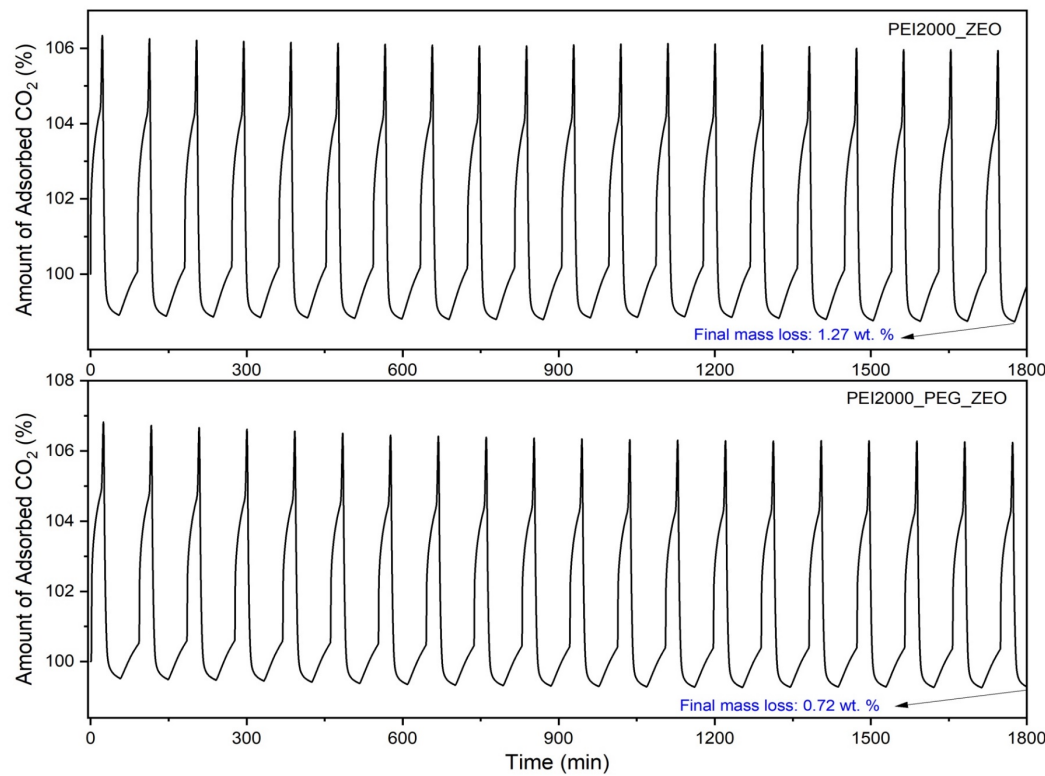


Figure 45 Adsorption-desorption measurements of PEI2000_ZEO and PEI2000_PEG_ZEO.

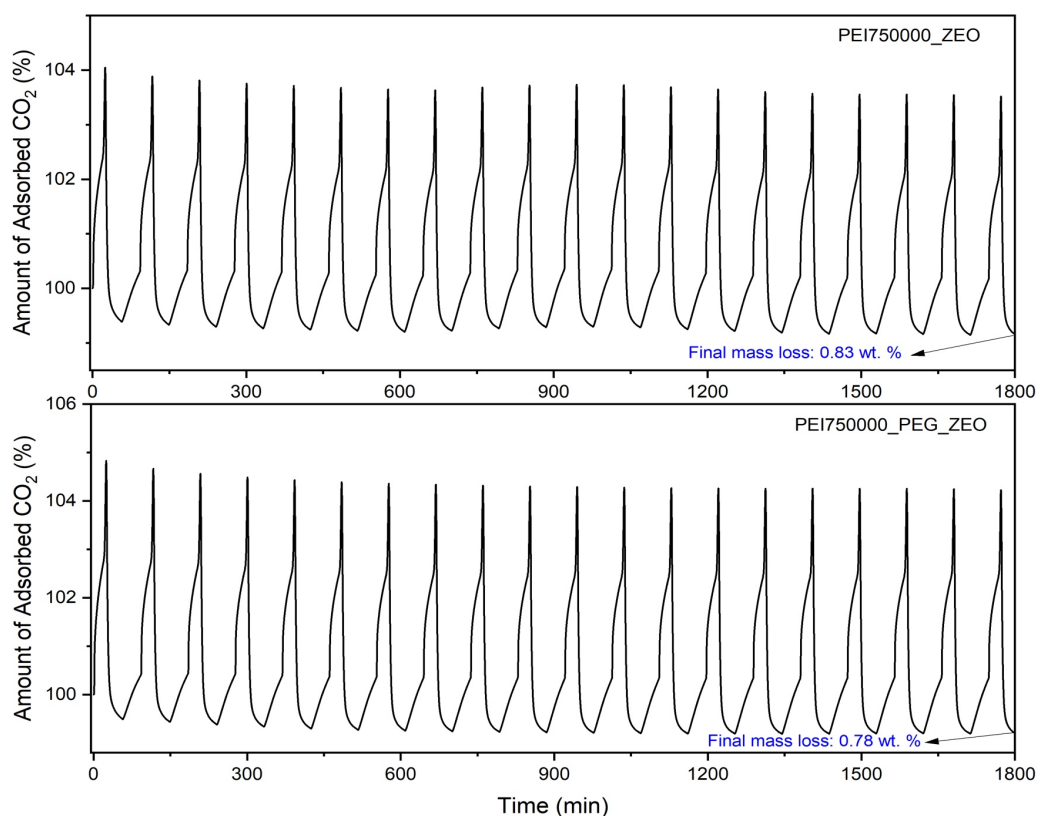


Figure 46 Adsorption-desorption measurements of PEI750000_ZEO and PEI750000_PEG_ZEO.

Under humid conditions, theoretically, only one amino group is needed to capture a molecule of CO_2 . Consequently, the CO_2 adsorption capacity of PEI is expected to be higher under humid conditions. In addition, the presence of water significantly stabilizes the adsorbents by inhibiting the formation of urea species. [29]

This is supported by the observation that PEI formulations with inherent water exhibit greater cyclic stability. For instance, PEI2000_ZEO and PEI2000_PEG_ZEO demonstrate better stability compared to PEI800_ZEO and PEI800_PEG_ZEO. A similar trend is observed for PEI750000_ZEO, where PEI750000_PEG_ZEO shows better stability (amine loss over cycles) compared to PEI25000_ZEO and PEI25000_PEG_ZEO.

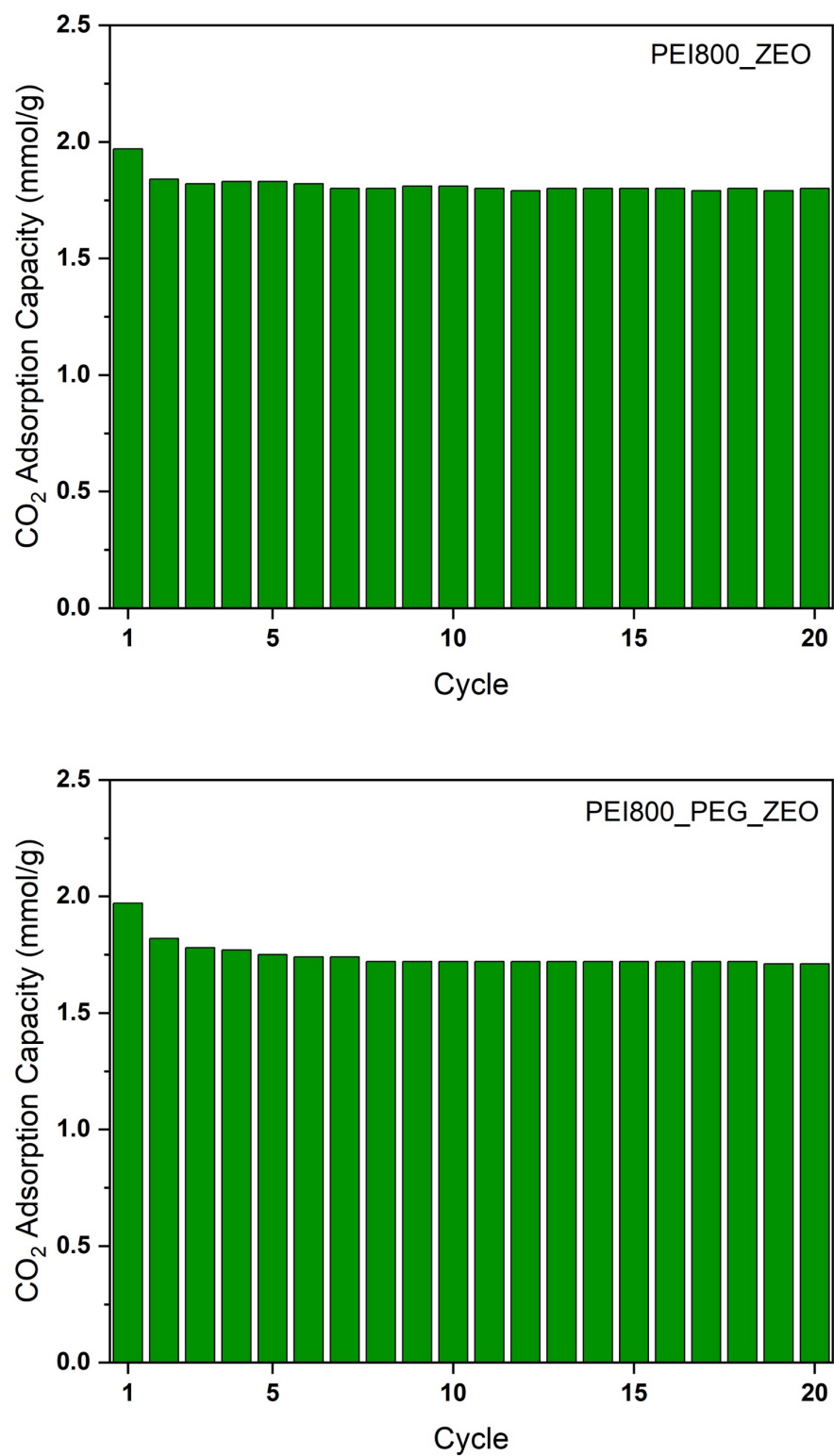


Figure 47 Cyclic stability and CO₂ adsorption capacity of PEI800_ZEO and PEI800_PEG_ZEO.

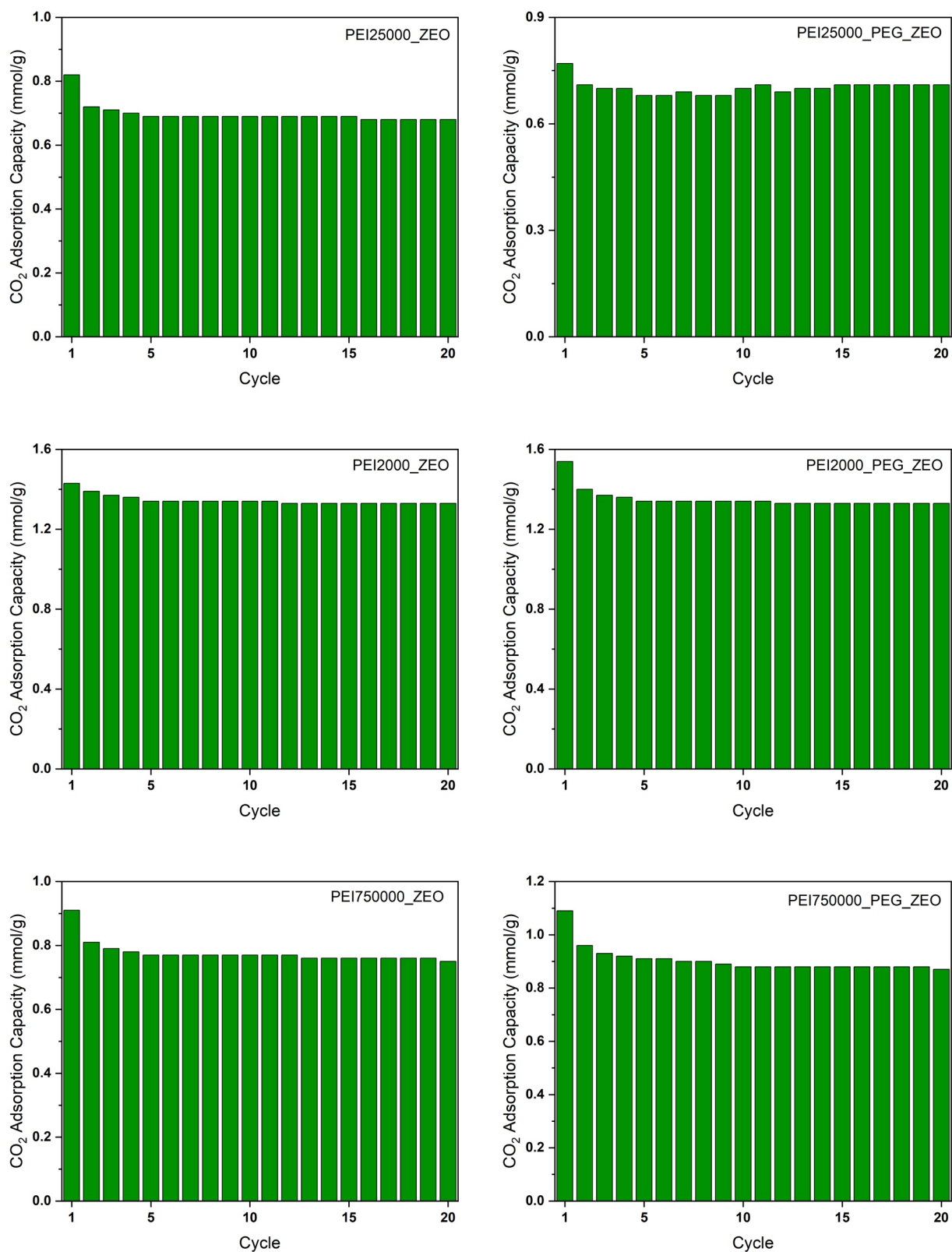


Figure 48 Cyclic stability and CO₂ adsorption capacity of PEI25000_ZEO, PEI25000_PEG_ZEO, PEI2000_ZEO, PEI2000_PEG_ZEO and PEI750000_ZEO, PEI750000_PEG_ZEO.

Literature reports that adsorbents with branched PEI (molecular weight of 800) achieved the highest CO₂ adsorption capacity.[20] This is supported by our findings, as PEI800_ZEO exhibited the highest CO₂ adsorption capacity at 1.81 mmol/g under %10 CO₂ conditions. However, the addition of PEG resulted in improved cyclic stability while slightly decreasing the adsorption capacity to 1.74 mmol/g for PEI800_PEG_ZEO.

Table 11 Amine loading, and CO₂ adsorption capacity of adsorbents using the TGA method. PEG molecular weight: 20000, all molecular weight shows in the table is only for PEI's.

Adsorbents	Molecular weight of PEI	Temp. (°C)	CO ₂ concent. (%)	Amine loading (%)	CO ₂ adsorption capacity (mmol/g)
PEI800_ZEO	800	30	10	50 wt%	1.81
PEI800_PEG_ZEO	800	30	10	47.5 wt%	1.74
PEI25000_ZEO	25000	30	10	50 wt%	0.69
PEI25000_PEG_ZEO	25000	30	10	47.5 wt%	0.70
PEI2000_ZEO	2000	30	10	50 wt%	1.34
PEI2000_PEG_ZEO	2000	30	10	47.5 wt%	1.35
PEI750000_ZEO	750000	30	10	50 wt%	0.77
PEI750000_PEG_ZEO	750000	30	10	47.5 wt%	0.90

Furthermore, PEI2000_ZEO and PEI2000_PEG_ZEO demonstrated higher capacity compared to the remaining adsorbents, namely PEI25000 and PEI750000 molecular weight as well as with addition of PEG synthesized adsorbents. The addition of PEG slightly increased the adsorption capacity of PEI2000_PEG_ZEO by 0.01 mmol/g compared to PEI2000_ZEO. Similarly, same amount of increasement was observed for the PEI25000_PEG_ZEO compared PEI25000_ZEO upon PEG addition. However, the addition of PEG notably increased the adsorption capacity of PEI750000_ZEO from 0.77 mmol/g to 0.90 mmol/g compared to PEI750000_PEG_ZEO.

7.10 CO₂ Adsorption Capacity of Amine-Grafted Adsorbents in 400 ppm CO₂ Environment

The adsorption capacity of amine-based solid adsorbents is significantly influenced by changes in the CO₂ partial pressure within the target gas. Belmabkhout et al. demonstrated that the equilibrium CO₂ adsorption capacity of a triamine-functionalized pore-expanded MCM-41 (TRI-PEMCM-41) decreased from 2.05 mmol/g to 1.20 mmol/g as the CO₂ concentration decreased from 5% to 1000 ppm.[51] In a more recent study by the same group, it was found that the adsorption capacity of triamine-functionalized MCM-41 varied with CO₂ concentration, yielding capacities of 2.18, 1.60, and 0.98 mmol/g at CO₂ concentrations of 10%, 1%, and 400 ppm respectively.[52], [53]

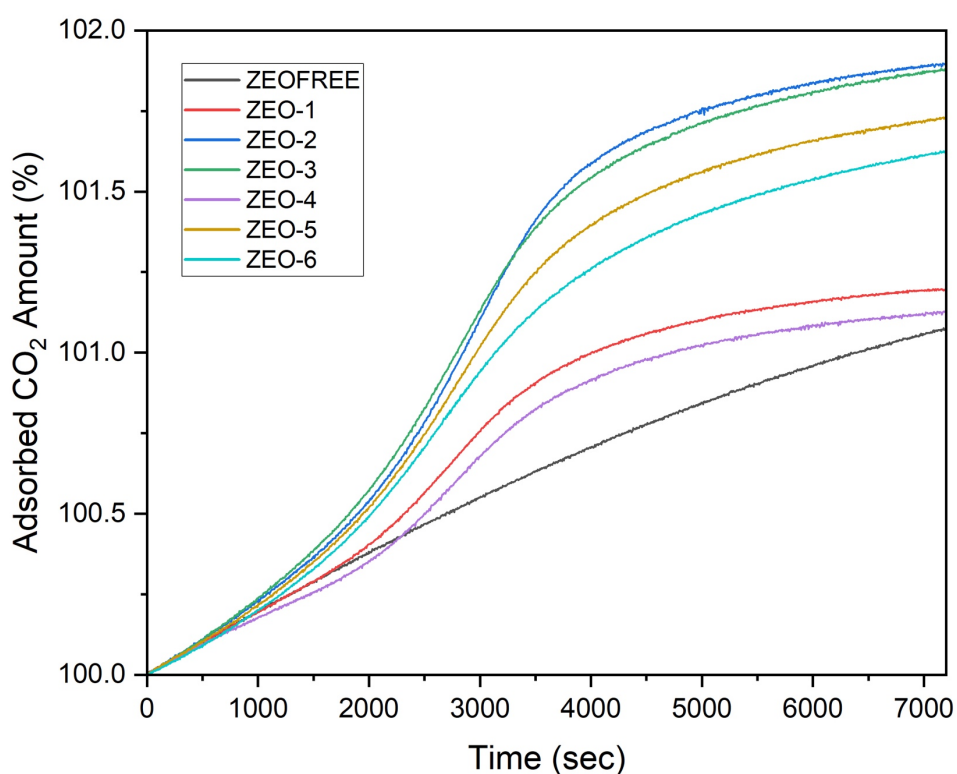


Figure 49 CO₂ adsorption capacity of ZEO series including ZEOFREE support under 400 ppm CO₂ conditions.

With a substantial decrease in CO₂ concentration, from 10% to 0.04%, the observations of CO₂ adsorption capacity of amine-based solid adsorbents prepared by chemical grafting shows a slight decrease in CO₂ adsorption capacity under 400 ppm compared to 10% CO₂. Even in the PEI series, adsorbents synthesized with molecular weights of 25000 and 750000 show increased CO₂ adsorption capacity compared to 10% CO₂ conditions.

Figure 49 illustrates the CO₂ adsorption cycle under 400 ppm CO₂ environment for the ZEO series, including the ZEOFREE pristine support. For this series, the adsorption time was set at 2 hours (7200 sec). The ZEOFREE pristine support curve shows slow adsorption for 2 hours, with a slight increase over time. There is no plateau of saturation observed. In contrast, ZEO-1 to ZEO-6 reach saturation

between 4000-5000 seconds, after which they show slow adsorption, with a slight increase until the end of the adsorption period.

Adsorbents synthesized under wet conditions or with undried support demonstrate better CO₂ adsorption capacity under 400 ppm conditions compared to those synthesized under dry conditions. Water content in the synthesis has a positive effect as mentioned before on CO₂ adsorption capacity under both 400 ppm and 10% CO₂, resulting in better adsorption capacity as well as better cycle stability under 10% CO₂ conditions.

7.11 CO₂ Adsorption Capacity of Amine-Impregnated Adsorbents in 400 ppm CO₂ Environment

The PEI series exhibits various adsorption capacities under 400 ppm conditions, as well as different saturation times. The PEI series was subjected to CO₂ adsorption for 3 hours (10800 sec) as well as ZEOFREE support. It is observed that the molecular weight of PEI influences the CO₂ adsorption capacity.

ZEOFREE exhibited a CO₂ absorption capacity of 0.27 mmol/g over both 2 and 3 hours. PEI800_ZEO and PEI800_PEG_ZEO show the highest CO₂ adsorption capacity under 400 ppm conditions, with capacities of 1.70 mmol/g and 1.68 mmol/g respectively. Both adsorbents reach saturation around 10000 sec and continue to adsorb CO₂ slowly until the end of the adsorption time.

In Figure 51, the adsorption time for PEI800_ZEO was set for 6 hours. It is evident that once the adsorbents reach 10000 sec, saturation occurs, and they continue to adsorb CO₂ slowly until the end of the adsorption time, showing a CO₂ adsorption capacity of 1.68 mmol/g.

PEI2000_ZEO and PEI2000_PEG_ZEO exhibit similar CO₂ adsorption capacities under 400 ppm conditions, with capacities of 1.24 mmol/g and 1.23 mmol/g respectively. Their adsorption capacities saturate with CO₂ after 8000 seconds.

The addition of PEG only influences PEI750000_PEG_ZEO, which shows a higher CO₂ adsorption capacity of 0.88 mmol/g compared to PEI750000_ZEO, which has a capacity of 0.80 mmol/g.

PEI25000_ZEO and PEI25000_PEG_ZEO show the lowest CO₂ adsorption capacities at 0.73 mmol/g and 0.75 mmol/g respectively. They reach CO₂ saturation within 5000 seconds and continue slow adsorption, while PEI750000_ZEO and PEI750000_PEG_ZEO saturate around 7000 seconds and continue slow adsorption.

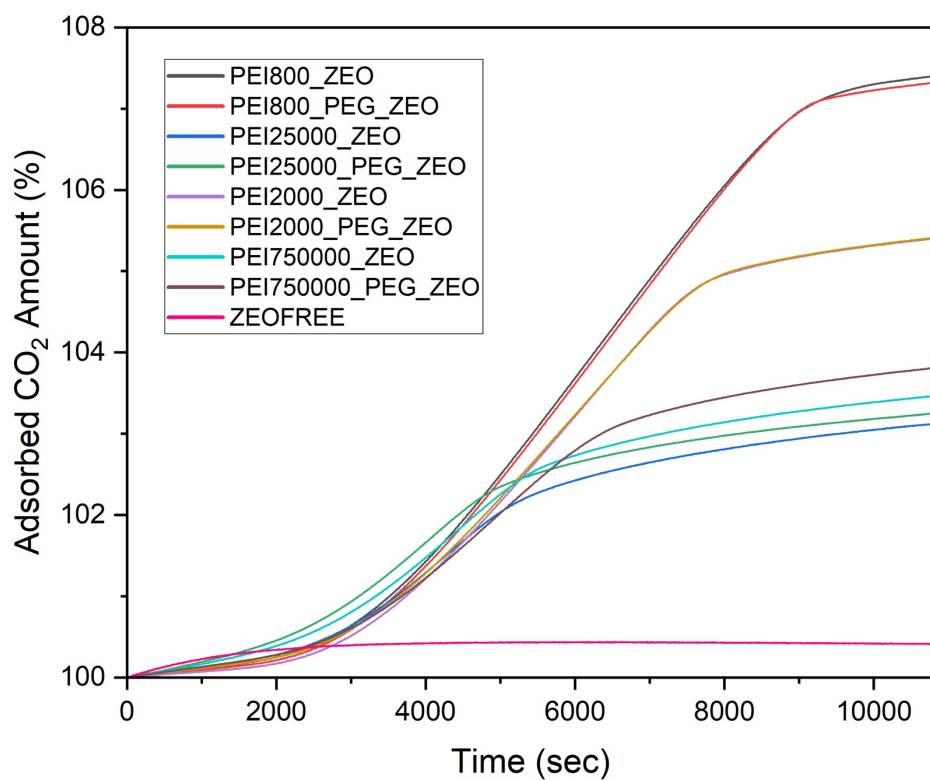


Figure 50 CO₂ adsorption capacity of PEI series and ZEOFREE support under 400 ppm CO₂ conditions.

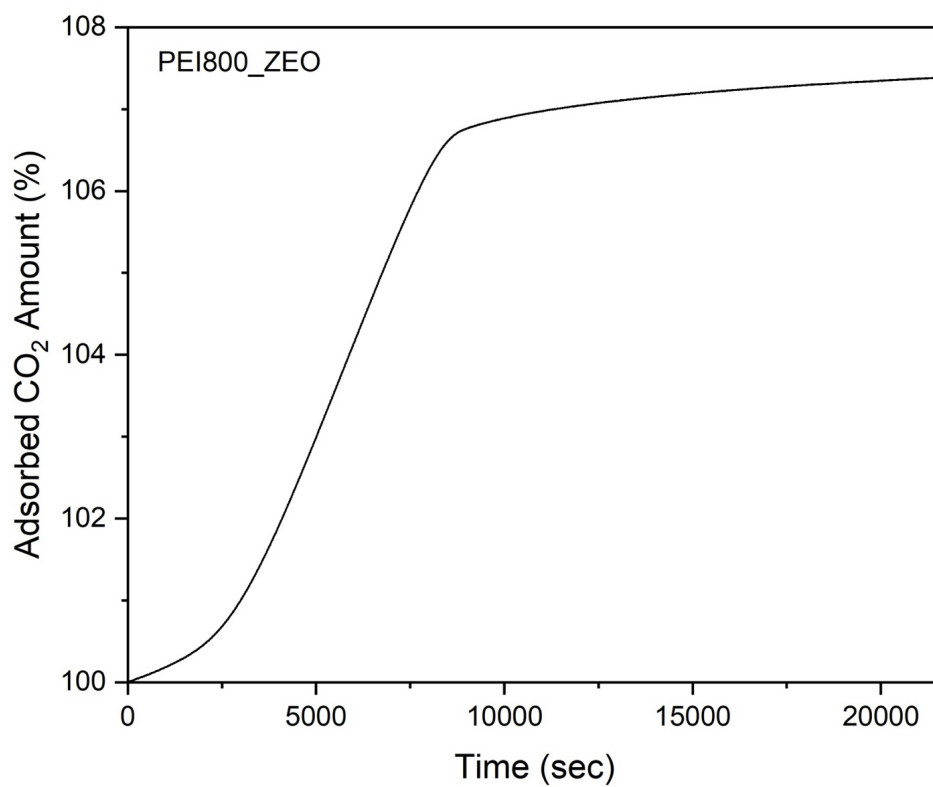


Figure 51 CO₂ adsorption capacity of PEI800_ZEO adsorbent in 6 hours adsorption under 400 ppm CO₂ conditions.

Table 12 CO₂ adsorption capacity of all samples including ZEOFREE support under 400 ppm CO₂ conditions.

Adsorbents	Amine type	Temp (°C)	CO ₂ concentr ation (ppm)	Amine loading (mmol of N per g of the adsorbent)	CO ₂ adsorption capacity (mmol/g)	Amine efficiency (mmol of CO ₂ per mmol of N)
ZEOFREE	-	30	400	-	0.27	-
ZEO-1	APTMS	30	400	3.64	0.27	0.07
ZEO-2	APTMS	30	400	3.76	0.44	0.11
ZEO-3	APTMS	30	400	3.69	0.44	0.12
ZEO-4	AEAPTMS	30	400	23.29	0.27	0.011
ZEO-5	AEAPTMS	30	400	3.54	0.40	0.11
ZEO-6	AEAPTMS	30	400	12.08	0.38	0.31
PEI800_ZEO	PEI	30	400	50 wt.%	1.70	-
PEI800_PEG_ZEO	PEI+PEG	30	400	47.5 wt.%	1.68	-
PEI25000_ZEO	PEI	30	400	50 wt.%	0.73	-
PEI25000_PEG_ZEO	PEI+PEG	30	400	47.5 wt.%	0.75	-
PEI2000_ZEO	PEI	30	400	50 wt.%	1.24	-
PEI2000_PEG_ZEO	PEI+PEG	30	400	47.5 wt.%	1.23	-
PEI750000_ZEO	PEI	30	400	50 wt.%	0.80	-
PEI750000_PEG_ZEO	PEI+PEG	30	400	47.5 wt.%	0.88	-

Among the adsorbents, pristine ZEOFREE shows an increase in adsorption capacity compared to 10% CO₂ conditions, with its capacity rising from 0.16 mmol/g to 0.27 mmol/g. Adsorbents synthesized with AEATPMS as the grafting agent show a greater decrease in CO₂ adsorption capacity under 400 ppm conditions compared to those synthesized with APTMS, but adsorbents synthesized with AEATPMS show better CO₂ adsorption capacity under 10% CO₂ conditions. ZEO-5 shows the highest decrease in CO₂ adsorption capacity under 400 ppm, decreasing from 0.60 mmol/g (%10 CO₂) to 0.40 mmol/g.

In the PEI series, the most significant decrease in adsorption capacity compared to 10% CO₂ conditions is observed in PEI2000_PEG_ZEO with a decrease of 0.12 mmol/g, followed by PEI800_ZEO adsorbent with a decrease of 0.11 mmol/g, PEI2000_ZEO with a decrease of 0.10 mmol/g, and PEI800_PEG_ZEO with a decrease of 0.06 mmol/g. The remaining PEI-based adsorbents show increases, with PEI25000_ZEO increasing by 0.04 mmol/g and PEI750000_ZEO increasing by 0.03 mmol/g, while PEI25000_PEG_ZEO increases by 0.05 mmol/g and PEI750000_PEG_ZEO increases by 0.02 mmol/g.

Table 13 CO₂ adsorption capacity amine-functionalized solid adsorbents synthesized by chemical grafting and impregnation processes presented from literature.

Support	Amine type	Temp. (°C)	CO ₂ concentration (ppm)	Amine loading (mmol of N per g of the adsorbent)	CO ₂ adsorption capacity (mmol/g)		Amine efficiency (mmol of CO ₂ per mmol of N)	Method	Ref
					Dry CO ₂	Humid CO ₂			
Hybrid silica	APTES	30	400	4.5	-	1.68	0.37	TGA	[54]
SBA-15	Z-L-lysine + APTMS	25	400	5.18	0.60	-	0.12	TGA	[55]
SBA-15 pellet	APTMS	25	395	-	0.09	0.13	-	TGA	[56]
SBA-15	APTMS	25	395	-	0.14	-	-	TGA	[56]
Mesocellular silica foam	APTMS	25	400	2.70	0.54	-	0.20	TGA	[57]
Com silica	PEI	25	400	10.5	2.36	-	0.22	TGA	[38]
Fumed silica	PEI	25	400	50 wt.%	2.44	-	-	IR	[40]
Mesocellular silica foam	PEI	25	400	10.7	1.74	-	0.16	TGA	[58]
γ-Alumina	PEI	25	400	11.2	1.74	-	0.16	TGA	[59]
SBA-15	PEI	25	400	9.23	1.05	-	0.11	TGA	[59]
SBA-15	PEI + PEG	30	400	5.75	0.79	-	0.14	TGA	[60]
Zr-SBA-15	PEI	25	400	8.3	0.85	-	0.10	TGA	[61]
CA-SiO ₂	PEI	35	395	16.1	0.59	1.60	-	TGA	[62]

CONCLUSIONS

The research presented in this thesis investigated the effect of different surface modification methods on the performance of ZEOFREE sorbents for CO₂ capture. Two different aminosilanes, APTMS and AEAPTMS, were introduced to the ZEOFREE sorbent via chemical grafting, while various molecular weights of polyethyleneimine (PEI) were impregnated onto the same sorbent to explore their impact on CO₂ adsorption capacity, thermal stability, cyclic stability, and textural properties.

The results of the ZEOFREE series revealed that the CO₂ adsorption capacity was primarily influenced by the type of silane used for grafting. Specifically, adsorbents grafted with AEAPTMS demonstrated higher CO₂ adsorption capacity under 10% CO₂ conditions compared to those grafted with APTMS. This was attributed to the additional aminoethyl group and primary/secondary amine present in AEAPTMS, leading to more amino silanes covalently bound to the support surface. However, under 400 ppm CO₂ conditions, no significant differences in CO₂ adsorption capacity were observed between sorbents grafted with APTMS and AEAPTMS this is due to high decrease of CO₂ partial pressure (400 ppm). Additionally, adsorbents synthesized with APTMS demonstrated higher thermal stability compared to AEAPTMS, as evidenced by amine degradation and evaporation occurring at higher temperatures.

In the PEI series, adsorbents synthesized with lower molecular weight of PEI demonstrated higher CO₂ adsorption capacities under both 10% CO₂ and 400 ppm CO₂ conditions compared to those synthesized with higher molecular weights. However, adsorbents synthesized with PEI 750000 molecular weight exhibited higher CO₂ adsorption capacity than those synthesized with PEI 25000 molecular weight under both 10% CO₂ and 400 ppm CO₂ conditions, attributed to the inherent water content in PEI 750000. Furthermore, PEI with inherent water, namely PEI 2000 and PEI 750000, showed improved cyclic stability compared to other PEIs without inherent water. Adsorbents synthesized with lower molecular weight PEI exhibited lower surface area but higher total pore volume, whereas those synthesized with PEI 750000 demonstrated reduced surface area and total pore volume due to the effect of inherent water.

We concluded that addition of poly(ethylene glycol) (PEG) to adsorbent synthesized with PEI 800 resulted in a notable increase in textural properties. This addition also helped reduce amine loss over multiple cycles for all samples except for adsorbents synthesized with PEI 25000 molecular weight. Moreover, this improvement was most pronounced in adsorbents synthesized with PEI 800 molecular weight. Therefore, the addition of hydroxy-rich poly(ethylene glycol) (PEG) has been shown to improve the stability and textural properties of adsorbents synthesized with PEI 800 molecular weight.

It can be concluded that adsorbents synthesized via chemical grafting offer high stability and easy regeneration during CO₂ adsorption–desorption cycles, even in humid conditions, compared to those obtained through physical impregnation. The covalent binding of amino silane to the support provides these materials with significant thermal stability, although they typically have a lower amine concentration, limiting their CO₂ uptake capacity due to surface saturation with amino silane species. In contrast, the physical impregnation method, while simpler and capable of accommodating substantial amounts of amine for higher CO₂ adsorption capacity, is prone to issues such as amine degradation and evaporation.

The most promising adsorbent synthesized via chemical grafting was ZEO-5, with a CO₂ adsorption capacity of 0.60 mmol/g under 10% CO₂, and 0.40 mmol/g under 400 ppm CO₂ conditions, along with superior cyclic stability. For sorbents synthesized with different molecular weights of PEI, PEI800_PEG_ZEO exhibited the significant CO₂ adsorption capacity, with 1.74 mmol/g under 10% CO₂ conditions and 1.68 mmol/g under 400 ppm CO₂ conditions. However, while PEI800_ZEO showed higher capacity, it exhibited poorer cyclic stability. With the addition of PEG, PEI800_PEG_ZEOFREE emerged as a promising adsorbent.

REFERENCES

- [1] N. Wang, K. Akimoto, and G. F. Nemet, 'What went wrong? Learning from three decades of carbon capture, utilization and sequestration (CCUS) pilot and demonstration projects', *Energy Policy*, vol. 158, Nov. 2021, doi: 10.1016/j.enpol.2021.112546.
- [2] S. Satyapal, T. Filburn, J. Trela, and J. Strange, 'Performance and properties of a solid amine sorbent for carbon dioxide removal in space life support applications', *Energy and Fuels*, vol. 15, no. 2, pp. 250–255, Mar. 2001, doi: 10.1021/ef0002391.
- [3] K. Calvin *et al.*, 'IPCC, 2023: Climate Change 2023: Synthesis Report. Contribution of Working Groups I, II and III to the Sixth Assessment Report of the Intergovernmental Panel on Climate Change [Core Writing Team, H. Lee and J. Romero (eds.)]. IPCC, Geneva, Switzerland.', Jul. 2023. doi: 10.59327/IPCC/AR6-9789291691647.
- [4] 'CO₂ and Greenhouse Gas Emissions - Our World in Data'. Accessed: Feb. 16, 2024. [Online]. Available: <https://ourworldindata.org/co2-and-greenhouse-gas-emissions>
- [5] S. Pattanaik and B. Nayak, 'A Review on CO₂ Sequestration: The Indian Scenario', *Journal of the Geological Society of India*, vol. 99, no. 8, pp. 1083–1093, Aug. 2023, doi: 10.1007/s12594-023-2434-6.
- [6] I. Energy Agency, 'Net Zero Roadmap: A Global Pathway to Keep the 1.5 °C Goal in Reach - 2023 Update', 2023. [Online]. Available: www.iea.org/t&c/
- [7] 'Politics and Particulates: New Delhi Fights Against Pollution - The New York Times'. Accessed: Feb. 16, 2024. [Online]. Available: <https://www.nytimes.com/2023/11/03/world/asia/new-delhi-india-pollution.html>
- [8] 'Data review: how many people die from air pollution? - Our World in Data'. Accessed: Feb. 16, 2024. [Online]. Available: <https://ourworldindata.org/data-review-air-pollution-deaths>
- [9] 'Wildfires'. Accessed: Feb. 16, 2024. [Online]. Available: <https://education.nationalgeographic.org/resource/wildfires/>
- [10] 'Wildfires'. Accessed: Feb. 16, 2024. [Online]. Available: https://www.who.int/health-topics/wildfires#tab=tab_1
- [11] 'NASA-STD-3001 Technical Brief Carbon Dioxide (CO₂)'.
- [12] A. Sodiq *et al.*, 'A review on progress made in direct air capture of CO₂', *Environmental Technology and Innovation*, vol. 29. Elsevier B.V., Feb. 01, 2023. doi: 10.1016/j.eti.2022.102991.
- [13] H. A. Patel, J. Byun, and C. T. Yavuz, 'Carbon Dioxide Capture Adsorbents: Chemistry and Methods', *ChemSusChem*, vol. 10, no. 7. Wiley-VCH Verlag, pp. 1303–1317, Apr. 10, 2017. doi: 10.1002/cssc.201601545.

- [14] J. A. Wurzbacher, C. Gebald, and A. Steinfeld, 'Separation of CO₂ from air by temperature-vacuum swing adsorption using diamine-functionalized silica gel', *Energy Environ Sci*, vol. 4, no. 9, pp. 3584–3592, Aug. 2011, doi: 10.1039/C1EE01681D.
- [15] T. Wang, K. S. Lackner, and A. Wright, 'Moisture swing sorbent for carbon dioxide capture from ambient air', *Environ Sci Technol*, vol. 45, no. 15, pp. 6670–6675, Aug. 2011, doi: 10.1021/es201180v.
- [16] S. Jin, M. Wu, Y. Jing, R. G. Gordon, and M. J. Aziz, 'Low energy carbon capture via electrochemically induced pH swing with electrochemical rebalancing', *Nat Commun*, vol. 13, no. 1, Dec. 2022, doi: 10.1038/s41467-022-29791-7.
- [17] K. Lackner, A. Hans-Joachim Ziock, P. Grimes, and G. Associates, 'Title: Carbon Dioxide Extraction From Air: Is It An Option? Los Alamos'.
- [18] S. Choi, J. H. Drese, and C. W. Jones, 'Adsorbent materials for carbon dioxide capture from large anthropogenic point sources', *ChemSusChem*, vol. 2, no. 9, Wiley-VCH Verlag, pp. 796–854, 2009. doi: 10.1002/cssc.200900036.
- [19] I. Energy Agency, 'Direct Air Capture: A key technology for net zero'. [Online]. Available: www.iea.org/t&c/
- [20] D. Panda, V. Kulkarni, and S. K. Singh, 'Evaluation of amine-based solid adsorbents for direct air capture: a critical review', *Reaction Chemistry and Engineering*, vol. 8, no. 1, Royal Society of Chemistry, pp. 10–40, Nov. 22, 2022. doi: 10.1039/d2re00211f.
- [21] A. Gambhir and M. Tavoni, 'Direct Air Carbon Capture and Sequestration: How It Works and How It Could Contribute to Climate-Change Mitigation', *One Earth*, vol. 1, no. 4, Cell Press, pp. 405–409, Dec. 20, 2019. doi: 10.1016/j.oneear.2019.11.006.
- [22] F. Sabatino, A. Grimm, F. Gallucci, M. van Sint Annaland, G. J. Kramer, and M. Gazzani, 'A comparative energy and costs assessment and optimization for direct air capture technologies', *Joule*, vol. 5, no. 8, pp. 2047–2076, Aug. 2021, doi: 10.1016/j.joule.2021.05.023.
- [23] 'Direct air capture technology: innovations in CO₂ removal'. Accessed: Feb. 16, 2024. [Online]. Available: <https://climeworks.com/direct-air-capture>
- [24] 'Direct Air Capture Explained: The Buzzy New Carbon Reduction Tech Gaining Exec Attention - CB Insights Research'. Accessed: Feb. 16, 2024. [Online]. Available: <https://www.cbinsights.com/research/direct-air-capture-corporate-carbon-reduction/>
- [25] 'Carbon Engineering | Direct Air Capture of CO₂ | Home'. Accessed: Feb. 16, 2024. [Online]. Available: <https://carbonengineering.com/>
- [26] A. Gambhir and M. Tavoni, 'Direct Air Carbon Capture and Sequestration: How It Works and How It Could Contribute to Climate-Change Mitigation', *One Earth*, vol. 1, no. 4, Cell Press, pp. 405–409, Dec. 20, 2019. doi: 10.1016/j.oneear.2019.11.006.

- [27] M. Jahandar Lashaki and A. Sayari, 'CO₂ capture using triamine-grafted SBA-15: The impact of the support pore structure', *Chemical Engineering Journal*, vol. 334, pp. 1260–1269, Feb. 2018, doi: 10.1016/j.cej.2017.10.103.
- [28] M. Karimi, M. Shirzad, J. A. C. Silva, and A. E. Rodrigues, 'Carbon dioxide separation and capture by adsorption: a review', *Environmental Chemistry Letters*, vol. 21, no. 4. Springer Science and Business Media Deutschland GmbH, pp. 2041–2084, Aug. 01, 2023. doi: 10.1007/s10311-023-01589-z.
- [29] X. Shi, Y. Lin, and X. Chen, 'Development of sorbent materials for direct air capture of CO₂', *MRS Bulletin*, vol. 47, no. 4. Springer Nature, pp. 405–415, Apr. 01, 2022. doi: 10.1557/s43577-022-00320-7.
- [30] S. Y. Lee and S. J. Park, 'A review on solid adsorbents for carbon dioxide capture', *Journal of Industrial and Engineering Chemistry*, vol. 23. Korean Society of Industrial Engineering Chemistry, pp. 1–11, Mar. 25, 2015. doi: 10.1016/j.jiec.2014.09.001.
- [31] R. Ben-Mansour *et al.*, 'Carbon capture by physical adsorption: Materials, experimental investigations and numerical modeling and simulations - A review', *Applied Energy*, vol. 161. Elsevier Ltd, pp. 225–255, Jan. 01, 2016. doi: 10.1016/j.apenergy.2015.10.011.
- [32] R. Chang, X. Wu, O. Cheung, and W. Liu, 'Synthetic solid oxide sorbents for CO₂ capture: State-of-the art and future perspectives', *Journal of Materials Chemistry A*, vol. 10, no. 4. Royal Society of Chemistry, pp. 1682–1705, Jan. 28, 2022. doi: 10.1039/d1ta07697c.
- [33] M. Songolzadeh, M. Soleimani, M. Takht Ravanchi, and R. Songolzadeh, 'Carbon dioxide separation from flue gases: A technological review emphasizing reduction in greenhouse gas emissions', *The Scientific World Journal*, vol. 2014, 2014, doi: 10.1155/2014/828131.
- [34] E. S. Sanz-Pérez, C. R. Murdock, S. A. Didas, and C. W. Jones, 'Direct Capture of CO₂ from Ambient Air', *Chemical Reviews*, vol. 116, no. 19. American Chemical Society, pp. 11840–11876, Oct. 12, 2016. doi: 10.1021/acs.chemrev.6b00173.
- [35] A. Goeppert, H. Zhang, R. Sen, H. Dang, and G. K. S. Prakash, 'Oxidation-Resistant, Cost-Effective Epoxide-Modified Polyamine Adsorbents for CO₂ Capture from Various Sources Including Air', *ChemSusChem*, vol. 12, no. 8, pp. 1712–1723, Apr. 2019, doi: 10.1002/cssc.201802978.
- [36] D. W. F. Brilman and R. Veneman, 'Capturing atmospheric CO₂ using supported amine sorbents', in *Energy Procedia*, Elsevier Ltd, 2013, pp. 6070–6078. doi: 10.1016/j.egypro.2013.06.536.
- [37] S. Choi, M. L. Gray, and C. W. Jones, 'Amine-tethered solid adsorbents coupling high adsorption capacity and regenerability for CO₂ capture from ambient air', *ChemSusChem*, vol. 4, no. 5, pp. 628–635, May 2011, doi: 10.1002/cssc.201000355.

- [38] S. Choi, M. L. Gray, and C. W. Jones, 'Amine-tethered solid adsorbents coupling high adsorption capacity and regenerability for CO₂ capture from ambient air', *ChemSusChem*, vol. 4, no. 5, pp. 628–635, May 2011, doi: 10.1002/cssc.201000355.
- [39] H. T. Kwon, M. A. Sakwa-Novak, S. H. Pang, A. R. Sujan, E. W. Ping, and C. W. Jones, 'Aminopolymer-Impregnated Hierarchical Silica Structures: Unexpected Equivalent CO₂ Uptake under Simulated Air Capture and Flue Gas Capture Conditions', *Chemistry of Materials*, vol. 31, no. 14, pp. 5229–5237, Jul. 2019, doi: 10.1021/acs.chemmater.9b01474.
- [40] A. Goeppert *et al.*, 'Easily regenerable solid adsorbents based on polyamines for carbon dioxide capture from the air', *ChemSusChem*, vol. 7, no. 5, pp. 1386–1397, 2014, doi: 10.1002/cssc.201301114.
- [41] A. R. Sujan *et al.*, 'Poly(glycidyl amine)-Loaded SBA-15 Sorbents for CO₂ Capture from Dilute and Ultradilute Gas Mixtures', *ACS Appl Polym Mater*, vol. 1, no. 11, pp. 3137–3147, Nov. 2019, doi: 10.1021/acsapm.9b00788.
- [42] K. A. S. Abhilash, T. Deepthi, R. A. Sadhana, and K. G. Benny, 'Functionalized Polysilsesquioxane-Based Hybrid Silica Solid Amine Sorbents for the Regenerative Removal of CO₂ from Air', *ACS Appl Mater Interfaces*, vol. 7, no. 32, pp. 17969–17976, Aug. 2015, doi: 10.1021/acsami.5b04674.
- [43] by J. Jason Lee *et al.*, 'SPECTROSCOPIC CHARACTERIZATION OF AMINE SORBENTS FOR CO₂ CAPTURE A Dissertation Presented to The Academic Faculty SPECTROSCOPIC CHARACTERIZATION OF AMINE SORBENTS FOR CO₂ CAPTURE', 2019.
- [44] A. Kumar *et al.*, 'Direct Air Capture of CO₂ by Physisorbent Materials', *Angewandte Chemie*, vol. 127, no. 48, pp. 14580–14585, Nov. 2015, doi: 10.1002/ange.201506952.
- [45] A. Goeppert *et al.*, 'Easily regenerable solid adsorbents based on polyamines for carbon dioxide capture from the air', *ChemSusChem*, vol. 7, no. 5, pp. 1386–1397, 2014, doi: 10.1002/cssc.201301114.
- [46] C. Lu, X. Zhang, and X. Chen, 'Advanced Materials and Technologies toward Carbon Neutrality', *Acc Mater Res*, 2022, doi: 10.1021/accountsmr.2c00084.
- [47] A. Goeppert, M. Czaun, R. B. May, G. K. S. Prakash, G. A. Olah, and S. R. Narayanan, 'Carbon dioxide capture from the air using a polyamine based regenerable solid adsorbent', *J Am Chem Soc*, vol. 133, no. 50, pp. 20164–20167, Dec. 2011, doi: 10.1021/ja2100005.
- [48] M. W. Hahn, J. Jelic, E. Berger, K. Reuter, A. Jentys, and J. A. Lercher, 'Role of Amine Functionality for CO₂ Chemisorption on Silica', *Journal of Physical Chemistry B*, vol. 120, no. 8, pp. 1988–1995, Mar. 2016, doi: 10.1021/acs.jpcb.5b10012.
- [49] Shaker, 'The interaction of CO₂ with amines as molecular control factor in catalytic processes'.

- [50] E. M. Hampe and D. M. Rudkevich, 'Exploring reversible reactions between CO₂ and amines', *Tetrahedron*, vol. 59, no. 48, pp. 9619–9625, Nov. 2003, doi: 10.1016/j.tet.2003.09.096.
- [51] Y. Belmabkhout and A. Sayari, 'Effect of pore expansion and amine functionalization of mesoporous silica on CO₂ adsorption over a wide range of conditions', *Adsorption*, vol. 15, no. 3, pp. 318–328, Jun. 2009, doi: 10.1007/s10450-009-9185-6.
- [52] Y. Belmabkhout, R. Serna-Guerrero, and A. Sayari, 'Adsorption of CO₂-containing gas mixtures over amine-bearing pore-expanded MCM-41 silica: Application for gas purification', *Ind Eng Chem Res*, vol. 49, no. 1, pp. 359–365, Jan. 2010, doi: 10.1021/ie900837t.
- [53] 'Belmabkhout Y, De Weireld G, Sayari A. Amine-bearing mesoporous silica for CO(2) and H(2)S removal from natural gas and biogas. *Langmuir*. 2009 Dec 1;25(23):13275-8. doi: 10.1021/la903238y. PMID: 19874010.'
- [54] K. A. S. Abhilash, T. Deepthi, R. A. Sadhana, and K. G. Benny, 'Functionalized Polysilsesquioxane-Based Hybrid Silica Solid Amine Sorbents for the Regenerative Removal of CO₂ from Air', *ACS Appl Mater Interfaces*, vol. 7, no. 32, pp. 17969–17976, Aug. 2015, doi: 10.1021/acsami.5b04674.
- [55] W. Chaikittisilp, J. D. Lunn, D. F. Shantz, and C. W. Jones, 'Poly(L-lysine) brush-mesoporous silica hybrid material as a biomolecule-based adsorbent for CO₂ capture from simulated flue gas and air', *Chemistry - A European Journal*, vol. 17, no. 38, pp. 10556–10561, Sep. 2011, doi: 10.1002/chem.201101480.
- [56] N. R. Stuckert and R. T. Yang, 'CO₂ capture from the atmosphere and simultaneous concentration using zeolites and amine-grafted SBA-15', *Environ Sci Technol*, vol. 45, no. 23, pp. 10257–10264, Dec. 2011, doi: 10.1021/es202647a.
- [57] C. Chen, S. Zhang, K. H. Row, and W. S. Ahn, 'Amine–silica composites for CO₂ capture: A short review', *Journal of Energy Chemistry*, vol. 26, no. 5. Elsevier B.V., pp. 868–880, Nov. 01, 2017. doi: 10.1016/j.jechem.2017.07.001.
- [58] W. Chaikittisilp, R. Khunsupat, T. T. Chen, and C. W. Jones, 'Poly(allylamine)-mesoporous silica composite materials for CO₂ capture from simulated flue gas or ambient air', *Ind Eng Chem Res*, vol. 50, no. 24, pp. 14203–14210, Dec. 2011, doi: 10.1021/ie201584t.
- [59] W. Chaikittisilp, H. J. Kim, and C. W. Jones, 'Mesoporous alumina-supported amines as potential steam-stable adsorbents for capturing CO₂ from simulated flue gas and ambient air', *Energy and Fuels*, vol. 25, no. 11, pp. 5528–5537, Nov. 2011, doi: 10.1021/ef201224v.
- [60] M. A. Sakwa-Novak, S. Tan, and C. W. Jones, 'Role of Additives in Composite PEI/Oxide CO₂ Adsorbents: Enhancement in the Amine Efficiency of Supported PEI by PEG in CO₂ Capture from Simulated Ambient Air', *ACS Appl Mater Interfaces*, vol. 7, no. 44, pp. 24748–24759, Nov. 2015, doi: 10.1021/acsami.5b07545.

- [61] Y. Kuwahara *et al.*, ‘Dramatic enhancement of CO₂ uptake by poly(ethyleneimine) using zirconosilicate supports’, *J Am Chem Soc*, vol. 134, no. 26, pp. 10757–10760, Jul. 2012, doi: 10.1021/ja303136e.
- [62] A. R. Sujan, S. H. Pang, G. Zhu, C. W. Jones, and R. P. Lively, ‘Direct CO₂ Capture from Air using Poly(ethylenimine)-Loaded Polymer/Silica Fiber Sorbents’, *ACS Sustain Chem Eng*, vol. 7, no. 5, pp. 5264–5273, Mar. 2019, doi: 10.1021/acssuschemeng.8b06203.

LIST OF ABBREVIATIONS

CO ₂ – Carbon dioxide	LCFS – Low Carbon Fuel Standard
CDR – Carbon Dioxide Removal	USD – United States Dollar
CCSU – Carbon Capture, Storage and Utilization	US – United States
CCS – Carbon Capture and Storage	IR – Infrared
DAC – Direct Air Capture	NMR – Nuclear Magnetic Resonance
S-DAC – Solid Direct Air Capture	SEM – Scanning Electron Microscope
L-DAC – Liquid Direct Air Capture	TGA – Thermogravimetric Analysis
IEA – International Energy Agency	BET– Brunauer-Emmett-Teller
BECCS – Bioenergy with Carbon Capture and Utilization or Storage	FTIR – Fourier Transform Infrared
DACS – Direct Air Capture and Storage	PEI – Polyethyleneimine
DAS – Delayed Action Scenario	PEG – Poly(ethylene glycol)
HSSSI – Hamilton Sundstrand Space Systems International	TEPA–Tetraethylenepentamine
WHO – World Health Organization	MOF – Metal-Organic Framework
IHME – Institute for Health Metrics and Evaluation	COF – Covalent Organic Framework
NASA – National Aeronautics and Space Administration	NO ₂ – Nitrogen dioxide
	LiOH – Lithium hydroxide
	NaHCO ₃ – Sodium bicarbonate
	Na ₂ CO ₃ – Sodium carbonate

NaOH – Sodium hydroxide

H – Hydrogen

CaO – Calcium oxide

N – Nitrogen

Ca(OH)₂ – Calcium hydroxide

S – Sulfur

CaO – Calcium oxide

Mw – Molecular weight

MgO – Magnesium oxide

ZEOFREE – Commercial calcium silicate

CaCO₃ – Calcium carbonate

APTMS – Amino propyl trimethoxy silane

Li₂CO₃ – Lithium carbonate

AEAPTMS – 3-[2-(2-aminoethylamino) ethyl amino] propyl-trimethoxy silane

K₂CO₃ – Potassium carbonate

LOD – Limit of Detection

Li₂ZrO₃ – Lithium zirconate

Gt – Gigaton

Li₄SiO₄ – Lithium silicate

°C – Degrees Celsius

COO⁻ – Carboxylate ion

kJ/mol–Kilojoules per mole

Si-O-Si – Silicon-Oxygen-Silicon

tCO₂/year–Metric tons of CO₂ per year

Si-OH – Silanol group

MtCO₂/year – Megatons of CO₂ per year

N-H – Amine group

Mbar – Millibar

C-H – Methyl group

Mmol/g – Millimoles per gram

H₂O – Water

nm – Nanometers

OH⁻ – Hydroxide ion

CO₂/N – Ratio of CO₂ to nitrogen

C – Carbon

HNO₃ – Nitric acid

400 ppm – Part per million

PM2.5 particulate matter 2.5 micrometers

mL – Milliliter

mL/min – Milliliter per minute

rpm – Revolutions per minute

kV – Kilovolt

μm – Micrometer

K – Kelvin

m^2/g – Square meters per gram

cm^3/g – Cubic centimeters per gram

nm – Nanometer

cm^{-1} – Inverse centimeter

I – one

II – two

III – three

IV – four

LIST OF FIGURES

Figure 1 Worldwide emissions of carbon dioxide due to the burning of energy sources and industrial activities from the year 1900 to 2022. [4]	12
Figure 2 Variation in worldwide carbon dioxide emissions from different fuels, compared to the baseline of 2019, from the years 2015 to 2022. [3].....	13
Figure 3 Worldwide carbon dioxide emissions categorized by industry, 2019 to 2022. [3]	13
Figure 4 Global average temperature variation. [4]	14
Figure 5 Extreme climate events harm smallholder farmers, reducing crop yields, food security, income, and well-being. [3].....	15
Figure 6 Air pollution in New Delhi November 3, 2023 [7].....	15
Figure 7 Every year, numerous forests endure drought conditions. [9].....	16
Figure 8 Leading Direct Air Capture companies around the world.	18
Figure 9 Direct Air Capture global operating capacity, 2010–2021 [6]	19
Figure 10 CO ₂ capture by Direct Air Capture, planned projects and in the Net Zero Emissions by 2050 Scenario, 2020-2030 [6].....	20
Figure 11 Adsorption and regeneration process of adsorbents. (Redrawn from [20]).....	21
Figure 12 Solid Direct Air Capture process. (Climeworks [24])	22
Figure 13 Liquid Direct Air Capture process. (Carbon Engineering [25])	22
Figure 14 Challenges of Direct Air Capture Technology.	23
Figure 15 Advantages of Direct Air Capture Technology.	24
Figure 16 Some of significant checkpoints for an effective CO ₂ adsorbent.	25
Figure 17 Porosity and chemistry have to be considered together in optimizing a sorbent choice. (Redrawn from [27])	26
Figure 18 Classification of adsorbents materials.	27
Figure 19 Capturing CO ₂ via calcination and carbonation with a calcium oxide (CaO) sorbent. 29	
Figure 20 Schematic representation of classification of amine based solid adsorbents. Redrawn from [20]	30
Figure 21 Representation of double functionalization. (Redrawn from [43]).....	32
Figure 22 Interaction of PEI with CO ₂ . (Redrawn from [40])	33
Figure 23 Synthesis of amine-grafting with ZEOFREE. (Created with BioRender.com).....	40
Figure 24 Synthesis of amine impregnating with ZEOFREE. (Created with BioRender.com)....	42
Figure 25 Scanning Electron Microscope (FEI, Nova NanoSEM 450).....	45
Figure 26 Thermo-gravimetric analyzer (TGA Q500 Thermogravimetric Analyzer) (left) and SETARAM Scientific & Industrial Equipment (SETSYS Evolution) TGA (right)	46
Figure 27 Brunauer-Emmett-Teller (BET) BELSORP-mini II Analyzer (left) and Fourier Transform Infrared Spectroscopy (FTIR) NICOLET 6700 FT-IR, Thermo Scientific (right).....	47
Figure 28 Flash Analyzer CHNS / O + MAS200R, Thermo Scientific.....	48

Figure 29 Representation of adsorption desorption cycles by temperature profile in 10% CO ₂ environment.....	49
Figure 30 Representation of adsorption desorption cycle by temperature profile in 400 ppm CO ₂ environment.....	50
Figure 31 SEM images of ZEOFREE and ZEO series. a) and b) ZEOFREE c) ZEO-1 d) ZEO-2 e) ZEO-3 f) ZEO-4 g) ZEO-5 and h) ZEO-6.	51
Figure 32 SEM images of PEI series. a) PEI800_ZEO b) PEI800_PEG_ZEO c) PEI25000_ZEO d) PEI25000_PEG_ZEO e) PEI2000_ZEO f) PEI2000_PEG_ZEO g) PEI750000_ZEO and h) PEI750000_PEG_ZEO	53
Figure 33 Thermal stability curves of ZEO series including ZEOFREE support.....	54
Figure 34 Thermal stability of PEI-based adsorbents without addition of PEG including ZEOFREE.	56
Figure 35 Thermal stability of PEI-based adsorbents with addition of PEG including ZEOFREE.	57
Figure 36 FTIR spectra of ZEO series including ZEOFREE support.....	60
Figure 37 FTIR spectra of PEI series and pristine PEIs as well as PEG and ZEOFREE support.....	61
Figure 38 Adsorption-desorption measurements of pristine ZEOFREE support.	64
Figure 39 Cyclic stability and CO ₂ adsorption capacity of ZEOFREE support over 20 cycles. ..	65
Figure 40 Comparative CO ₂ uptake of the ZEO series under 10% CO ₂ conditions.	66
Figure 41 Adsorption-desorption measurements of ZEO series.	67
Figure 42 Cyclic stability and CO ₂ adsorption capacity of ZEO series.	68
Figure 43 Adsorption-desorption measurements of PEI800_ZEO and PEI800_PEG_ZEO.	70
Figure 44 Adsorption-desorption measurements of PEI25000_ZEO and PEI25000_PEG_ZEO.....	71
Figure 45 Adsorption-desorption measurements of PEI2000_ZEO and PEI2000_PEG_ZEO....	71
Figure 46 Adsorption-desorption measurements of PEI750000_ZEO and PEI750000_PEG_ZEO.	72
Figure 47 Cyclic stability and CO ₂ adsorption capacity of PEI800_ZEO and PEI800_PEG_ZEO.	73
Figure 48 Cyclic stability and CO ₂ adsorption capacity of PEI25000_ZEO, PEI25000_PEG_ZEO, PEI2000_ZEO, PEI2000_PEG_ZEO and PEI750000_ZEO, PEI750000_PEG_ZEO.....	74
Figure 49 CO ₂ adsorption capacity of ZEO series including ZEOFREE support under 400 ppm CO ₂ conditions.	76
Figure 50 CO ₂ adsorption capacity of PEI series and ZEOFREE support under 400 ppm CO ₂ conditions.	78
Figure 51 CO ₂ adsorption capacity of PEI800_ZEO adsorbent in 6 hours adsorption under 400 ppm CO ₂ conditions.	78

LIST OF TABLES

Table 1 List of materials and chemicals used for the synthesizes.....	38
Table 2 Materials and chemicals used for the synthesizes.....	39
Table 3 Comparative table of grafting experiments performed using ZEOFREE support.....	41
Table 4 Comparative table of dry impregnation synthesis.....	43
Table 5 Comparative table of wet impregnation synthesis.	44
Table 6 Corresponding table detailing water loss and overall weight loss as well as estimated organic content.	55
Table 7 Actual amine loading and total weight loss of PEI series.....	58
Table 8 Surface area, pore diameter and total pore volume of all samples including ZEOFREE support.....	59
Table 9 Determination of C, H, N, (S) content in Diatoms (DE) and ZEOFREE based sorbents and samples using the FLASH method. Values given in weight percent % (m/m), methionine (C 5 H 11 NO 2 S) standard used.....	63
Table 10 CO ₂ capture capacity of amine-functionalized ZEO series adsorbents synthesized by chemical grafting.....	69
Table 11 Amine loading, and CO ₂ adsorption capacity of adsorbents using the TGA method. PEG molecular weight: 20000, all molecular weight shows in the table is only for PEI's.....	75
Table 12 CO ₂ adsorption capacity of all samples including ZEOFREE support under 400 ppm CO ₂ conditions.	79
Table 13 CO ₂ adsorption capacity amine-functionalized solid adsorbents synthesized by chemical grafting and impregnation processes presented from literature.	80